Development of Adaptive Artificial Pancreas Systems for Personalized Glucose Management

By

Navid Resalat

A DISSERTATION

PRESENTED TO THE DEPARTMENT OF BIOMEDICAL ENGINEERING
AND THE OREGON HEALTH & SCIENCE UNIVERSITY
SCHOOL OF MEDICINE
IN PARTIAL FULLFILLMENT OF THE
REQUIREMENT FOR THE DEGREE OF
DOCTOR OF PHILOSOPHY

Summer 2019

School of Medicine

Oregon Health & Science University

CERTIFICATE OF APPROVAL

This is to certify that the PhD dissertation of

Navid Resalat

has been approved

Peter Jacobs, Ph.D. (Advisor)

Alexander Kain, Ph.D.

Joseph El Youssef, MD

Kyle Ellrott, Ph.D.

Daniel Zuckerman, Ph.D.

TABLE OF CONTENTS

List of Figures

List of Tables

Acknowledgments

I would like to express my gratitude to my advisor Prof. Peter Jacobs for his support during my PhD program, for his patience, motivation, and knowledge. His guidance helped me in all the time of research and in writing of this thesis. I could not have imagined having a more respectful advisor during my study.

In addition to my advisor, I would like to thank the rest of my thesis committee: Prof. Alexander Kain, Dr. Joseph El. Youssef, and Prof. Kyle Ellrott for not only their insightful comments, but also for incentivizing me to widen my research from various perspectives with their thought-provoking questions

I thank my fellow labmates: Arun, Nick, Taha, Ravi, Nichole, and Joe for their stimulating discussions and comments and for all the fun we have had in the last four years. In addition, I thank my friends: Dr. Meysam Asgari in the Center for Spoken Language Understanding and Mr. Jonathan Savage, a PhD student in the Program of Molecular and Cellular Biosciences.

Lastly, I would like to thank my family: my lovely wife, my parents, my wife's parents and grandparents, and my brother and sister for supporting me spiritually and financially throughout my life and my PhD program.

To my parents, sister, brother and my lovely wife and her parents and grandparents

Life is a unique stage of art

Everybody sings a song and goes from the stage

Stage is always on

Good for the song that people commit to memory

ABSTRACT

Type 1 diabetes (T1D) is a chronic disease where the pancreas does not produce sufficient insulin. Exogenous insulin is required to be delivered. Over delivery of insulin can cause hypoglycemia, which can cause coma or death if not treated. Under delivery can cause hyperglycemia; long-term exposure can cause chronic health problems including neuropathy, retinopathy, and limb loss. The artificial pancreas (AP) is an automated technology for helping people with T1D control their glucose. A single-hormone (SH) AP consists of three main components: a glucose sensor that is inserted in the body, a control algorithm for calculating insulin infusion based on the glucose levels, and an insulin pump. A dual-hormone (DH) AP system includes a glucagon pump; glucagon stimulates endogenous glucose production. Exercise is challenging for people with T1D as it can cause hypoglycemia. Glucagon can help avoid exercise-induced hypoglycemia. In AP systems, the control algorithm is a critical component that affects how well glucose is managed including avoidance of hypoglycemia and hyperglycemia. Model predictive control (MPC) is a state-of-the-art method for controlling glucose levels in people with T1D. There is currently not an adaptive MPC for single and dual-hormone AP control systems that can effectively handle exercise.

In this dissertation, I contributed the following. First, I developed a new virtual patient population (VPP) simulator that can be used to mathematically represent people with type 1 diabetes and can be used for in-silico simulations before a clinical trial. We compared the results of this VPP with patients with T1D under equivalent test conditions and found that the VPP behaved similarly to the patients. Second, I developed a SH- and a DH-MPC that appropriately model exercise. I assessed the importance of model complexity on controller performance for the SH-MPC. Both controllers were validated with real-world meal scenarios, and designed for fast action insulin delivery. I demonstrated the importance of including an exercise model within the MPC, showing that time in hypoglycemia could be reduced by 40 minutes per day on average. Third, I have developed an adaptive algorithm to personalize insulin dosing after meals. The Adaptive Learning Postprandial Hypoglycemia-prevention Algorithm (ALPHA) was developed to reduce post-prandial hypoglycemia. ALPHA reduced time in hypoglycemia from 1.92% to 0.54%. Lastly, I developed an adaptive algorithm called the Insulin Sensitivity Adaptation (ISA) algorithm to personalize each patient's insulin sensitivity model parameter within the MPC controllers. ISA reduced average glucose significantly to 136.5 mg/dl from 140.2 mg/dl.

1 Introduction

Type 1 diabetes (T1D), known as insulin-dependent diabetes, is an autoimmune disease which typically has onset in childhood or early adolescence. The autoimmune system suppresses the β-cell production of insulin. Without exogenous insulin delivery, glucose fails to get absorbed into cells and tissues for energy production, and the blood glucose becomes elevated. Elevated glucose levels are particularly problematic during mealtime where carbohydrates increase glucose levels.

When glucose exceeds 180 mg/dl, hyperglycemia occurs, according to American Diabetes Association (ADA). On the other hand, when glucose utilization increases (e.g. during physical activity and exercise), glucose uptake of glucose within the body increases and blood glucose can drop sharply. It can be dangerous and even deadly if glucose levels should not drop below a minimum threshold. The ADA has identified a low boundary (70 mg/dl or 3.9 mmol/L), below which is defined as hypoglycemia. Severe health problems may occur if hypoglycemia remains [1].

According to ADA, 1.25 million people with T1D live in the United States and approximately 40,000 people are diagnosed with T1D each year [2]. Because diabetes mellitus is the seventh leading cause of death in the US, with more than

252,000 death certificates in 2015 [3], it is essential to maintain glucose in the target range and reduce time spent in hyper- and hypoglycemia. If hyperglycemia remains untreated, people with T1D will be exposed to long-term complications such as kidney disease, nerve disease and blindness [4]-[5]. To treat hyperglycemia, exogenous insulin is infused; however; over-delivery of exogenous insulin may lead to hypoglycemia. If hypoglycemia remains untreated, even for a short period, diabetic coma may occur [1]. In general, symptoms of people with T1D are divided into two categories: acute and chronic. Acute symptoms of hypoglycemia occur instantaneously and are divided into adrenaline and neurological-based symptoms. Acute symptoms of hyperglycemia occur after several months to several years. Table I categorizes the symptoms of hyper- and hypoglycemia.

Table I Symptoms of hyper/hypoglycemia

<table>
<tr><td>Symptoms</td><td>Hyperglycemia</td><td colspan="2">Hypoglycemia</td></tr>
<tr><td rowspan="2">Acute</td><td rowspan="2">1. Blurry vision
2. Thirst
3. Frequent urination</td><td>Adrenaline based</td><td>1. Shakily
2. Nervousness
3. Sweeting
4. palpitation</td></tr>
<tr><td>Neurological based</td><td>1. Confusion
2. Seizures
3. Stroke-like coma</td></tr>
<tr><td>Chronic</td><td>1. Retinopathy
2. Neuropathy
3. Nephropathy</td><td colspan="2">1. Unawareness
2. Lose adrenaline response</td></tr>
</table>

1.1 Diabetes Diagnosis and Treatment

For pre-evaluating diabetes, the rate of glucose changes and the diabetic symptoms are examined. If frequent diabetic symptoms exist or the rate of glucose reduction in urine is significant, the likelihood of diabetes increases and three main tests will be performed for diagnosis.

1- Fasting glucose test: glucose is measured before breakfast. If it exceeds 7 mmol/L (126 mg/dl), diabetes mellitus may be present [6].

2- Oral glucose tolerance test: glucose is given orally and the glucose level is measured every 30 to 60 minutes up to 3 hours. If the glucose level exceeds 200 mg/dl, diabetes mellitus may be present [6], [7].

3- A1c test: average of glycated hemoglobin during the past 2-3 months is measured. If it exceeds 7%, likelihood of diabetes mellitus increases [8].

To determine the type of diabetes, a zinc transporter-8 autoantibody (ZnT8Ab) test is performed [9]. Zinc transporter-8 is a membrane protein of the pancreatic β-cells, which is an autoantigen in people with T1D. ZnT8Ab can be used as a marker to identify T1D [10].

Diabetes treatment is generally divided into two categories: islet-cell transplantation and insulin therapy. Islet cell transplantation is a costly treatment where donor cells are transferred to patients resulting in higher production of endogenous insulin.

Although it shows significant improvements for patients with a history of neuropathy, it may not perform appropriately for patients under insulin therapy [11].

Insulin therapy is a prevalent type of diabetes treatment where insulin is exogenously injected. Insulin therapy is divided into two modes: open loop and closed-loop. Open loop insulin therapy is also divided into two main categories based on the type and the quality of insulin. These categories are multiple daily insulin injection (MDI) and continuous subcutaneous insulin infusion (CSII).

In MDI therapy, multiple blood glucose measurements are taken throughout the day using a lancing device to prick the finger to extract blood that is put into a glucose meter. Both short-acting and long-acting insulin (e.g. Lantus, Levemir) with prolonged action of 24 hours are injected using a needle [12]. Because the absorption time (1-4 hours) and the time-to-maximum of peak effect (4-12 hours) of insulin in MDI therapy are high, management with MDI can be challenging. CSII therapy is an alternative therapy whereby fast acting insulin is dosed continuously throughout the day to improve glucose management [12]-[13]. In CSII therapy, rapid-acting insulin (e.g. Humalog, Novolog) with faster absorption time (10-30 minutes) and shorter time-to-maximum of peak effect (0.5-3 hours) is infused via an insulin pump (e.g. Tandem t:slim, Insulet Omnipod, Medtronic) [13]. An insulin pump delivers a small amount of basal insulin continuously throughout the day pre-set by the patient.

The pump has the ability to alarm the user when insulin is not delivered or is discontinued.

Many studies have shown improved glucose control with the CSII therapy compared to the MDI therapy [12], [14]-[15]. In the latest version of the CSII therapy, known as Sensor Augmented Pump therapy (SAP), a subcutaneously inserted glucose sensor (e.g. Dexcom, Medtronic) is mounted used for continuous glucose monitoring (CGM) [16] -[17]. Because CGM data are measured subcutaneously, they are less precise than the blood-based finger-stick measurements made by a glucose meter; however, SAP therapy has shown better clinical performance in terms of reduced time spent in hyper- and hypoglycemia [18]. If a CGM detects hypoglycemia, it prompts the users to shut down insulin infusion manually. The CGM enables patients to adjust basal insulin rates based on real-time glucose measurements and also be enabling patients to review prior CGM data.

Notice that in MDI therapy long-acting basal insulin is injected multiple times per day whereas in CSII and SAP therapies, short-acting basal insulin is infused continuously throughout the day. For all therapies described above, extra insulin is dosed for meals; we call this meal *bolus insulin*. Bolus insulin is a larger amount of insulin delivered at the start, or some minutes before, a meal is consumed and is used

to lower carbohydrate-induced high glucose levels. The magnitude of administered bolus insulin is directly proportional to the amount of carbohydrate intake.

While insulin pumps deliver a constant amount of insulin throughout the day, in closed-loop control, known as Artificial Pancreas (AP), basal insulin rate is updated continually based on the measured CGM. The sampling interval of the CGM data with advanced glucose sensors is 5 minutes, and the basal insulin rates are computed at each 5-minute time interval, enabling more rapid response to rapidly changing glucose levels. Generally, clinical studies have shown that AP systems result in better glycemic management compared with SAP therapy, especially during nighttime [19, 20]. If low glucose levels occur during sleep, AP systems reduce or turn off basal insulin delivery. In an advanced version of the SAP therapy called predictive low glucose suspend therapy (PLGS), insulin is suspended for impending hypoglycemia if glucose level reaches a threshold of 90 mg/dl [21].

1.2 Clinical Metrics

Seven clinical metrics have been proposed to evaluate the performance of the insulin therapy methods across patients. These clinical metrics are:

1- Time spent in hypoglycemia: period of day that glucose levels are below 70 mg/dl (%).

2- Time spent in hyperglycemia: period of day that glucose levels are above 180 mg/dl (%).

3- Time spent in euglycemia: period of day that glucose levels are between 70 mg/dl and 180 mg/dl (%).

4- Number of rescue carbs: When blood glucose drops below 70 mg/dl, a 20-gram carbohydrate is given to patients and blood glucose is re-measured after 20 minutes. If it is still less than 70 mg/dl, another 20-gram of carbs is given until no more hypoglycemia is observed. In this situation, when a rescue carb is given to patients, basal rates are turned down to 25% for 40 minutes. If the glucose level drops below 50 mg/dl, intravenous carbohydrates will be given to increase blood sugar faster [22].

5- Average glucose level: the most desirable average glucose level for people with T1D is when it is less than 154 mg/dl per each 2-3 months.

6- Glycated Hemoglobin, HbA_{1c}, is another metric for evaluating diabetes mellitus. The concentration of HbA_{1c} is measured every 8-12 weeks and is considered reasonable if it is less than 7% [23]-[24].

7- Low Blood Glucose Index (LBGI): LBGI shows the risk of getting hypoglycemia. It considers the number of glucose levels less than 112 mg/dl.

8- High Blood Glucose Index (HBGI): HBGI shows the risk of getting hyperglycemia. It considers the number of glucose levels greater than 112 mg/dl.

Although there is a positive correlation between LBGI and hypoglycemia and HBGI and hyperglycemia, LBGI and HBGI show the skewness of the distribution of glucose levels around 112 mg/dl. Whereas, time in hypoglycemia and hyperglycemia only show the amount of time spent below 70 mg/dl and above 180 mg/dl, respectively. Particularly, LBGI and HBGI indicate the probability of hypoglycemic and hyperglycemic episodes, respectively. Table II shows the ranges of the LBGI and HBGI during glucose control [25].

Table II Ranges of LBGI and HBGI

Risk	LBGI	HBGI
Minimal	≤ 1.1	≤ 5.0
Low	> 1.1 - ≤ 2.5	> 5.0 - ≤ 10.0
Medium	> 2.5 - ≤ 5.0	> 10.0 - ≤ 15.0
High	> 5.0	> 15.0

1.3 Background on AP systems

The Artificial Pancreas (AP) is an emerging technology which was developed initially in the 1970s. Albisser et al. [26] designed the first AP in 1974 and evaluated it across 3 subjects with T1D. In the first day of the experiment, subcutaneous insulin and measured meals were given to the subjects. On the second day, intravenous (IV)

insulin with the same pattern of meals were administered. Their control algorithm calculated the basal insulin rates based on the glucose concentrations and the rate of glucose changes.

They found that IV insulin better managed glucose levels and reduced the time spent in hyperglycemia; however, the time spent in hypoglycemia was increased. A similar approach was performed by Mirouze et al. [27] in 1977. They designed a simple AP and evaluated it across 20 subjects with T1D. Their algorithm used both the current glucose level and the rate of change of glucose to estimate intravenous insulin injection. They found no severe hypoglycemic episodes; however, time spent in hypoglycemia was not negligible due to the frequent over-delivery of postprandial insulin doses. In the aforementioned AP systems, the apparatus for recording glucose and delivering intravenous insulin rates was bulky and not convenient. Furthermore, delivery of insulin directly into a vein is not practical and can be dangerous in real-world situations. Various research groups have been working on new generations of the AP to improve glucose control and to miniaturize the system. Generally, AP systems consist of three main components: Insulin and glucagon pumps, CGM sensor and controller algorithm device (Figure 1.1) [28].

Insulin and glucagon pumps are electromechanical devices, which deliver basal insulin and glucagon subcutaneously. In dual-hormone APs, both pumps are active;

whereas, in the single-hormone AP, insulin is the only hormone for glucose regulation. Glucagon is an alternative to rescue carbs for increasing glucose level. It is delivered when low glucose levels are observed. Lack of glucagon causes people with T1D to be vulnerable to hypoglycemia [29].

CGM sensor consists of a glucose sensor, a transmitter and a receiver to measure interstitial glucose level. The transmitter sends the glucose readings to the receiver wirelessly, and the receiver displays and stores the data. CGM sensor can measure glucose every 5 minutes and provide more data than the conventional finger-stick approach. The only disadvantage of the CGM data is that they are not as accurate as the finger-stick measurements and are prone to measurement noises. This measurement noise is random at each time-point and its highest magnitude is 15% from the capillary glucose level [30].

The controller algorithm runs on a smart phone. The smart phone uses Bluetooth Low Energy (BTLE) to wirelessly receive the CGM data and calculate the basal insulin doses. Then, it sends the insulin dose to the pumps [31]-[32]. In some APs, the CGM requires calibration by a glucose meter, which measures capillary blood glucose [33].

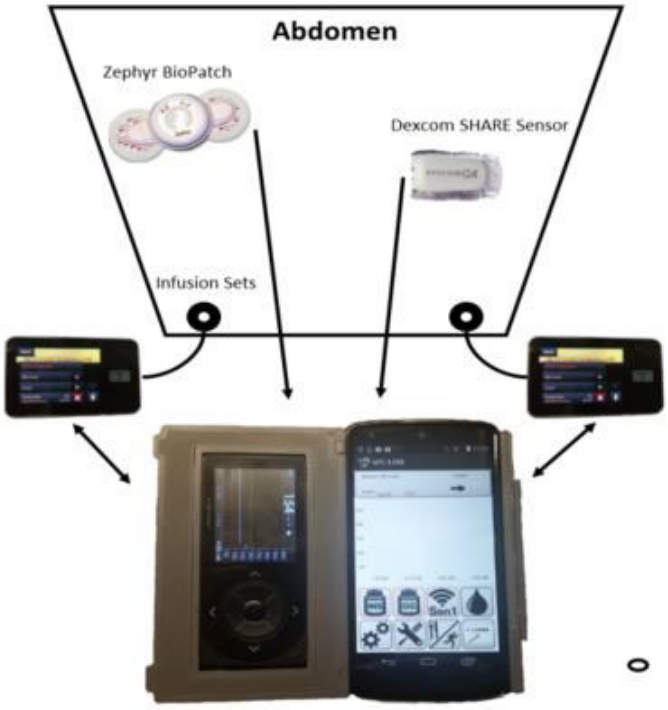

Figure 1.1 Hardware components of the OHSU dual-hormone AP

The accurate functionality of all the components in an AP is important. The control algorithm or controller is a critical component of the AP role maintaining good glucose management. If the controller misestimates basal rates, frequent hypo- and hyperglycemic episodes will occur.

The general schematic of a control system is depicted in Figure 1.2. It consists of three components. The plant is the controllable system. In diabetes glucose management control system, the plant is either the patient's body or a virtual patient during in-silico simulations. In this dissertation, all the results and methods were

evaluated during in-silico simulations using the virtual patient population. The second component of a control system is the controller that considers the error between the control target level and the processed output received from the feedback component.

In diabetes glucose management control systems, the output of the plant is glucose level and the output of the controller (or input to the plant) is insulin and optionally glucagon for dual-hormone control systems. The feedback component processes the output before it is used in the controller. In some studies, the feedback component is a low-pass filter for de-noising the output. Subcutaneous glucose measurements include noise and so filtering is oftentimes required prior to use within a controller.

There are three popular controllers that have been designed for AP systems: model predictive control (MPC), proportional integral derivative (PID) controller and fuzzy logic controllers.

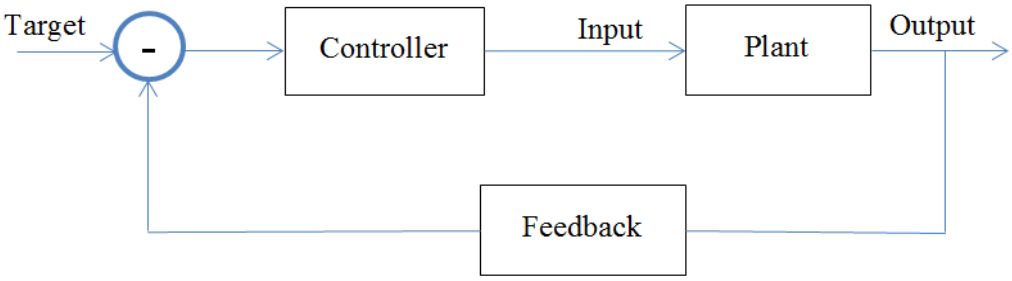

Figure 1.2 General schematic of control systems

1.4 MPC-based APs

Model Predictive Control uses a mathematical model to predict glucose levels over a prediction horizon and then calculates the optimum basal insulin/glucagon rates over the control horizon by minimizing the error between the projected target trajectory and the predicted values. This mathematical model (known as glucoregulatory model) describes the relationship between carbohydrate consumption, insulin, glucagon and glucose. Models that are more accurate can yield better glucose control. Single- and dual-hormone MPCs can be designed and are presented below.

1.4.1 Single-Hormone MPC

The first use of an MPC within an AP system was published by Parker et al. [34] in 1999. They used a linearized nineteenth-order mathematical model within the controller. In the first implementation of the MPC (standard MPC), they used a step-response function for relating insulin to glucose. The coefficients of the function were determined by an identified impulse response of the model [34]. In the second implementation, they used state-space representation of the mathematical model (MPC/SE). The control horizon was set to 10 minutes for both implementations. The prediction horizon was 40 and 50 minutes for the standard MPC and the MPC/SE, respectively. They compared the performance of these two implementations with a 50-gram oral glucose tolerance test in one diabetic patient. Their finding showed that

MPC/SE had a tighter glucose control along with a higher time spent in euglycemia compared to the standard MPC [34].

In the year 2000, Kan et al. [35] compared the performance of a single-hormone MPC with a Proportional Derivative (PD) controller on 11 diabetic dogs. They used a STG-22 glucose sensor to monitor venous blood glucose levels. The sampling interval of the glucose sensor was 10 seconds. And, the controller calculated the intravenously injected basal insulin rate every 2 minutes [35]. When glucose fell below a target level (100 mg/dl), an intravenous glucose was injected to prevent hypoglycemia. In their MPC controller, the control and the prediction horizons were set to 10 seconds and 15 minutes, respectively. They found that the mean insulin infusion rate was significantly lower with the MPC compared to the PD.

In 2004, Hovorka et al. [36] designed a non-linear MPC algorithm. They used eight differential equations to represent the MPC's model and defined a 4-hour prediction horizon. They tested the MPC algorithm across 10 subjects with T1D for 8-10 hours during nighttime where no meals were given. The sampling interval for measuring glucose concentration and delivering insulin was 15 minutes. They found no overnight hypoglycemic episodes.

The following studies from the same research group utilized this MPC algorithm for glucose control. Hovorka et al. [37] examined the feasibility of their MPC controller

across 19 young people with T1D. They designed three randomized therapies starting form CSII therapy over all studies and then switched to three different closed-loop (CL) therapies. At one CL study (Arm_1), glucose levels were controlled overnight (from 20:00 to 8:00). At the other CL study (Arm_2), glucose levels were controlled when subjects had both slowly-and rapidly- absorbed large meals. At the last CL study (Arm_03), subjects had a 45-gram meal at 16:00 followed by a 45-minute aerobic exercise bout on a treadmill with 55% PVO_{2max} at 18:00. Glucose levels were controlled by the CSII therapy, and CL system from 20:00 to 8:00.

Although there was no significant difference between the performances of the above arms, overnight time spent in hypoglycemia was significantly less with the CL systems compared to the CSII therapy. Elleri et al. [38] assessed the effect of low glucose suspend during overnight closed-loop control across seven young subjects with T1D. Insulin delivery was suspended if either glucose levels fell less than a low glucose threshold or predicted glucose levels were less than a hypoglycemia threshold or the rate of the glucose drop was rapid [38]. Insulin delivery was suspended 3 hours on average across subjects. In addition, plasma glucose levels increased at 0.01 mmol/L/min for 105 minutes after the suspension.

Kumareswaran et al. [39] examined the efficacy of overnight CL control across 17 adolescents and 24 adults with T1D. Each group underwent CL control or CSII therapy resulting in four randomized crossover studies. The adolescents had an evening meal followed by a 40-minutes moderate aerobic exercise. Adults had either 60-grams or 100-gram of carbs followed by a glass of white wine. They found that the average time in euglycemia increased significantly across both groups with the CL control compared to the CSII therapy. The CL control reduced average time spent in hypoglycemia across both groups.

Elleri et al. [40] investigated the effect of CL initiation time on glucose regulation across eight children with T1D in an overnight study. Subjects had a meal in the evening followed by a snack three hours afterwards. The closed loop control started on two occasions (18:00 or 21:00). They found similar results between these two CL control strategies. Finally, Hovorka et al. [41] evaluated the feasibility and efficacy of the MPC-based CL control in an overnight study across 16 adolescents with T1D. Glucose levels were controlled through SAP therapy during daytime whereas either CL control or SAP therapy were used during nighttime from 23:00 to 7:00. They found that mean glucose level and time spent in euglycemia were improved significantly with the CL control.

Later, in 2007, Magni et al. [42] designed two MPC algorithms (one non-linear and one linear) by using a more complex MPC's model defined by differential equations. They tested their MPC algorithms versus a PID controller during in-silico simulations. The prediction horizon for both MPC algorithms was 4 hours. They found that the non-linear MPC algorithm outperformed the linear one, and hence, did not provide the results of the linear MPC in their paper. Generally, the non-linear MPC performed more appropriately in term of smaller maximum postprandial glucose peaks and smaller minimum glucose level during the nighttime, compared to the PID controller.

Then, in 2009, Magni et al. [43] designed another MPC algorithm with a different model structure. They used the autoregressive with exogenous input (ARX) model to represent the MPC's model. In addition, they individualized their algorithm by tuning one parameter to determine the aggressiveness of glucose regulation based on a run-2-run control. In the run-2-run control, the performance of the controller was analyzed on any given day in order to modify the parameters of the controller for the following day. Their MPC algorithm was tested with a 100 virtual patient population generated in the University of Padova's (UVa).

They found that the majority of the postprandial glucose peaks across the virtual patients were below 180 mg/dl. In another study by Magni et al. [44], the non-linear

MPC defined by the differential equations was compared to the enhanced linear MPC. In the enhanced linear MPC, the model was determined by AR-modeling of the full model defined by the differential equations. Likewise, they found that the non-linear MPC outperformed the enhanced linear MPC, and time spent in hyperglycemia was fewer with the non-linear MPC. For both MPC algorithms, time spent in hypoglycemia was zero.

Later, in 2014, Del Favero et al. [45] were the pioneers for evaluating their developed model predictive control algorithm. They tested their algorithm across six people with T1D. Each subject underwent a 42-hr study and their glucose levels were controlled by SAP in the first 14-hr of the study (at the first night) and by the AP in the remaining 28hr of the study. Results showed a significant improvement for time in euglycemia with the AP compared to the SAP during nighttime. In addition, overnight hypoglycemia significantly reduced to 0% with AP compared to 8.2% with the SAP.

In 2010, Grosman et al. [46] designed a Zone model predictive control (Zone-MPC) algorithm. The Zone-MPC was created based on an ARX model. And it was developed to maintain the coefficient of variation of the glucose ($CV = \frac{\sigma}{\mu}$, σ: standard deviation, μ: mean) within acceptable boundaries. In the zone-MPC, at each control-time interval (i.e. 5 minutes), predicted glucose levels and the CV for three

regions were computed. The regions included the samples below the lower boundary, between lower and upper boundary and above the upper boundary. CV values were used to adjust the cost function to obtain more appropriate insulin doses by reducing the number of predicted samples outside of the desired boundary.

Grosman et al. [46] compared the performance of the Zone-MPC with the conventional open-loop therapy during in-silico simulations across 10 UVa virtual patients. They also investigated the performance of the Zone-MPC with announced and unannounced meals. When a meal was announced to the controller, the controller delivered the bolus insulin. They found that Zone-MPC outperformed the open-loop therapy during the both meal strategies. In addition, when meals were announced, time spent in euglycemia substantially increased whereas, time spent in hypoglycemia worsened.

In another study by the same research group, Forlenza et al. [47] used the zone-MPC across 19 adults with T1D and compared its performance with the SAP therapy. They found that the time spent in euglycemia and hypoglycemia significantly improved with the CL therapy during both overnight and all-day periods. Dassau et al. [48] evaluated their developed MPC algorithm, designed by Parker et al. [34] in 1999, across 17 subjects with T1D. In addition, they investigated the effect of various glucose levels at the start of the CL control (84 to 251 mg/dl). In this

scenario, a small-unannounced meal was given to all subjects. They found that the low and high glucose indices (LBGI and HBGI) were 0.34 and 0.51 respectively; and the time spent in euglycemia was 70%.

Boiroux et al. [4] designed an individualized MPC algorithm using a less complex model and tested it against a more complex plant. They used a priori information of the patient such as basal insulin, insulin sensitivity factor and insulin action time to create a personalized model. They used eight differential equations reported in Hovorka et al. [36]. And, they proposed a second order approximation of the Hovorka's model by using an autoregressive moving average model with exogenous input (ARIMAX). This was done to maintain a less complex model in the MPC algorithm.

The AR and the MA components were related to glucose and insulin levels respectively, and the exogenous input was referred to sensor noise and artifacts. The order of the AR, the MA and the sensor noise were 2, 2 and 3 respectively. The prediction and the control horizon in this study were set to 10 hours. They created 100 virtual patients for the in-silico simulations. They also changed the insulin sensitivity factor of the controller by ±30% at the midnight to move the system towards more extreme conditions. During the overnight simulations, they found no hypoglycemic episodes by reducing the insulin sensitivity factor. However, time

spent in hyperglycemia significantly increased. In addition, they tested their developed controller across 1 subject with T1D and found few hypoglycemic episodes.

In this dissertation in chapter 5, I show how my work has extended the above work in that I have developed [49] evaluated the feasibility of a new exercise-enabled single-hormone MPC algorithm during in-silico simulations. In this work, I varied the complexity of the MPC's model and tested the different complexity models against a more complex plant. I combined simpler insulin kinetics, insulin dynamics and glucose kinetics models to create simpler glucoregulatory models for the MPC's model. I proposed four different models and tested them across 163 virtual patients. The glucoregulatory model used as the plant was derived from Hovorka et al. [36]. I found that the rising and settling time decreases with more complex MPC models. In addition, time spent in euglycemia and hyperglycemia was improved with models that were more complex. I also simulated the effect of 45-minutes aerobic exercise by integrating an exercise model into the MPC model and I found that the time spent in hypoglycemia was reduced by approximately 40 min by including this model.

1.4.2 Dual-Hormone MPC

Batora et al. [50] designed a switchable model predictive controller. They modeled insulin and glucagon responses reported by Hovorka et al. [36] and Herrero et al.

[51] with two separate ARMAX models, similar to the study done by Boiroux et al. [4] with the insulin-only model. Then, they designed the dual-hormone MPC with two separate single-hormone MPCs. For glucose levels above 90 mg/dl the insulin-only MPC was controlling glucose levels. When glucose dropped below 90 mg/dl, the glucagon-only MPC was activated. They compared the performance of this dual-hormone MPC with another dual-hormone controller where insulin and glucagon were computed using the insulin-only MPC and a glucagon-only PD controller, respectively. They used 3 subjects with T1D and found that time spent in hypoglycemia and euglycemia worsened with the dual-hormone MPC. However, the glucagon dosages were substantially smaller.

In this dissertation in chapter 4, I describe how we [52] evaluated the performance of our single-hormone and dual-hormone MPC algorithms across virtual patients. In the dual-hormone controller, unlike the prior dual-hormone MPC designs, glucagon and insulin could be delivered simultaneously. We also incorporated the effect of exercise into the controller and found that time spent in hypoglycemia reduced significantly with the dual-hormone MPC compared to the single-hormone MPC. In addition, we found that adding the model of exercise into the MPC could prevent exercise-induced hypoglycemia substantially.

1.4.3 Summary of MPC-based APs

Parker et al. [34], in 1999, published the first SH-MPC for AP using a nineteenth-order mathematical model, and he linearized the nonlinearities in the model.

Kan et al. [35], in 2000, designed a SH-MPC for intravenous insulin injection.

Hovorka et al. [36], in 2004, designed a non-linear SH-MPC with sampling intervals of 15 minutes using eight differential equations. They have been testing the controller only during overnight trials.

Magni et al. [42], in 2007, designed a non-linear and a linear SH-MPC using a thirteen-order mathematical model. He found that nonlinear SH-MPC outperformed the linear SH-MPC without publishing the results of the latter. He, later in 2009, developed another MPC by using an autoregressive model [43].

Grosman et al. [46], in 2010, designed a Zone MPC using an autoregressive model which was followed by Boiroux et al. [4] in 2012.

In this dissertation, I have developed a SH-MPC [49] that is:

- Designed with a less complex model – specifically, a fifth-order mathematical model.
- Linearized and updated at each time point based on the latest states of the mathematical model.

- Compatible for subcutaneous insulin delivery since the mathematical models are designed for subcutaneously injected insulin.
- Designed based on the mathematical models defined by differential equations rather than autoregressive models. This approach enables us to interpret the parameters of the model more appropriately.

Batora et al. [50], in 2014, designed a switching DH-MPC which functioned like two separate SH-MPC designs. They used an autoregressive moving average model to model the relationship between glucose levels, insulin and glucagon. When glucose levels were above 90 mg/dl, insulin-only SH-MPC was controlling the glucose levels. When they fell below 90 mg/dl, glucagon-only SH-MPC governed the system. In this dissertation, I designed a DH-MPC where glucagon and insulin could manage glucose levels simultaneously [52].

1.5 PID-based APs

Proportional Integral Derivative (PID) controllers calculate insulin and optionally glucagon rates based on the current and past glucose measurements. A PID consists of three components: proportional, derivative and integral components. The proportional component takes the deviation of the current glucose level from the target glucose level (also known as the control error function) into consideration. The derivative component takes the rate of change of the error function into account, and

the integral component considers the area under the error curve resulting from the deviation of the prior data relative to the target value. In the PID controllers, the derivative component decreases overshoots, increases steady-state oscillations and decreases rising time. On the other hand, the integral component reduces the steady-state error, decreases rising time and increases overshoot. As a result, the integral component of the PID controller may cause an over-delivery of insulin and hypoglycemia may occur [53]. Therefore, some studies preferred to design PD controllers for T1D.

1.5.1 Single-Hormone PID

Shimoda et al. [54] investigated the effect of 3 different insulin delivery methods: intravenous regular insulin (IV insulin), subcutaneously injected regular insulin and insulin Lispro. A PD controller was used for insulin delivery across all methods. They found that the performance of the system with the insulin Lispro was similar to the IV insulin. In addition, they found that the postprandial hypoglycemia was less with the insulin Lispro compared to the regular insulin [53], [54].

Matsuo et al. [55] designed a closed-loop PD controller and investigated the effect of injecting Lispro insulin subcutaneously and intraperitoneally on 10 diabetic dogs. They gave an oral glucose tablet of 2 grams/kg to the dogs and observed the postprandial glucose excursions. They found that glucose levels were controlled

more appropriately by injecting insulin intraperitoneally, where no hypoglycemic episodes were observed.

O'Grady et al. [56] designed a PID controller-based Closed Loop (CL) system and tested it across eight subjects with T1D for 16 overnight trials (from 21:00 to 7:00). The performance of the CL controller was also compared with the SAP therapy. They found that the time spent in euglycemia and hypoglycemia improved significantly with the CL system compared to the SAP therapy. Steil et al. [57] examined the feasibility of a PID-based CL controller compared to a SAP therapy across 10 subjects with T1D. In the PID controller, the proportional and derivative components were defined similarly to the other PD components in the literature; whereas, the integral component only took the current and the latest glucose level into consideration. No difference was found between the two therapies in terms of the mean glucose level and the hypoglycemic episodes, while time spent in euglycemia was significantly higher with CL therapy.

In another study by this group, Weinzimer et al. [58] compared the performance of the above PID controller (called fully closed-loop: FCL), developed by Steil et al. [57], with a modified version. In the modified version (called Hybrid closed-loop: HCL), 25-50% of the meal bolus insulin was given 15 minutes in advance of each meal. They examined the FCL and the HCL across 17 pediatric subjects with T1D.

They found that the mean glucose level during night- and daytimes was insignificantly less with the HCL. However, daytime mean glucose level was significantly smaller with the HCL. They also found no significant difference between the FCL and the HCL during overnight control.

Van Bon et al. [59] investigated the feasibility of a 48-hr dual-hormone closed-loop therapy versus a 48-hr SAP therapy across 11 people with T1D. They used a PD controller. Insulin delivery was personalized relative to the insulin sensitivity factor of the subjects. Insulin sensitivity factor was reduced and raised if changes of postprandial glucose levels exceeded 5 mmol/L (90 mg/dl) or fell below 3.5 mmol/L (63 mg/dl), respectively [59]. Small amount of glucagon (less than 1 mg to treat severe hypoglycemia) was administered if glucose was less than 6.5 mmol/L (117 mg/dl). Time spent in euglycemia and hyperglycemia was similar between the two therapies however, time spent in hypoglycemia was improved at the second day of the experiment with the CL therapy.

1.5.2 Dual-Hormone PID

Castle et al. [60] compared the performance of a dual-hormone CL control with a CSII therapy. They also examined the effect of delivering high-glucagon versus low-glucagon dosages. Seven subjects received the high glucagon dosages and six subjects received the low glucagon dosages, both under the CL trial. The dual-

hormone controller, designed by Gopakumaran et al. [61], consisted of a PD controller to calculate insulin and glucagon delivery rates. Insulin was given if both proportional and derivative errors were positive. And glucagon dosages were called if they were negative.

For calculating more accurate insulin and glucagon rates in the controller, fading memory of past glucose levels were used such that most recent glucose levels had more influence to change the delivery rates. Castle et al. [60] named the controller as fading memory proportional derivative (FMPD) controller. They found that the time spent in hypoglycemia significantly reduced with the CL trial compared to the CSII therapy. However, this reduction was not significant between the CSII and the CL trial with the low glucagon dosages approach.

Jacobs et al. [22] designed an improved version of the FMPD controller. In the controller, glucagon was delivered relative to the proportional and derivative errors, independent of their signs. For better glucose management, the controller filtered insulin and glucagon delivery rates through a few decision tree algorithms to prevent hypoglycemia and hyperglycemia. In addition, the improved FMPD controller consisted of validated strategies for managing meals and safety mechanism. It also adjusted nighttime target glucose differently to prevent overnight hypo and hyperglycemia.

Jacobs et al. [22] evaluated the controller across eight subjects with T1D in an inpatient trial using the Dexcom 7+ CGM sensor. They found that the average time spent in euglycemia was 73.1% along with 5 hypoglycemic episodes. In another study by Jacobs et al. [22], glucose levels of 5 subjects with T1D were managed using another CGM sensor (Dexcom G4) and no hypoglycemia was observed.

1.5.3 Mixed PID and MPC Controllers

El-Khatib et al. [62] examined the efficacy of a dual-hormone AP across 4 diabetic pigs. They conducted 11 experiments on the pigs. Insulin and glucagon infusion rates were computed by a MPC and a PD controller, respectively [33], [62]. They found no hypoglycemic episodes. Moreover, the average percent of time spent in euglycemia was 74%. Later, Haidar et al. [63] evaluated the dual-hormone AP across 15 adults with T1D in a randomized crossover study. Each subject underwent either a CL control or a CSII therapy at each trial. Each trial lasted for 15 hours including a 30-minutes aerobic exercise bout at 60% PVO_{2max} followed by a medium-sized meal (60 g for females and 80 g for males). They found that the percent time spent in euglycemia improved significantly with CL control, and only one subject had hypoglycemic episodes compared to eight subjects with the CSII therapy.

Haidar et al. [19] compared the performance of the dual-hormone AP with the single hormone AP and the SAP therapy. Each study lasted 24 hours and was selected

randomly by the subjects. In the single-hormone AP, inulin was delivered based on a predictive dosing algorithm. In the dual-hormone AP, glucagon was delivered relative to glucose concentration and the rate of glucose changes. In the SAP therapy, insulin was pre-programmed and delivered based on the prior glucose profile of each subject. They found no significant difference across the dual and single hormone APs, while both APs significantly outperformed the SAP therapy. In addition, the number of hypoglycemic episodes was significantly lower with the APs compared to the SAP.

1.5.4 Summary of the PID-based APs

Single-hormone PID controllers have been designed since 1997 by Shimoda (1997), Matsuo (2003), Steil (2006), Weinzimer (2008), O'Grady (2012), and Van Bon (2014) [54-59]. Gopakumaran et al. [61], in 2005, designed the first dual-hormone PD controller. Jacobs et al. [22], in 2014, designed a more advanced dual-hormone PD controller. It, known as Fading Memory Proportional Derivative controller, has been widely used since 2004 [28, 64, 65].

However, despite their acceptable performance, PD (in general, PID) controllers are unable to account for the inherent delayed kinetics of subcutaneous insulin delivery and the action of insulin in plasma [66], which may cause hypoglycemic episodes. In addition, they do not take the kinetics of insulin into account. Therefore, I have used

MPC in this dissertation, which includes information about the subcutaneously infused insulin. I hypothesize that MPC will improve time in target range and reduce hypoglycemic episodes compared with PID controllers.

1.6 Fuzzy-logic based AP

Fuzzy logic is another controlling concept that changes the pattern of the manipulated input (insulin) from a "crisp" pattern to a "fuzzy" pattern. In other words, fuzzy logic provides a smoother relationship between the output and the input of a system. The fuzzy logic controller can be used in an artificial pancreas. Mauseth et al. [67] developed the first fuzzy logic controller for AP.

In this study, glucose levels and their rates were fuzzified to determine the insulin rates. Glucose level (GL) was fuzzified into five categories: very high (250 < GL mg/dl), high (180 < GL < 250 mg/dl), medium (120 < GL < 180 mg/dl), low (80 < GL < 120 mg/dl) and very low (GL < 80 mg/dl). The glucose rate (GR) was fuzzified into five categories: very negative (GR < -2.5 mg/dl/min), negative (-2.5 < GR < -1.25 mg/dl/min), zero (-1.25 < GR < 1.25 mg/dl/min), positive (1.25 < GR < 2.5 mg/dl/min) and very positive (2.5 < GR mg/dl/min). Then, two fuzzy inputs (between 0 and 1), based on the actual values of GL and GR, were determined.

A ruler 2-dimensional matrix, based on the Mamdani's fuzzy logic inference rules, was created to map the fuzzy inputs to a range of possible fuzzy outputs; then, the final value (e.g. Insulin infusion rate) was determined by aggregating the fuzzy outputs [68]. Mauseth et al. [67] examined the algorithm across four subjects who received either one high (1 gram/kg) or one small (30 grams) carbohydrate intake. Ten and two postprandial hypoglycemic episodes were observed with the high and low carb intake, respectively, compared to zero hypoglycemic episodes during the fasting condition.

In another study by Mauseth et al [69], the above fuzzy controller was tested during a 24-hour trial across 7 subjects with T1D. Subjects were given a 30 gram carbs followed by a 60 gram carbs for breakfast and lunch. They found that the average glucose level was 165 mg/dl, and the average time spent in euglycemia was 76%.

1.7 Challenges of Diabetes

Insulin therapy methods can typically regulate blood glucose properly when there are no interventions. The interventions are meals, exercise and stress [70], [71]. Meals and stress increase glucose levels, leading to postprandial hyperglycemia [70]. High glucose levels induced from meals are compensated with bolus insulin. However, over-delivery of the bolus insulin may lead to postprandial hypoglycemia. On the

other hand, exercising can instigate serious challenges for diabetes because it increases sensitivity of cells to insulin and enhances glucose utilization [72], [73].

If the effect of exercise is overlooked, hypoglycemia may occur and people with T1D may fall into a state of coma. The effect of exercise lasts from several minutes to several hours (up to 12 hours [74]) and may cause hypoglycemia, even when glucose level is high at the start of the exercise [20]. Figure 1.3 shows the effect of exercise and meals on glucose profiles obtained from 21 people with T1D in an inpatient closed-loop study done by our lab (Permission to reproduce this figure has been granted by John Wiley and Sons and Copyright Clearance Center) [20].

In this study, a moderate-intensity exercise bout was started at the beginning of the experiment following breakfast; and lunch was given approximately 6 hours afterwards. Two randomized AP algorithms, APX and APN, were used to control the glucose levels. APX was aware of the exercise while APN was not. Glucose levels dropped below 70 mg/dl (≈ 4 mmol/l) for a few patients after and during the exercise bout. Moreover, postprandial hypoglycemia was observed during the first 4 hours following lunchtime, demonstrating the over delivery of pre-meal bolus and postprandial basal insulin. However, more post-exercise hypoglycemic episodes were observed with APN compared to APX.

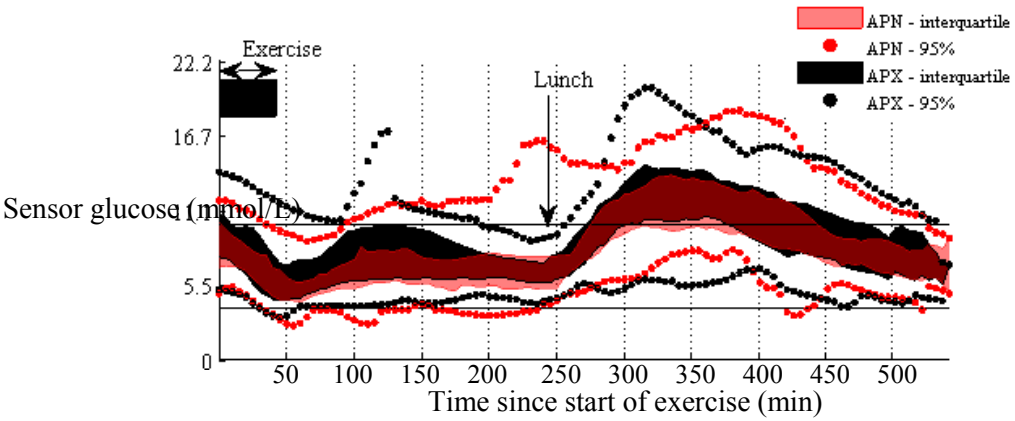

Figure 1.3 Glucose profiles showing the effect of exercise and meals

1.7.1 Meals

Meals are the major source of disturbance for people with T1D. Eating a meal increases glucose levels leading to hyperglycemia. To prevent hyperglycemia, a pre-meal insulin bolus proportional to the amount of carbohydrate is injected. However, an insulin bolus cannot rapidly reduce glucose due to the inherent delay between the subcutaneous insulin delivery and the action of insulin in plasma. Over delivery of insulin can expedite the glucose drop and may cause postprandial hypoglycemia.. Additional factors such as meal composition, alcohol consumption and abnormalities in gastric emptying may aggravate meals-induced hyperglycemia.

Elleri et al. [75] investigated the effect of glycemic load (GL) of meals on glucose levels under the MDI therapy across people with T1D. Eight subjects consumed a low-glycemic-load meal (macaroni cheese) and eight subjects consumed a high-glycaemic-load meal (vegetable shepherd's pie). The amount of carbohydrate for

both meal types was 121 grams; however, the ratio of protein to fat differed for each of the two meal types. At each gram of meal, the ratio of protein to fat for low- and high-GL meals was 20/9 and 35/31, respectively. Elleri et al. [75] found that the rate of glucose appearance was significantly faster with high-GL meals.

In another study by this group, Hovorka et al. [76] investigated the effect of meal size across 24 adults with T1D under either a CL therapy or the CSII therapy. Twelve of the subjects underwent the "eating-in" scenario where they consumed a medium-size evening meal (60 gram of carbs). The other 12 subjects underwent the "eating-out" scenario where they consumed a large evening meal (100 gram of carbs) followed by a glass of white wine. They found that time spent in hyperglycemia was significantly lower with the eating-in scenario compared to the eating-out scenario, across both the CSII and CL therapy methods. Time spent in euglycemia and hypoglycemia significantly improved in both meal scenarios with the CL therapy.

Woerle et al. [77] examined the effect of the gastric emptying rate on postprandial glucose excursions across people without diabetes. Fourteen subjects consumed a mixed meal followed by a 30 μg of Pramlintide (PRAM) or placebo (PBO). Pramlintide is an anti-diabetic medication used to slower the gastric emptying rate. They found that plasma insulin and postprandial glucose excursions were lower with

pramlintide compared to placebo. In another similar study, Weinzimer et al. [78] examined the effect of injecting pramlintide on glucose control across 8 people with T1D. The control algorithm used in their study was a PID controller designed in Weinzimer et al. [58]. In the control group, no pramlintide was given while in the treatment group, 30 μg of pramlintide was given prior to each meal. They found that the average time to peak after meals increased from 1.5 hour to 2.5 hour with Pramlintide. In addition, the magnitude of the glycemic excursion reduced significantly with Pramlintide.

1.7.2 Exercise

Exercising is another major challenge for people with T1D. It decreases the amount of glucose in blood stream by enhancing glucose utilization. It is generally recommended for people with T1D to exercise 2-3 times per week to have their high glucose levels reduced [79]-[80]. Manohar et al. [81] recruited 12 people with and 12 people without diabetes to investigate the effect of post-meal walking. They divided each day into two parts. During the first part, one meal followed by no physical activity was given, and in the other part, two meals followed by a 30-minute walk at a speed of 1.9 mph were given. The Dexcom SevenPlus sensor and triaxial accelerometer were used to record the CGM and physical activity data, respectively. In both groups, time spent in hyperglycemia and postprandial area under the curve

were reduced; however, this reduction was more significant across people with diabetes [81].

The effect of exercising on glucose levels occurs instantly, lasts for several hours, and may cause nocturnal hypoglycemia [82], [83]. Maran et al. [82] investigated the effect of different types of exercise on glucose control. Eight people with T1D interchangeably underwent a 30-minute of either high-intensity intermittent exercise or moderate-intensity exercise. They found that the mean glucose levels during nighttime were significantly lower with the high-intensity intermittent exercise. And, the number of hypoglycemic episodes was higher with high-intensity intermittent exercise for the entire trial.

Iscoe et al. [83] investigated the effect of two types of exercise across eleven athletes with T1D. Subjects underwent 45 minutes of continuous moderate-intensity exercise (CON) and continuous moderate-intensity exercise + intermittent high-intensity exercise (CON+IHE). During the CON, three subjects and during the CON+IHE, seven subjects experienced hypoglycemia. During nighttime, the mean glucose was significantly lower with the CON compared to the CON+IHE. Reddy et al. [65] investigated the effect of late-afternoon exercise on sleep and nocturnal hypoglycemia across 10 adults with T1D. Subjects underwent two 45-minute bouts of either aerobic or resistance exercise per week and the glucose levels were

compared with the events with no exercise. Sleep loss was significantly less with the aerobic exercise while it did not change significantly with the resistance exercise. Severe hypoglycemia (glucose < 54 mg/dl) occurred eight times with the aerobic and three times with the resistance exercise.

Exercise also affects the duration and severity of post-exercise hypoglycemia. Yardley et al. [84] examined the impact of resistance vs. aerobic exercise on 12 subjects with T1D. Subjects underwent 45 minutes of resistance exercise consisting of three sets of eight repetitions, and 45 minutes of aerobic exercise consisting of running on a treadmill at 60% of VO_{2max}. Plasma glucose decreased significantly during both resistance and aerobic exercise, and mean glucose level was significantly lower from 4.5 to 6 hours after the resistance exercise. This demonstrated that the resistance exercise caused prolonged reduction of glucose levels in comparison to the aerobic exercise.

The order of exercise also affects the glycemic control in people with T1D. In another study by Yardley et al. [85], 12 people with T1D were recruited to perform either 45 minutes of aerobic exercise followed by a 45 minute of resistance exercise (called AR) or vice versa (called RA). They found no significant difference in the frequency of post-exercise hypoglycemic episodes; however, the duration of hypoglycemia was greater after RA compared with AR. Despite the above studies

showing the impact of different exercise intensities and types, Tonoli et al. [86] conducted a meta-analysis to determine the effect of exercise on acute and chronic glycemic control across people with T1D. They found that HbA1c was only improved by regular aerobic exercise. In addition, time spent in hypoglycemia was minimized with the aerobic exercise incorporated with short bouts of high-intensity intermittent exercise. In general, ADA does not have a comprehensive guideline for exercise across T1D. However, it suggests that people with T1D consume a snack if their pre-exercise glucose level is less than 100 mg/dl [79].

As mentioned earlier, exercise can instigate serious complications for T1D. Selecting the most appropriate insulin therapy method (MDI, CSII, and AP) and providing systematic approaches to prevent exercise-induced complications have been the attention of different studies. Yardley et al. [87] examined the effect of exercise on glycemic control governed by MDI and CSII therapies. Nine subjects were recruited for the MDI and ten subjects were recruited for the CSII therapy. Both groups underwent 45 minutes of aerobic exercise (either cycling or running) at 60% of VO_{2max}. To prevent exercise-induced hypoglycemia, fast-acting glucose tablets were given to five out of nine MDI subjects and three out of 10 CSII subjects. Results showed that post-exercise time spent in hyperglycemia was more significantly reduced with the CSII therapy than the MDI therapy, while no significant difference

for the glucose drop and time spent in hypoglycemia was observed during the exercise periods.

Elleri et al. [88] investigated the efficacy of AP and CSII on glucose control during meals and unannounced exercise and sleep across 12 adolescents with T1D. Subjects underwent moderate-intensity exercise for 40 minutes in the morning and 20 minutes in the afternoon. Elleri et al. [88] found better glycemic control with the AP. Time spent in euglycemia and hyperglycemia was significantly higher during night-time and day-time without effecting the time spent in hypoglycemia. In another similar study, Breton et al. [89] investigated the effect of exercise on glucose levels controlled by either CSII or AP across 11 adolescents and 27 adults with T1D. Subjects underwent a 30-minute moderate-intensity exercise at 50% VO_{2max} followed by a dinner 2.5 hours afterwards. They found significant improvement for time in euglycemia and hypoglycemia with the AP during day- and nighttime.

Russell et al. [90] tested a dual-hormone AP with high-carb meals and a moderate-intensity exercise bout across 6 subjects with T1D. The testing scenario, which lasted 51 hours for each subject, consisted of six meals (mean ± std = 78 ± 12 grams) and a 30-minute exercise on a stationary bicycle at a target heart rate of 120-140 bpm. A model predictive controller and a customized proportional derivative controller were used to calculate insulin and glucagon delivery rates, respectively. They found that

the average time in hypoglycemia and euglycemia were 0.6% and 69%, respectively. In another study by Russel et al. [91], the effectiveness of a randomized 5-day outpatient study controlled by either a dual-hormone artificial pancreas or SAP therapy across 20 adults and 32 adolescents was examined. Time in hypoglycemia, hyperglycemia and euglycemia across the adults were significantly improved with the CL therapy compared to the SAP therapy. Time in euglycemia and hyperglycemia were only improved across the adolescents with the dual-hormone CL therapy.

Based on the above studies, selecting the most desirable type of exercise (aerobic vs. anaerobic) is a disputable concept for people with T1D, and it may relate to each patient's physiological behavior. Nevertheless, any type of exercise can still cause hypoglycemia. The following studies have developed algorithms to mitigate exercise-induced hypoglycemia independent of the type of exercise. Jacobs et al. [28], [20] incorporated an exercise detection and grading algorithm for people with T1D. They adjusted insulin and glucagon delivery rates more appropriately during and after exercise. Accelerometry and heart rate data were used to estimate energy expenditure (EE). When EE exceeded 4 kcal/min, exercise was detected and announced to the controller. The controller turned off insulin for 30 minutes and

reduced post-exercise insulin by 50% for 60 minutes. Meanwhile, the amount of glucagon was increased by 2 folds during this 90-minute window.

In addition, the glucose target for delivering glucagon was increased from 95 to 110 mg/dl. This feature increased the safety mechanism of the system by which the glucagon was delivered earlier once glucose dropped below 110 mg/dl. They evaluated the algorithm across 21 subjects with T1D [20] in a randomized crossover study. Eight subjects underwent the SAP therapy. Six subjects underwent the CL control without exercise dosing adjustments (APN). And, nine subjects underwent the CL control with exercise dosing adjustments (APX). They found significantly less time spent in hypoglycemia with APX compared to APN and SAP. However, there were no significant differences between the APN and SAP therapy methods.

In addition to the above algorithms for reducing exercise-induced hypoglycemia, the following studies were done to assess the exercise effects with mathematical models. These assessments can be incorporated with the current treatment plans to provide insights about hypoglycemia during and after exercise. Roy et al. [92] were among the first developers of an exercise model. They incorporated the exercise model into the Bergman's minimal glucoregulatory model [93]. They added the following compartments to the Bergman's minimal model: exercise-induced rate of glycogenolysis, increased rate of glucose uptake and glucose production, and

increased rate of insulin removal from plasma. Each of the added compartments changed with respect to the exercise intensity, PVO_{2max}, which was assumed constant 5 minutes after the start of exercise. In that exercise model, PVO_{2max} changed from 8% (average PVO_{2max} in the basal state) to 92%. However, they only showed the results of mild and moderate exercise bouts. Although the results showed good fits between the actual and the simulated data during mild exercise for subjects without diabetes, they did not fit properly for people with T1D.

Later, Balakrishnan et al. [94] modified the Roy and Parker model among 34 children and adolescents with T1D. They first fitted the Roy and Parker model consisting of 16 free parameters to the clinical dataset of two adolescents and found out that 6 of the parameters were the most sensitive parameters across people with T1D. Then, these 6 parameters were estimated for each of the 34 patients using the actual clinical CGM data. To identify the intensity of the exercise, they used Rate of Perceived Exertion (RPE) method. In the RPE, users reported their feelings about the physical activity and allocated a number to them ranging from 6 (no physical exertion) to 20 (maximally hard exertion) [95]. They linearly scaled the percent of the reported RPE values to PVO_{2max}, which was used to calculate the exercise level and intensity. Exercise intensity was then used to determine the declining rate of

glycogenolysis. Exercise level was used to determine the incremental rate of hepatic glucose production and declining rate of glucose uptake.

In this dissertation, we did not use the exercise models developed by Roy and Balakrishnan. The glucoregulatory model used in my study is more complex than the minimal glucoregulatory model. The exercise model used in this dissertation was developed by Hernandez-Ordonez et al. [73] and was integrated into the more complex glucoregulatory model. Hernandez-Ordonez quantified the incremental effects of exercise on periphery glucose and insulin uptakes and hepatic glucose production using the percent of active muscular mass (PAMM) and percentage of maximum oxygen consumption (PVO_{2max}). They verified the model with experimental data for light and moderate exercise.

1.7.3 Stress

Stress is another source of perturbation for people with T1D. Stress releases two hormones: catecholamine and glucocorticoids. They not only make the body more resistance to insulin but also increase endogenous glucose production, leading to hyperglycemia [70].

1.7.4 Summary

Eating a meal is a major challenge for people with T1D. It increases glucose concentration which leads to high glucose levels and hyperglycemia. To reduce time in hyperglycemia:

Hovorka et al. [76] recommended using closed loop control therapy (i.e. artificial pancreas) along with smaller meal sizes.

Woerle et al. [77] and Weinzimer et al. [78] recommended using a 30 μg of Pramlintide following meals. Pramlintide is an anti-diabetic medication used to slower the gastric emptying rate.

In this dissertation, I incorporated a meal model, developed by Hovorka et al. [36], into the MPC algorithm. The MPC can adjust postprandial basal delivery, accordingly. Our preliminary study showed that time in hyperglycemia was reduced substantially by incorporating the meal model.

Exercising is another major challenge for people with T1D. It increases glucose utilization, which reduces time in hyperglycemia [81]. However, it may also lead to hypoglycemia [82, 83]. To reduce time in hypoglycemia:

- Yardley et al. [87] suggested people with T1D under the MDI therapy to switch to the CSII therapy. He also recommended having fast-acting glucose tablets.

- Maran et al. [82] recommend having moderate-intensity aerobic exercise rather than high intensity intermittent intervals. Similarly, Iscoe et al. [83] recommended having continuous moderate-intensity exercise rather than continuous moderate-intensity exercise followed by an intermittent high-intensity exercise.
- Jacobs et al. [28] proposed an algorithm to modify insulin delivery during and after exercise.
- Balakrishnan et al. [94] used an exercise model to compute glucose drops during exercise. However, the study was only validated across two adolescents with T1D.

In this dissertation, I show in chapters 4 and 5 how we incorporate a better-validated exercise model into the MPC. The MPC automatically adjusts the insulin rates once exercise is announced.

1.8 Thesis Contributions

Meals and exercise are major sources of disturbances for people with T1D and must be handled appropriately by an AP algorithm. In this dissertation, I developed AP algorithms to manage meals and exercise more appropriately for people with T1D. These algorithms were embedded in the MPC algorithms. Moreover, I created a validated virtual population for enabling pre-clinical trial studies in-silico on single-

hormone and dual-hormone control studies. This section outlines my contributions to the field.

Chapter 2: The AP control algorithm should be first evaluated in-silico by using simulators (plants, shown in Figure 1.2), before being used in-vivo. Plants are virtual populations created using glucoregulatory models. Accurate modeling of insulin and glucagon kinetics and dynamics is critical for doing single-hormone and dual-hormone simulation studies. In the field of diabetes, other virtual patient populations have been created, but they did not include good models for glucagon or models for exercise [31]. The goal of this chapter is to present two new open source virtual patient populations (VPP) for T1D that use statistical sampling to create an unlimited number of virtual patients. We present the mathematical model of both the dual-hormone VPP and the single-hormone VPP, and we validate the VPP with clinical data.

Chapter 3: Postprandial hypoglycemia can be observed across many people with T1D, caused by inappropriate insulin delivery. Postprandial hypoglycemia can even be a problem in people using an AP because the controller may not have been designed to handle all physiologies appropriated. The goal of this chapter is to describe an adaptive algorithm that adjusts the postprandial basal and bolus insulin individually, based on the glucose measurements. I present two approaches to

prevent postprandial hypoglycemia using a new Adaptive Learning Postprandial Hypoglycemia-prevention Algorithm (ALPHA), designed to be used in hybrid AP insulin therapy.

Chapter 4: The importance of using dual-hormone AP systems to reduce time in hypoglycemia has been the core part of many dual-hormone AP studies. As there is no published dual-hormone AP with the MPC algorithm, a dual-hormone MPC is developed in this chapter. The goal of this chapter is to introduce a dual-hormone MPC algorithm that can switch between dual hormone and single hormone operation based on the sensed glucose level of the patient. The dual-hormone MPC algorithm also includes a model for exercise, such that if exercise is detected or if a user announces an exercise event to the controller, the algorithm can respond appropriately.

Chapter 5: In this chapter, we evaluate the feasibility of the MPC algorithm for the in-vivo study. In clinical studies, the plant (human body) is always more complex than the MPC's mathematical control model. We investigate less complex MPC's mathematical models against a more complex plant structure. We assess models within the MPC controller that are of lower complexity than the plant and evaluate these models of order 4, 5, and 6 with respect to control and clinical metrics. Lastly,

we consider whether the added complexity of an exercise model within the controller adds benefit, specifically in preventing exercise-induced hypoglycemia.

Chapter 6: Creating personalized, adaptive control algorithms for people with type 1 diabetes is currently an important topic whereby the design and structure of AP systems for each patient are adapted over time to match each patient's physiology. In my MPC design, the insulin sensitivity factor is updated adaptively based on the glucose data from the plant. Insulin sensitivity is the most important parameter in the MPC algorithm that describes the body's response to insulin. The goal of this chapter is to reduce the model-plant mismatch existing in the MPC design via a model identification approach. The MPC's model is fit to the plant's output at each non-meal period and the most sensitive parameter of the model (i.e. insulin sensitivity factor) is updated and used for the following day. We show in this chapter that the time in hyperglycemia can be reduced significantly.

Chapter 7: this chapter summarizes the entire dissertation and explains future directions of the MPC design. We will be talking about how the state-of-the art techniques of integrating exercise and meals should be to receive the optimum performance from the MPC. In addition, we will challenge the MPC's structure toward calculating more accurate insulin deliveries by including the estimates of the future glucose levels for current insulin delivery.

2 A statistical virtual patient population for the glucoregulatory system in type 1 diabetes with integrated exercise model

In this chapter, two open-source virtual patient populations compatible with the characteristics of type 1 diabetes are introduced. The virtual populations are used in-silico to evaluate control algorithms before the clinical studies. The virtual populations are validated with real-world clinical datasets.

Chapter Summary:

- Virtual populations have to be developed to evaluate control algorithms.
- Two virtual populations are created, one for single-hormone AP and one for dual-hormone AP analysis.
- Both populations are validated with real-world scenarios.
- Results show consistency with the real-world data, showing the feasibility of the virtual populations to be used in-silico.

This work was originally published in 2019:

Navid Resalat, Joseph El Youssef, Nichole Tyler, Jessica Castle and Peter G. Jacobs, "A statistical virtual patient population for the glucoregulatory system in type 1 diabetes with integrated exercise model", PLOS ONE, volume 14, Issue 7, e0217301, July 2019 [96],

2.1 Abstract

Purpose: We introduce two validated single (SH) and dual hormone (DH) mathematical models that represent an in-silico virtual patient population (VPP) for type 1 diabetes (T1D). The VPP can be used to evaluate automated insulin and glucagon delivery algorithms, so-called artificial pancreas (AP) algorithms that are currently being used to help people with T1D better manage their glucose levels. We present validation results comparing these virtual patients with true clinical patients undergoing AP control and demonstrate that the virtual patients behave similarly to people with T1D. *Methods*: A single hormone virtual patient population (SH-VPP) was created that is comprised of eight differential equations that describe insulin kinetics, insulin dynamics and carbohydrate absorption. The parameters in this model that represent insulin sensitivity were statistically sampled from a normal distribution to create a population of virtual patients with different levels of insulin sensitivity. A dual hormone virtual patient population (DH-VPP) extended this SH-VPP by incorporating additional equations to represent glucagon kinetics and glucagon dynamics. The DH-VPP is comprised of thirteen differential equations and a parameter representing glucagon sensitivity, which was statistically sampled from a normal distribution to create virtual patients with different levels of glucagon sensitivity. We evaluated the SH-VPP and DH-VPP on a clinical data set of 20

people with T1D who participated in a 3.5-day outpatient AP study. Twenty virtual patients were matched with the 20 clinical patients by total daily insulin requirements and body weight. The identical meals given during the AP study were given to the virtual patients and the identical AP control algorithm that was used to control the glucose of the virtual patients was used on the clinical patients. We compared percent time in target range (70-180 mg/dL), time in hypoglycemia (<70 mg/dL) and time in hyperglycemia (>180 mg/dL) for both the virtual patients and the actual patients. *Results*: The subjects in the SH-VPP performed similarly vs. the actual patients (time in range: 78.1 ± 5.1% vs. 74.3 ± 8.1%, p = 0.11; time in hypoglycemia: 3.4 ± 1.3% vs. 2.8 ± 1.7%, p = 0.23). The subjects in the DH-VPP also performed similarly vs. the actual patients (time in range: 75.6 ± 5.5% vs. 71.9 ± 10.9%, p = 0.13; time in hypoglycemia: 0.9 ± 0.8% vs. 1.3 ± 1%, p = 0.19). While the VPPs tended to over-estimate the time in range relative to actual patients, the difference was not statistically significant. *Conclusions*: We have verified that a SH-VPP and a DH-VPP performed comparably with actual patients undergoing AP control using an identical control algorithm. The SH-VPP and DH-VPP may be used as a simulator for pre-evaluation of T1D control algorithms.

2.2 Introduction

Mathematical models of the glucoregulatory system have been used within in-silico virtual patient simulations for many years [97, 98]. The FDA-approved UVA/Padova simulator, which was developed in 2008 (known as S2008 simulator), was one of the first simulators to model glucose-insulin metabolism. In the S2008 simulator, 100 virtual adults, 100 virtual adolescents, and 100 virtual children were generated by randomly drawing samples from the joint distribution of the parameters of the model [31]. At first, the 100 virtual adults were produced from a given nominal insulin sensitivity value and then the virtual children and adolescents were generated with higher and lower insulin sensitivity values. Since 2008, many studies have used the 2008 version of the UVA/Padova simulator for open loop [97, 99] and AP [100, 101] computer analyses. In 2013, due to hypoglycemia underestimation of the S2008 simulator, three new features were integrated. Dalla Man et al. [31] incorporated the non-linear effect of insulin action for glucose levels below a threshold. In addition, they added the glucagon kinetics and dynamics models to simulate the counter-regulatory behavior of glucagon for glucose levels below a threshold. They also modified the insulin-to-carb ratio as well as the correction factor for better representation of postprandial glucose excursions. The new simulator was named the S2013 simulator. Visentin et al. [102] validated the S2013 simulator with a database consisting of two sets of 24 glucose profiles recorded during one open loop study and one AP study across type 1 diabetes. Each glucose profile was controlled for 22

hours with two meal intakes. In both control trials, the variations of the meal intakes were negligible at each meal event across the patients. To validate the S2013 simulator, actual insulin profiles were given to the 100 virtual adults and the closest virtual adults were selected whose clinical outcomes were similar to the patients. Finally, the performance of the selected virtual adults were compared with the patients in terms of percent time spent in hyper- and hypoglycemia along with low and high blood glucose indices. They found better clinical consistency with the S2013, however unlike the S2008 simulator, the S2013 simulator overestimated the percent time spent in hypoglycemia significantly [102]. Later in 2016, to validate the S2013 simulator across type 1 diabetes and to better model time spent in hypoglycemia, Visentin et al. [103] fit the simulator to the actual dataset recorded from 47 people with T1D using a Bayesian approach. They found that the insulin sensitivity was around 30% less than the nominal values, showing that the insulin sensitivity of the S2013 simulator should be further modified to represent people with type 1 diabetes. While the S2013 simulator has been used by various research institutions to validate AP algorithms prior to running clinical studies, it is no longer commercially available and there is a need in the field for alternative VPPs to validate AP control algorithms. The Cambridge single-hormone simulator is another simulator developed for type 1 diabetes, which consists of 18 virtual patients [104]. The simulator was validated with a clinical dataset during overnight periods. In

2013, Haidar et al. [105] used the Cambridge simulator and developed a single-hormone virtual patient population by fitting the glucoregulatory model to glucose data of 12 young people with type 1 diabetes using a Markov chain Monte Carlo sampling method. In this paper, the glucoregulatory model used is similar to the Cambridge glucoregulatory model, except the insulin kinetics model is different. Our preliminary testing on the virtual populations showed that the insulin kinetics model published in Hovorka et al. [36] better reflects the physiological characteristics of adults with T1D.

The goal of this paper is to present two new open source VPPs that use statistical sampling to create an unlimited number of virtual patients. We present the mathematical model of both the dual-hormone VPP (DH-VPP) and the single-hormone VPP (SH-VPP). In the models, the most sensitive inter-subject parameters were statistically sampled to create the VPPs. The parameters associated with the insulin and glucagon sensitivity factors within the models were the parameters that were statistically sampled within the mathematical models. We describe how we validated the VPPs using glucose data, insulin data, and meal data collected from adults with type 1 diabetes during 3.5-day outpatient AP studies that involved self-selected meals, typical activities of daily living, and in-clinic aerobic exercise at 60% of the participant's maximal VO_2. We matched each virtual patient with one of the

true patients from the AP study, matching them by their nearest TDIR and their weight. We then used the same control algorithm that was used in the AP outpatient studies [22, 28, 64] to control the glucose of the virtual patients under the identical meal scenarios that were given during the outpatient studies. We compared the clinical outcome measures from the outpatient study with those done on the VPP in-silico studies to validate the VPP. The SH-VPP and DH-VPP that are presented in this paper are made available through source code in Matlab as online supplementary material or by downloading from the Artificial Intelligence for Medical Systems (AIMS) lab GIT repository.

2.3 Materials and Methods

The SH-VPP and DH-VPP were generated based on glucoregulatory models consisting of insulin and glucagon kinetics and dynamics models and a glucose kinetics model. The SH-VPP was generated by statistically sampling the most sensitive inter-subject parameters of the insulin dynamics model. To generate the DH-VPP, the parameters of the insulin and glucagon dynamics models as well as one parameter in the glucose kinetics model were statistically sampled. Both VPPs were validated with experimental data.

2.3.1 Glucoregulatory Model

The glucoregulatory models presented in this section have been previously published. The block diagram of the glucoregulatory model used in this study is shown in Figure 2.1. The single-hormone glucoregulatory model used in the SH-VPP is comprised of three main compartments: an insulin kinetics model, an insulin dynamics model and a glucose kinetics model. The DH-VPP is identical to the SH-VPP except that for the DH-VPP, two additional compartments were included: a glucagon kinetics and a glucagon dynamics model. Aerobic exercise can cause hypoglycemia in people with T1D [106] and it may be important for AP control algorithms to incorporate exercise detection and modified dosing to help avoid exercise-induced hypoglycemia [20, 107]. We have integrated an aerobic exercise model [73] into both the SH and DH-VPPs. Lastly, we have incorporated a meal absorption model into both VPPs.

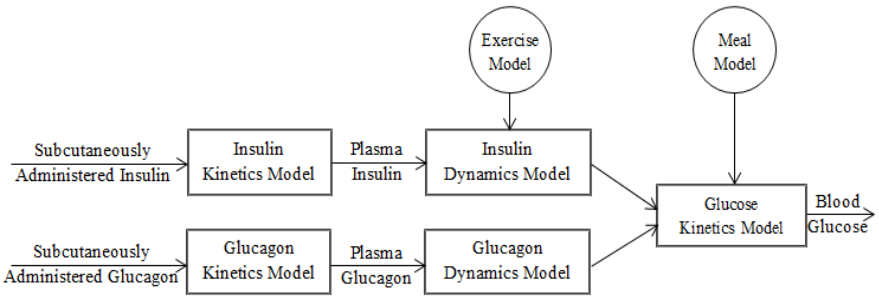

Figure 2.1 Block Diagram of the glucoregulatory model

The insulin kinetics model demonstrates the relationship between the subcutaneously administered insulin and plasma insulin concentration. In this study, we employed an

insulin kinetics model developed by Hovorka et al. [108]. This model is outlined below:

$$\begin{aligned} \dot{S_1} &= u_I - \frac{S_1}{t_{max}} \\ \dot{S_2} &= \frac{S_1}{t_{max}} - \frac{S_2}{t_{max}} \\ \dot{I} &= \frac{S_2}{t_{max} V_I} - k_e I \end{aligned} \tag{1}$$

where, S_1 and S_2 represent the masses of insulin in two subcutaneous compartments [mU/kg], u_I represents the rate of insulin infusion [mU/kg/min], I represents the plasma insulin concentration [mU/L], and t_{max}, V_I and k_e are the time-to-maximum absorption [min], distribution volume [L/kg] and elimination rate [min^{-1}] of insulin. The insulin dynamics model, which describes the action of plasma insulin on glucose, was presented by Hovorka et al. [108]:

$$\begin{aligned} \dot{X_1} &= -k_{a1} X_1 + S_{f1} k_{a1} I \\ \dot{X_2} &= -k_{a2} X_2 + S_{f2} k_{a2} I \\ \dot{X_3} &= -k_{a3} X_3 + S_{f3} k_{a3} I \end{aligned} \tag{2}$$

where x_1 [min^{-1}], x_2 [min^{-1}] and x_3 [unitless] represent the effect of insulin on glucose distribution, disposal and suppression of Endogenous Glucose Production (EGP). S_{f1} [min^{-1} per mU/L], S_{f2} [min^{-1} per mU/L] and S_{f3} [per mU/L] are the insulin sensitivity factors and are the most sensitive inter-subject variables for describing variability in the glucoregulatory system of people with T1D. Selection of new insulin sensitivity

factors enables us to generate new subjects within the VPPs. The variables k_{a1}, k_{a2} and k_{a3} [min^{-1}] are used as both appearance rates of insulin into the action compartments as well as the elimination rates of the insulin effects. The glucagon kinetics model, which represents the absorption rate of subcutaneously injected glucagon into plasma, was designed by Lv et al. [109]:

$$\begin{aligned} \dot{X_{1g}} &= -(k_{1g} + k_{ge1})X_{1g} + u_g \\ \dot{X_{2g}} &= k_{1g}X_{1g} - k_{2g}X_{2g} \\ \dot{X_{3g}} &= k_{2g}X_{2g} - k_{ge2}X_{3g} \end{aligned} \tag{3}$$

where X_{1g} and X_{2g} represent subcutaneous glucagon mass compartments and X_{3g} is plasma glucagon mass, all measured in mg/kg. u_g is the glucagon basal rate [mg/kg/min] infused from the glucagon pump. k_{1g} and k_{2g} are constant transfer rates [min-1]. k_{ge1} and k_{ge2} are elimination rates of glucagon from the inaccessible and accessible (plasma) compartments, respectively [min-1]. The glucagon dynamics model which describes the interaction between the plasma glucagon concentration and the EGP was previously described by Jacobs et al. [28]:

$$\begin{aligned} \dot{Y} &= \frac{10^6 \times k_c \times S_{fGG}}{V_{dGG}} X_{3g} - k_c Y = k_g X_{3g} - k_c Y \\ \dot{Y} &= Z \\ \dot{Z} &= k_g k_{2g} X_{2g} - k_g k_{ge2} X_{3g} - k_c Z \end{aligned} \tag{4}$$

Y represents the effect of glucagon on EGP. Because the rate of change of Y had an effect on EGP, we introduced the variable Z in our equations. k_c is the clearance rate of glucagon from the remote compartment [min-1], S_{fGG} is the glucagon sensitivity factor [(ng/L)-1.min-1] and V_{dGG} is the glucagon volume of distribution [L/kg]. Similar to the insulin sensitivity factors, S_{fGG} is another sensitive inter-subject parameter and is used to generate the dual-hormone VPP. The glucose kinetics model, which estimates blood glucose with respect to insulin and glucagon actions and non-insulin mediated glucose uptake, was presented in Hovorka et al. [108] and Jacobs et al. [28]:

$$\dot{Q_1} = -X_1 Q_1 - F_{01}^c - F_R + k_{12} Q_2 + U_G + EGP_0(1 - X_3 + Y + k_{g3} Z)$$
$$\dot{Q_2} = X_1 Q_1 - k_{12} Q_2 - X_2 Q_2 \quad (5)$$

where Q_1 and Q_2 are the masses of glucose in the accessible (plasma) and non-accessible (rapidly-equilibrating interstitial) compartments, respectively [mmol/kg]. EGP_0 is the basal endogenous glucose production at a theoretical zero insulin concentration [mmol/kg/min]. F_{01}^c and F_R are the non-insulin mediated glucose uptake and the renal glucose clearance rate, respectively [mmol/kg/min]. For the SH-VPP, the Y and Z variables in Equation 5 are zero since no exogenous glucagon is considered to be given to the single-hormone virtual patient. U_G represents the glucose absorption rate from meals [mmol/kg/min]:

$$U_G = \frac{D_G A_G (t - t_0) e^{-\frac{t - t_0}{t_{max,G}}}}{t_{max,G}^2} \quad (6)$$

where, $t_{max,G}$ is the time-to-maximum appearance rate of glucose in Q_1 [min], A_G is the carbohydrate bioavailability [unitless], t_0 is the meal announcement time [min] and D_G is the estimated carbohydrate intake [mmol/kg]. Note that, for the in-silico simulations, D_G is converted from grams to mmol/kg to be compatible with the variables of the glucose kinetics model.

2.3.2 Integration of exercise into the glucoregulatory model

Previously, we showed how an exercise model described by Hernandez-Ordonez et al. [73] could be incorporated into a VPP [28, 49, 52]. In the current paper, we include this exercise model in both the SH-VPP and DH-VPP and validate these populations relative to clinical data sets. We used the Hernandez et al. model to enable exercise to impact the peripheral insulin uptake, the peripheral glucose uptake, and the hepatic glucose production components of the model. Specifically, in the insulin dynamics model in Equation 2, the three insulin sensitivity factors (S_{f1}, S_{f2} and S_{f3}) are increased during the exercise bout as shown below in Equation 7.

$$\begin{aligned} S_{f1-EX} &= M_{PGU} M_{PIU} S_{f1} \\ S_{f2-EX} &= M_{PGU} M_{PIU} S_{f2} \\ S_{f3-EX} &= M_{HGP} S_{f3} \end{aligned} \quad (7)$$

where, M_{PGU} represents a percentage increment with respect to the basal peripheral glucose uptake (35 mg/min); M_{PIU} represents an increment of peripheral insulin uptake and M_{HGP} represents a percentage increment with respect to the basal hepatic glucose production (155 mg/min). These parameters are defined below:

$$\begin{aligned} M_{PGU} &= 1 + \frac{\Gamma_{PGUA} \times PAMM}{35} \\ M_{PIU} &= 1 + 2.4 \times PAMM \\ M_{HGP} &= 1 + \frac{\Gamma_{HGPA} \times PAMM}{155} \end{aligned} \tag{8}$$

where, PAMM represents the percentage of active muscular mass. In the testing described further below, the value of PAMM was set to 50% because the study participants were running on a treadmill with moderate intensity. Smaller values of PAMM (≈ 25%) were reported in [72, 73] for two-legged exercises. Γ_{PGUA} and Γ_{HGPA} are the glucose uptake and production from the active tissues respectively, and are assumed to have identical values during short-duration exercise according to equation (9).

$$\dot{\Gamma}_{PGUA} = -\frac{1}{30}\Gamma_{PGUA} + \frac{1}{30}\Gamma_{\overline{PGUA}} \tag{9}$$

$\Gamma_{\overline{PGUA}}$ represents the peripheral glucose uptake by active tissue in steady state and is a function of PVO_{2max} according to the following equation:

$$\Gamma_{\overline{PGUA}} = 0.006(PVO_{2max})^2 + 1.2264(PVO_{2max}) - 10.1958 \tag{10}$$

where, PVO_{2max} is the percentage of the maximum oxygen consumption during exercise. It was calculated using the metabolic equivalents (MET) as shown below:

$$PVO_{2max} = \frac{MET}{MET_{max}} \tag{11}$$

where MET_{max} is the maximum energy expenditure estimated during a VO_{2max} test. The values of MET and MET_{max} were estimated in the clinical evaluations described further below with the heart rate and accelerometry data recorded by a Zephyrlife BioPatch. The MET estimation was further personalized by incorporating anthropometric characteristics of each individual [110]. During non-exercise periods, M_{PGU}, M_{PIU} and M_{HGP} are close to one, and insulin sensitivity factors do not change.

2.3.3 Clinical Data

Real-world meal scenarios were used from 20 patients with T1D who underwent two separate 3.5-day randomized outpatient AP trials. In one trial, glucose levels were controlled with insulin and in the other, glucose levels were controlled with both insulin and glucagon. Subjects were enrolled at the Oregon Health and Science University and the control algorithm used was the OHSU-FMPD controller [20, 22]. Participants in the study spent the first and fourth day of the study at the hospital eating known meals and participating in formal aerobic exercise at 60% of their maximal VO2. The formal in-clinic exercise bouts lasted for 45 minutes and were

performed 2 hours after lunch. Table III summarizes the characteristics of the participants of the study. For more information about the study and participants, refer to Castle et al. [64] and the study listed on clinicaltrials.gov (Clinical trial reg. no. NCT02862730)

Table III Baseline characteristics of the participants in the AP study

			Value	Range
Age		(years)	35 ± 4.7	27 – 45
Sex	Female		14 (70%)	
	Male		6 (30%)	
Weight		(kg)	76.3 ± 14.6	55.6 -- 104.7
Height		(cm)	172 ± 10.1	156 – 189
HbA1c		(%)	7.6 ± 0.8	6 -- 9.1
TDIR		(units)	42.3 ± 16	18 – 93
Duration of Diabetes		(year)	20.2 ± 8	8 – 37
Maximum HR_{Ex}		(bpm)	182.4 ± 9	170 – 199
Maximum MET_{Ex}			11.7 ± 2.5	6.5 -- 16.5

HR_{Ex}: heart rate during exercise; MET_{Ex}: metabolic equivalent during exercise. Data is reported as

mean ± standard deviation.

2.3.4 Single-Hormone VPP

A Single-hormone VPP was generated for running single-hormone simulations. The nominal values given for S_{f1}, S_{f2}, and S_{f3} from equation (2) were derived for people without T1D [108]. We updated S_{f1}, S_{f2} and S_{f3} to represent the sensitivity of insulin for people with T1D. TDIR was used to personalize insulin sensitivity for each virtual patient. TDIR is the amount of insulin required by a person with diabetes during 24 hours. Insulin sensitivity is inversely proportional to TDIR. Insulin sensitivity is a measure of how sensitive the body is to insulin. Generally, subjects with higher weight have higher TDIR because a larger body oftentimes requires more insulin. To consider a range of TDIR values that relate to different insulin sensitivities, we created a sensitivity composite (Sc) that ranged from 0.1 to 2; this sensitivity composite was multiplied by the nominal values of S_{f1}, S_{f2} and S_{f3} in equation (2) to generate a range of basal insulin values. Basal insulin (I_{basal}) for each sensitivity composite was determined through simulations where the basal insulin rates at each value of Sc yielded a steady state glucose level of 115 mg/dl. The units of I_{basal} is mU/kg/min, which is also shown in Equation 1. To convert the units of I_{basal} to U/hr., we multiplied I_{basal} by a fixed weight of 76.3 kg obtained from the average weight across a clinical dataset of people with T1D, shown in Table

III. The daily basal requirement was then computed as $I_{basal} \times 24$. This total daily basal insulin requirement (basal-TDIR) did not include insulin given for meals. The TDIR, which includes meals and basal insulin, was estimated by multiplying the TDIR by a factor of 1.8 which was empirically validated on an OHSU clinical dataset across people with T1D, implying that our VPP obtained 44.4% of their daily insulin from meals and 55.6% of their daily insulin from basal. Walsh *et al*. [111] introduced a similar impact of basal-TDIR on TDIR. They showed that the basal-TDIR is approximately 48% of the TDIR.

Figure 2.2 shows the relationship between the Sc value and the TDIR. Based on the mean TDIR from a clinical dataset of approximately 45 units/day, an Sc of 0.4 was chosen as the insulin sensitivity modifier across subjects with T1D. Selection of an Sc of 0.4, results in a corresponding reduction of insulin sensitivity of people in our VPP such that they have a 60% lower insulin sensitivity than people without T1D. A similar relationship between the insulin sensitivity of people with and without T1D was investigated by Rickels *et al*. [112] in a euglycemic clamp study. It is important to note that this Sc of 0.4 for generating a large VPP was determined using an average weight of 76.3 kg obtained from a clinical data set of people with T1D. Under the section "Validating VPPs under real-world meal scenarios" we will show how to generate Sc values for individual patients with specific weights.

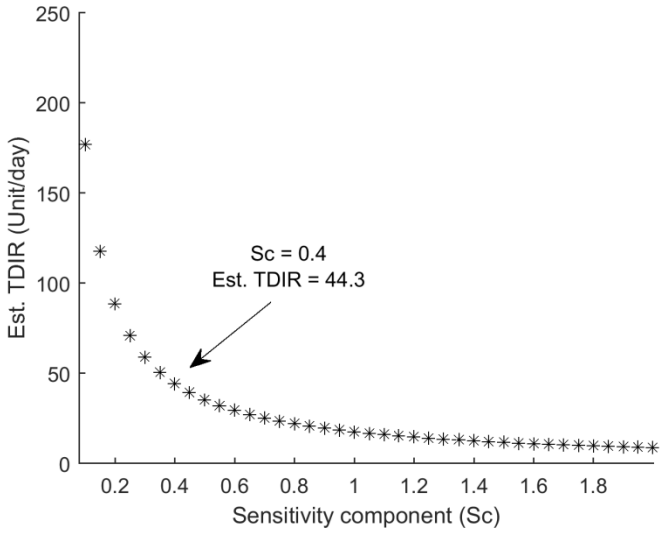

Figure 2.2. Estimated TDIR across Sc values.

Next, virtual patients with T1D were created by statistically sampling from the distributions of the updated insulin sensitivity factors given an ad-hoc 75% correlation between S_{f1} and S_{f2}, and 25% correlation between S_{f2} and S_{f3}. In addition, the weight of the virtual patients was sampled from a normal distribution, with mean of 76.3 kg and standard deviation of 14.6 kg that was obtained based on the clinical data described further above.

After sampling the parameters of each virtual patient, the physiologic feasibility of each virtual patient was evaluated through two tests:

A) Steady-state glucose levels of each virtual patient in the absence of insulin should exceed 300 mg/dl.

B) Delivery of high-dose insulin (15 unit/hr) to each virtual patient should result in a low steady-state glucose level (typically less than 100 mg/dl from the baseline steady-state glucose)

A total of 99 virtual individuals out of 100 passed the above criteria. Figure 2.3 shows the histogram of the TDIR values of the single-hormone VPP.

2.3.5 Dual-hormone VPP

For generating DH-VPP, we first followed the instructions of generating single-hormone VPP and reduced insulin sensitivity factors (S_{f1}, S_{f2} and S_{f3}) by 60%. Then, we changed the most sensitive inter-subject parameters (EGP_0, S_{f1}, S_{f2} and S_{f3}, S_{fGG}, k_c and k_{g3}) of the glucoregulatory model across each subject. Similar to the single-hormone VPP, we assumed a normal distribution of these parameters and we randomly sampled from these distributions to create a new virtual patient. To determine the physiologic feasibility of the randomly drawn parameters, each parameter set was required to pass four clinically-relevant criteria, listed below.

A) Steady-state glucose levels in each virtual patient in the absence of insulin should exceeds 300 mg/dl.

B) Delivery of high-dose insulin (15 U/hr) to each virtual patient should result in a low steady-state glucose level (typically less than 100 mg/dl from the baseline steady-state glucose).

C) Delivery of high-dose glucagon (20 mcg/kg) to each virtual patient should result in a significant rise in glucose within 2 hours of the dose, greater than 50 mg/dl above the baseline steady-state glucose.

D) Delivery of a small dose of glucagon (0.2 mcg/kg) to each virtual patient should not result in a response greater than 100 mg/dl above baseline steady-state glucose.

A total of 90 out of 100 virtual patients passed the below criteria and were selected for the dual-hormone VPP. Figure 2.3 shows the histogram of the TDIR values of the DH-VPP. Table IV shows all the numerical values of the parameters of the glucoregulatory models. The parameters that were statistically sampled to create the virtual patient populations are shown along with their standard deviation.

Table IV The numerical values of the parameters of the glucoregulatory models

Parameters	Values	**Parameters**	Values	**Parameters**	Values	**Parameters**	Values
F_{01}^{c}	0.0097	V_G	0.16	k_{12}	0.066	$t_{max,G}$	40
t_{max}	55	k_e	0.138	V_I	0.12	A_G	0.8
k_{a1}	0.006	k_{a2}	0.06	k_{a3}	0.03	k_{1g}	0.0065
k_{ge1}	0.0772	k_{ge2}	0.0357	V_{dGG}	0.19	k_{ge1}	0.0772
S_{f1} ($\times 10^{-4}$)	21 ± 5.9	S_{f2} ($\times 10^{-4}$)	3.5 ± 1.4	S_{f3} ($\times 10^{-4}$)	214 ± 5.9	EGP_0 ($\times 10^{-2}$)	1.61 ± 0.15
S_{fGG} ($\times 10^{-2}$)	1.7 ± 0.47	k_c ($\times 10^{-2}$)	6.0 ± 1.95	k_{g3}	140 ± 39.9	k_{2g}	0.02777

Data is shown as the mean and standard deviation for the variable parameters.
For the SH-VPP, only S_{f1}, S_{f2}, S_{f3} were sampled across the virtual subjects.
For the DH-VPP, only S_{f1}, S_{f2}, S_{f3}, S_{fGG}, k_c, k_{g3} and EGP_0 were sampled across the virtual subjects.

2.3.6 Validating VPPs under real-world meal scenarios

To validate the VPPs, we matched clinical patients with T1D with their virtual twin from the virtual patient population. In this section, we describe how we matched real-world patients with T1D with their virtual twin. The 99 single-hormone virtual patients and 90 dual-hormone virtual patients described above are the patients that should be used typically to run simulations on a glucose control algorithm. For the purpose of validation, we generated 20 new virtual patients that were created to match actual patients with T1D by weight and TDIR. The only difference between the methods described above and those used to match the clinical patients with their

virtual twin was the determination of Sc values. Unlike the methods described above whereby the Sc vs. TDIR relationship (Figure 2.2) was generated using the *average weight* of patients (76.3 kg from Table III), the Sc vs. TDIR for the validation data was generated individually for each clinical patient using their *actual weight*. Meal scenarios describing daily meal content and pattern of consumption were acquired from a previous clinical study assessing single hormone and dual hormone artificial pancreas technologies [64]. Twenty 3.5-day meal scenarios from the single-hormone clinical trial and twenty 3.5-day meal scenarios from the dual-hormone clinical trial were collected and used to deliver to the virtual patient population. Virtual patients were matched to clinical study participants by closest match of TDIR and weight. Matching a virtual patient to a study participant was done by first creating a TDIR vs. sensitivity component (Sc) graph like the one shown in Figure 2 using the participant's actual weight. The Sc that most closely corresponded to a given participant's TDIR was determined and a temporary set of 100 virtual patients was generated using the methods described above under the sections Single-hormone VPP and Dual-hormone VPP. Then, the TDIR of each of the temporary virtual patients was compared to the participant's TDIR and finally the desired virtual patient whose TDIR was the closest was identified. By using this approach, we ensured that both weight and TDIR of each actual patient were used to identify the closest virtual patient. This approach was repeated for all 20 actual patients from

each clinical study trial and the 20 closest virtual twins were identified. We then used the same OHSU-FMPD control algorithm that was used in the outpatient AP studies to control the glucose levels of each of the 20 virtual patients under the dual-hormone and single-hormone meal scenarios. The control algorithm was implemented in Java and has been previously described [22, 28]. The glucose profiles of the virtual patients were compared with the related actual glucose profiles controlled by the same controller during the in-vivo trial. For the in-silico simulations, the system was further challenged by introducing a randomly selected -30% to 30% meal uncertainty applied to each carbohydrate intake at each meal scenario. Since insulin is known to vary during the day [113], circadian variability of insulin sensitivity was introduced to the insulin sensitivity parameters (S_{f1}, S_{f2} and S_{f3}) within each virtual patient by varying these parameters with respect to time of day using equation (12):

$$S_{fi}(t)=S_{fi}^{*}\times(1+0.3\sin(\frac{2\pi}{24\times60/Ts}\times t+2\pi\times RND),\ i=1,2,3 \tag{12}$$

where, RND is a random variable generated from a uniform distribution between 0 and 1; Ts is the sampling interval (5 minutes). S_{fi}* denotes the nominal value of each of the insulin sensitivity factors. Notice that the phase of the circadian insulin sensitivity was randomly initialized at the start of the study using the RND command, and this phase was fixed for all virtual patients. This approach helped us

to compare the performance of all virtual patients similarly as the phase shift remained constant. We additionally modeled glucose sensor noise using the glucose sensor noise model described by Facchinetti et al. [30, 114]. During this study, meal scenarios and exercise sessions were imposed on the virtual subjects as determined by the existing study data. And as described under the section 'Integration of exercise into the glucoregulatory model', the nominal insulin sensitivity (S_f*) in Equation 12 is changed during exercise according to Equation 7. It is increased during the exercise period and returned to the original value at the end of exercise.

2.3.7 Evaluation metrics and statistical analysis

We assessed accuracy of the VPP by comparing the primary outcome measures of the VPP with primary outcome measures acquired during the clinical study. The primary outcome measures for the validation of VPPs included the percent time in hypoglycemia (<70mg/dl) and the percent time in target range (70-180 mg/dl). The secondary outcome measures for validation of the VPPs included the percent time in hyperglycemia (>180mg/dl) and the low and high blood glucose indices [25]. We report errors in the clinical outcome metrics (e.g. time in range, time in hypoglycemia, time in hyperglycemia) as mean absolute error (MAE) whereby error in the VPP outcome metrics are calculated relative to the outcome metrics obtained from the clinical study. To assess the statistical difference between the simulated and

the actual glucose profiles, the student t-test was used, with significance level set to 5%.

$$MAE = \frac{1}{M}\sum_{i=1}^{M}|Outcome_{clinical} - Outcome_{simulation}| \quad (13)$$

Where M is the number of meal scenarios used in the validation step of the VPPs. The MAE was computed for each of the outcome metrics

2.4 Results

Figure 2.3 show the histogram of the patients, SH-VPP and DH-VPP. The range of the TDIR values of SH-VPP started at 20 units and ended at 120 units. The peak of the histogram was around 40-45 units showing that the TDIR values of the SH-VPP were well-scaled regarding the average TDIR value shown in Table III. A similar range is also observable in DH-VPP. The peak of the histogram occurred for TDIR values between 40-45 units, however the minimum TDIR spanned to smaller levels for several virtual patients simulating the situations where certain individuals with T1D may require less insulin.

Figure 2.4 and Figure 2.5 show the comparison between the simulated and the actual glucose profile for one representative subject in SH and DH trials. Overall, the dynamic responses of the simulated glucose profiles during meal events and exercise bouts were similar to the actual one.

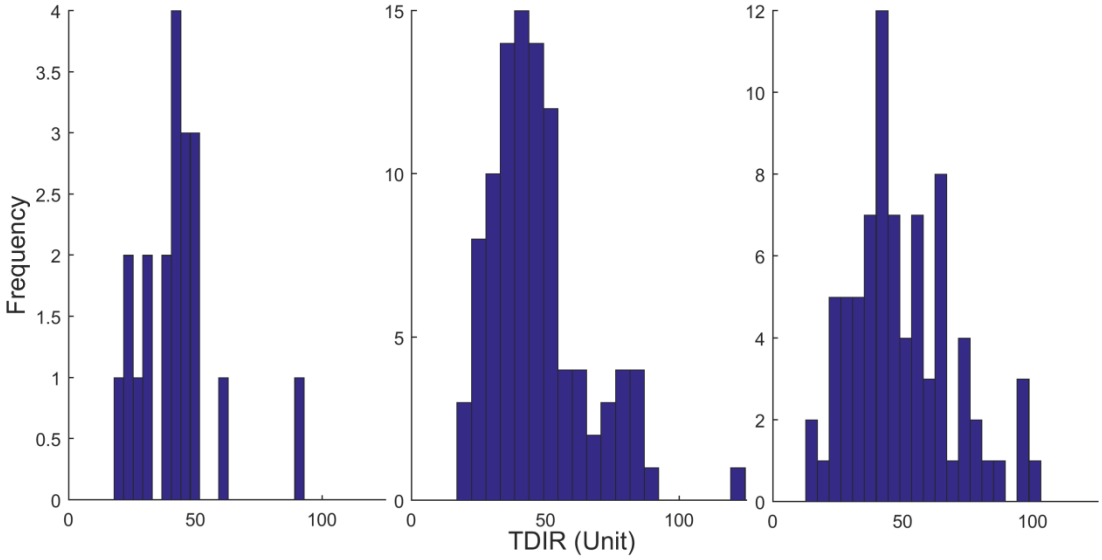

Figure 2.3 Histogram of the TDIR values of the clinical patients (left), SH-VPP (middle) and DH-VPP (right).

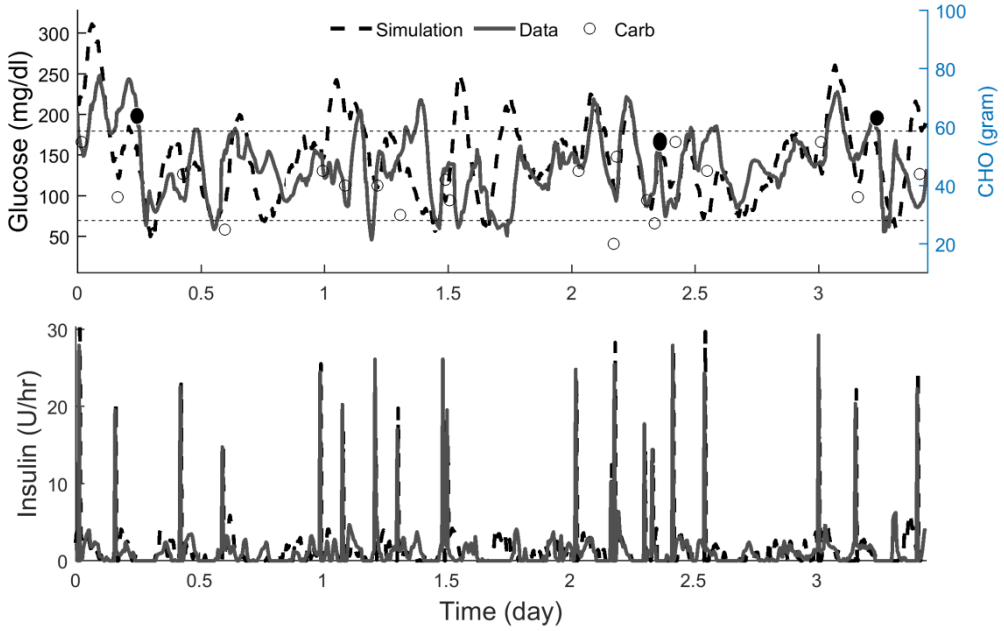

Figure 2.4 Simulated vs. actual glucose and insulin profiles of one representative subject in single-hormone trial. Both experiments were initialized at 8:00 am. Carbs are shown with

circles. Filled circles show the start of exercise. Higher resolution data from this study is shown in Supplemental Figure 2.6.

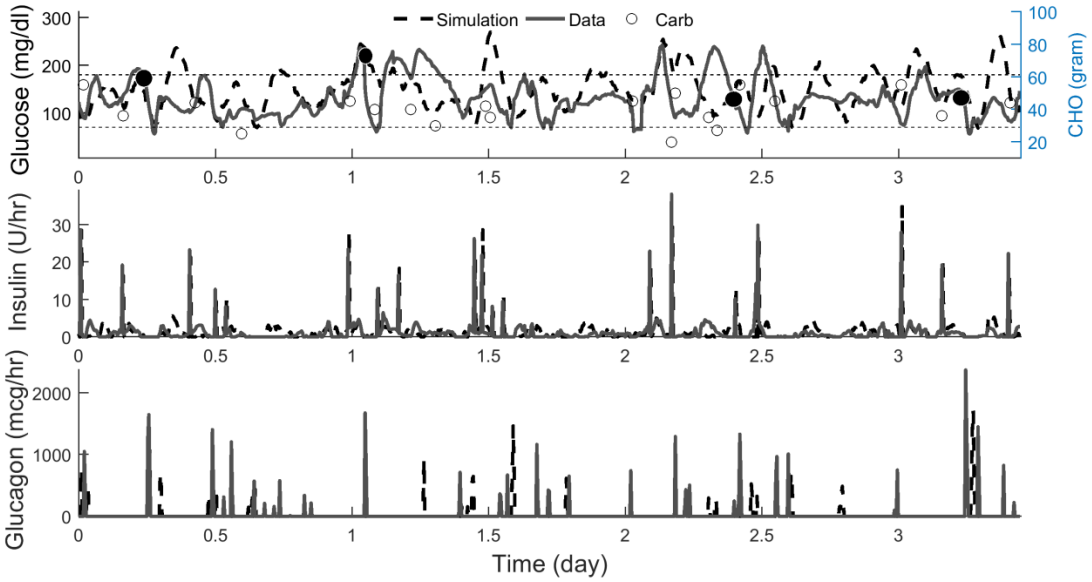

Figure 2.5 Simulated vs. actual glucose and insulin profiles of one representative subject in dual-hormone trial. Both experiments were initialized at 8:00 am. Carbs are shown with circles. Filled circles show the start of exercise. Higher resolution data from this study is shown in Supplemental Figure 2.7.

Table V and Table VI show the clinical study outcomes in comparison with the in-silico control simulation outcomes of the VPPs. Table V shows results from the single-hormone study and Table VI shows results from the dual-hormone study. The tables also show the statistical analysis of each outcome and a p-value indicating whether the VPP outcome was statistically different than the clinical outcome using a two-tailed t-test analysis. For all outcome measures, the SH-VPP was not statistically different than the true population. The time spent in hyperglycemia was slightly underestimated by the SH-VPP, which was not significant but was trending

towards significant (p=.08). The MARE of time spent in hyperglycemia was high for SH-VPP showing that the meal model should be further improved to better represent glucose levels above 180 mg/dl. The outcome measures for the DH-VPP during the in-silico AP simulation are not statistically different than the outcome measures for the actual patients during the AP clinical study as shown in Table VI, however the HBGI is trending towards being significant (p=.06).

Table V Outcome metrics of the single-hormone VPP across the selected virtual patients

Single Hormone VPP	Clinical Results	Simulated Results	p-value	MAE (%)
Time in hypoglycemia (%)	2.8 ± 1.7	3.4 ± 1.3	0.23	2
Time in hyperglycemia (%)	22.9 ± 8.8	18.4 ± 5.3	0.08	9.6
Time in range (%)	74.3 ± 8.1	78.1 ± 5.1	0.11	8.4
LBGI	3.1 ± 1	3.5 ± 0.9	0.24	1.2
HBGI	6.2 ± 1.7	5.9 ± 1.2	0.47	1.9

Table VI Outcome metrics of the dual-hormone VPP across the selected virtual patients

Dual Hormone VPP	Clinical Results	Simulated Results	p-value	MAE (%)
Time in hypoglycemia (%)	1.3 ± 1	0.9 ± 0.8	0.19	1.1

Time in hyperglycemia (%)	26.7 ± 11.4	23.5 ± 5.7	0.21	8.8
Time in range (%)	71.9 ± 10.9	75.6 ± 5.5	0.13	8.3
LBGI	2.3 ± 1.3	1.9 ± 0.8	0.3	1.3
HBGI	7.2 ± 2.3	6.2 ± 1.1	0.06	1.9

2.5 Discussion and Conclusion

In this paper, we described the design of two T1D virtual patient populations that can be used to evaluate single-hormone and dual-hormone control algorithms within automated drug delivery systems for helping people with T1D better manage their glucose levels. These virtual populations were validated against clinical data acquired from real-world patients with T1D [64]. The results showed no significant difference between the performance outcome measures of the VPPs and the true patients when treated with an automated control algorithm intervention and when given identical meals. In this study, we were able to validate the VPP on a clinical data set whereby patients with T1D were matched with their in-silico virtual twin by TDIR and weight. Both real patients and virtual patients were given the same meals and exercise regimen while their glucose was controlled using the same control algorithm. It is important to emphasize that, while we used just one control algorithm to validate the VPPs, this does not mean that these VPPs are compatible with just a

single control algorithm. Any control algorithm can now be used with the VPPs. We have simply used a single control algorithm to validate that when virtual patients and actual patients are given comparable amounts of insulin, glucagon, meals, and exercise, the glycemic outcome metrics between the virtual and actual patients are not statistically different.

For further evaluating the VPPs, we compared the performance of the SH-VPP with the free version of the single-hormone UVA/Padova simulator. In this comparison, we only used 10 of the real-world meal scenarios because the UVA/Padova simulator deletes meal events that occur within 30 minutes of a prior meal. For the purpose of comparison, we eliminated 10 of the 20 meals, which had meal events occurring within 30 minutes of each other. For each of the 10 selected meal scenarios, a relevant UVA/Padova virtual subject was identified based on weight and TDIR, similar to the selected virtual patients descried above. Because the single-hormone UVA/Padova simulator does not have an exercise model, we could only compare the performance of the UVA simulator with the VPP population at the second day, when no exercise took place in the study. Table VII shows the comparison between the single-hormone VPP, the single-hormone UVA/Padova simulator and the clinical data across the 10 selected meal scenarios. Both simulators agreed closely on average with the clinical data for the time in range outcome

measure and time in hyperglycemia. However, they misestimated the time in hypoglycemia compared to the clinical data. The MAE of the UVA simulator relative to the clinical data for time in range was 33.4%, which was significantly higher than the MAE of the SH-VPP, which was 15.8%. The MAE for the percent time in hypoglycemia of the UVA/Padova simulator relative to the clinical data was comparable with the SH-VPP showing slightly higher error (0.76% for UVA/Padova vs. 1.7% for SH-VPP).

Table VII Comparison between the simulators and the clinical data across the 10 selected meal scenarios

Simulators/outcomes	Time in hypoglycemia (%)	Time in hyperglycemia (%)	Time in range (%)
Clinical data	0.77	24.72	74.51
SH-VPP	2 (0.01)	15.4 (0.11)	82.6 (0.16)
UVA/Padova	0 (0.02)	30.4 (0.62)	69.6 (0.67)

Data is shown as the mean, and the p-value in parenthesis for the comparison.

While the SH-VPP and the DH-VPP on average resulted in a good match with the clinical data, the MAE was higher than we would prefer for the percent time in range and the percent time in hyperglycemia. This indicates that for certain individuals, there was not always a good match between the in-silico model and the weight/TDIR matched clinical participant. There are several reasons why this was the case. First,

for the clinical study we did not know the true meal amount consumed by the patient and instead could only estimate based on their input during the clinical study. This is why we imposed a +/- 30% variability in the carbohydrate consumed by the virtual patients at each meal. This meal estimation uncertainty will inevitably cause error between the participant and the in-silico matched patient. Second, there was uncertainty of the time when clinical study participants delivered their rescue carbs for times when their glucose dropped below 70 mg/dl. In our simulations, the virtual patient was given a rescue carbohydrate 10 minutes after glucose dropped below 70 mg/dl. For the clinical participant, the rescue carbohydrate delivery could have been given at a different time, which would contribute to error. Third, it is known that insulin sensitivity can vary throughout the day. We modeled this insulin sensitivity variability by varying each virtual patient's insulin sensitivity by +/- 30% throughout the day. This potentially inaccurate estimation of circadian insulin sensitivity variability could further explain the error observed. Fourth, the exercise model that we used in the VPP was validated on continuous and non-intermittent aerobic exercise with constant PVO_2 [73]. We further assumed in the exercise model that the PAMM was 50% for all subjects. However, we know that there was some variability in the exertion of the subjects throughout the exercise sessions and it is probable that the PAMM for all of the subjects was not exactly 50%. This would have been a cause for further error observed. Palumbo et al. [115] describe how PVO_{2max} can be

adapted to a patients' specific physiology and adapt based on duration and intensity of exercise. In the future, we will need to do a similar type of adaptation to better model the impact of exercise duration, type, and intensity on glycemic control. A further reason for differences between the VPPs and the clinical subjects was that the VPP used a model of the CGM noise that was derived using the Dexcom G4 glucose sensor, whereas the data collected from the clinical study was done using the Dexcom G5 sensor. Despite these various factors that contributed to individual differences between the virtual patients and the clinical study participants, we remain confident that on average the SH-VPP and DH-VPP are sufficiently accurate for use in designing and evaluating AP control algorithms prior to an actual clinical study. The average outcome measures from the clinical study were not statistically significantly different than those of the in-silico study. And the MAE was lower than other stimulators that have been used in the past to evaluate AP control algorithms prior to in-vivo studies. In the future, we plan to leverage the clinical data set to try to improve our models by using system identification approaches such as Markov Chain Monte Carlo (MCMC) approaches. While the goal of the current work was to use the clinical data to estimate the accuracy of the VPP, we can certainly try to achieve a closer match to the clinical data by identifying each individual's insulin sensitivity, carbohydrate sensitivity, and exercise model parameters.

In conclusion, two new single and dual-hormone VPPs were presented and validated against a clinical data set. On average, there was not a significant difference in outcome measures between the clinical data and the in-silico data, indicating that both VPPs may be used for pre-clinical evaluation of AP algorithms.

2.6 Supplementary Materials

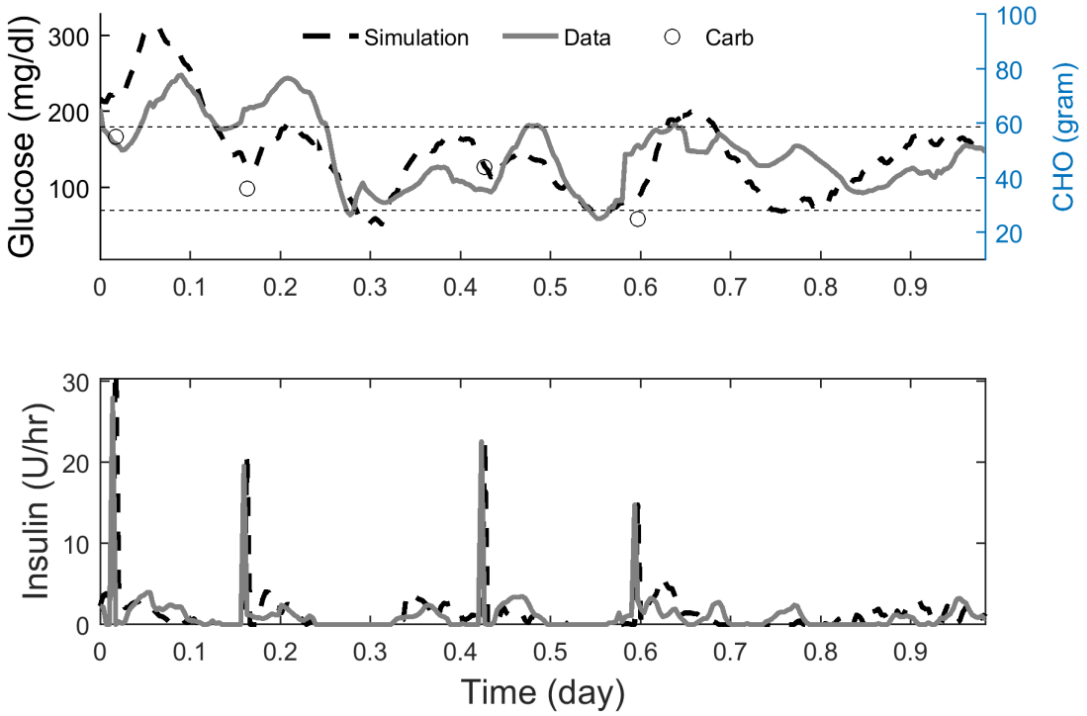

Figure 2.6 Simulated vs. actual glucose and insulin profiles of the representative subject shown in Figure 2.4 for one-day simulation. Both experiments were initialized at 8:00 am. Carbs are shown with circles.

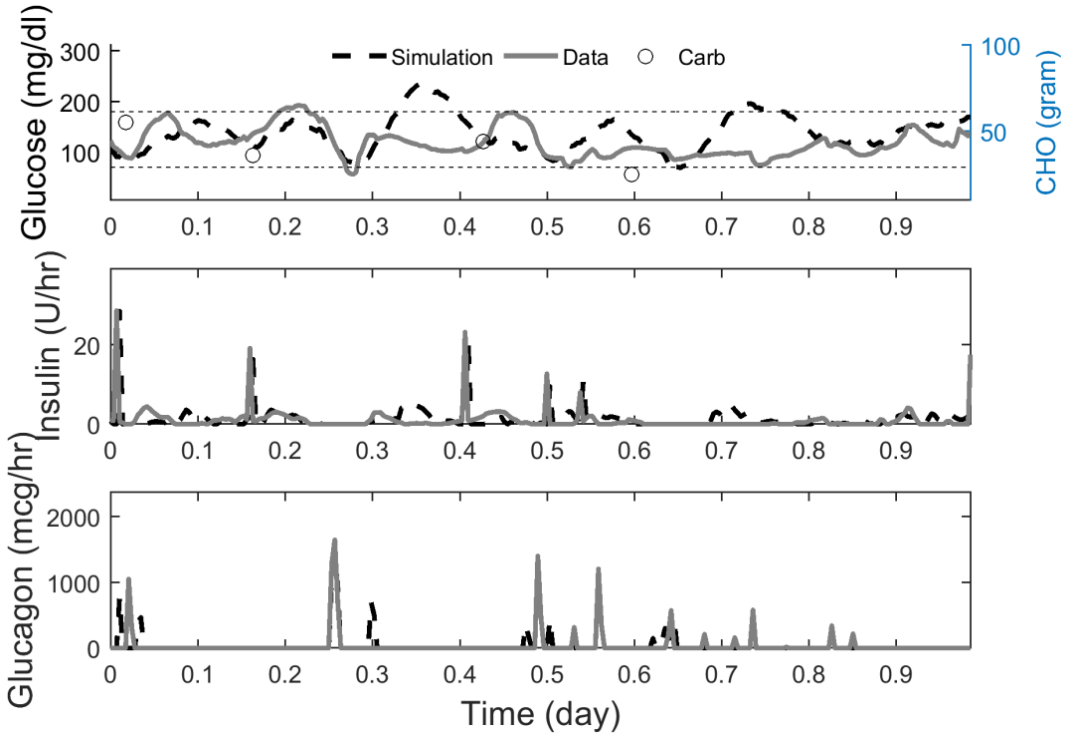

Figure 2.7 Simulated vs. actual glucose, insulin and glucagon profiles of the representative subject shown in Figure 2.5 for one-day simulation. Both experiments were initialized at 8:00 am. Carbs are shown with circle.

Table VIII Information of the meal scenarios

Meal Scenario	Mean carbs and std
1	40.2 ± 9.9
2	72.8 ± 36.6
3	45.1 ± 8.7
4	42.6 ± 30.1

5	42.8 ± 28.7
6	47.4 ± 21.9
7	46.4 ± 15.5
8	32.6 ± 18.9
9	40.2 ± 34.7
10	38.9 ± 20
11	45.1 ± 25.4
12	31.6 ± 16.9
13	40.4 ± 30.4
14	55.8 ± 35.2
15	57.2 ± 15.9
16	33.9 ± 21.6
17	48.4 ± 24.8
18	32.2 ± 11.1
19	40.9 ± 21.7
20	38.9 ± 2.6
Average	43.7 ± 9.7

3 Adaptive Tuning of Basal and Bolus Insulin to Reduce Postprandial Hypoglycemia in a Hybrid Artificial Pancreas

Patients sometimes experience postprandial hypoglycemia. Inappropriate pre-meal insulin bolus and postprandial basal insulin may cause postprandial hypoglycemia. In this chapter, two adaptive algorithms are developed based on postprandial glucose levels to better adjust insulin delivery rates.

Chapter Summary:

- Two adaptive learning postprandial hypoglycemia prevention algorithms (ALPHA) are implemented.
- In one implementation, only postprandial basal insulin (ALPHA-BR) is adaptively modified. In the other implementation, only insulin to carb ratio (ALPHA-ICR) is changed without changing the basal insulin.
- Both implementations are evaluated with real-world scenarios. They successfully reduce time in hypoglycemia.
- ALPHA-BR reduces time in hypoglycemia more than ALPHA-ICR and is selected to be used for in-vivo studies.

This work was originally published in 2019:

Navid Resalat, Joseph El Youssef, Ravi Reddy, Jessica Castle and Peter G. Jacobs, "Adaptive Tuning of Basal and Bolus Insulin to Reduce Postprandial Hypoglycemia in a Hybrid Artificial Pancreas", Journal of Process Control, vol. 80, August 2019, pp. 247-254 [116], Reprinted with permission from Elsevier.

3.1 Abstract

Objective: We introduce an adaptive learning algorithm to better adjust postprandial basal and pre-meal bolus insulin for reducing postprandial hypoglycemia in a hybrid artificial pancreas (AP). An AP uses a control algorithm and sensed glucose to automate the delivery of insulin to people with type 1 diabetes (T1D). A hybrid AP requires the person to dose insulin in advance of a meal. Insulin sensitivity is dynamic in people with T1D, making it challenging for an AP to maintain euglycemia. Adaptive approaches to meal dosing can help prevent postprandial hypoglycemia. *Methods:* An adaptive learning postprandial hypoglycemia-prevention algorithm (ALPHA) is introduced. One implementation of ALPHA adjusts the rate of postprandial insulin (ALPHA-BR) proportionally in response to prior postprandial episodes. This is achieved by an adaptive aggressiveness factor applied to postprandial basal insulin. The second implementation adaptively updates the pre-meal bolus insulin by changing the insulin-to-carbohydrate ratio (ALPHA-ICR), also proportionally in response to prior postprandial hypoglycemia. Both

implementations were evaluated within an AP on an in-silico T1D virtual population of 99 subjects with circadian insulin sensitivity variations and 30% errors on meal estimations. Twenty real-world 4-day meal scenarios were given and glycemic outcomes were compared with an AP with no adaptation. *Results:* Out of the 99 in-silico subjects, 23 of them experienced postprandial hypoglycemia leading to greater than 1% overall time in hypoglycemia. Of these 23 subjects, we evaluated the benefit of using ALPHA-BR and ALPHA-ICR to prevent postprandial hypoglycemia. ALPHA-BR yielded substantially fewer percent time in hypoglycemia compared to AP (0.54% vs 1.92%, $p < 0.001$) and fewer rescue carbs per day (0.36 vs. 1.29, $p<0.001$). For the control algorithm evaluated, it yielded an average aggressiveness factor of 0.72 for reducing postprandial basal insulin. ALPHA-ICR slightly reduced time in hypoglycemia compared to AP (1.77% vs. 1.92%, $p=0.09$). *Conclusion:* Incorporating adaptive meal dosing into an AP can help reduce postprandial hypoglycemia, and the reduction is primarily due to changes in postprandial insulin delivery rather than pre-meal bolus. *Significance:* Adapting postprandial insulin can lead to substantial reduction in postprandial hypoglycemia and the adaptive algorithm presented can be used both to tune an algorithm prior to a study and to adapt to individuals during real-time usage.

3.2 Introduction

People with type 1 diabetes produce little or no insulin and therefore require insulin for survival. Different insulin therapy methods are used by people with T1D to control glucose levels. Multiple daily injection (MDI) is where long-acting basal insulin is administered once or twice per day, and rapid-acting insulin is administered for meals. Continuous subcutaneous insulin infusion (CSII) therapy is another type of open-loop therapy where rapid-acting insulin is delivered via an insulin pump. MDI and CSII therapies require multiple adjustments by the user throughout the day. Closed-loop therapies have been developed to reduce patient burden by automating delivery of insulin and optionally glucagon to enable better glucose control with less patient interaction. The artificial pancreas (AP) is a closed-loop therapy where the delivery rate of rapid-acting insulin is calculated based on continuous glucose measurements (CGM) and delivered by an insulin pump.

Many AP systems are hybrid, meaning that patients are still required to announce meals and in certain systems estimate the amount of carbohydrates consumed so that a pre-meal bolus can be delivered. Dosing of insulin for meals is a challenging aspect of T1D glucose management. Pre-meal insulin boluses help to reduce postprandial excursions, though the delayed pharmacokinetics of subcutaneously delivered insulin limits this effect resulting in some hyperglycemia. Over-estimation of the amount of pre-meal insulin, on the other hand, leads to postprandial hypoglycemia, a common

and dangerous situation. Severe hypoglycemia (< 54 mg/dl) if left untreated can lead to coma and can be life threatening. In a recent hybrid insulin-only AP study by our group [64], we observed that some of the participants experienced postprandial hypoglycemia. A number of factors can lead to postprandial hypoglycemia in hybrid AP systems. First, there is variability in insulin kinetics of people with T1D making it challenging for a single control algorithm to work well for all patients. Second, insulin sensitivity tends to vary throughout the day making the estimation of the optimal dose of insulin a challenge. Third, people commonly misestimate the amount of carbohydrates consumed for a given meal, which can lead to over or under-delivery of pre-meal insulin. An adaptive system would be helpful to respond to meal-based insulin deliveries within a hybrid AP system. An adaptive system can modify the insulin-to-carbohydrate (ICR) or the post-prandial basal insulin in response to postprandial hypoglycemia.

Adaptive AP systems have been presented by a number of research groups. Palerm et al. [117]-[118] presented a run-to-run control algorithm to adjust pre-meal bolus insulin each day based on glucose readings of the previous day with similar meal amounts. They showed higher rates for both time in range and hypoglycemia. Dassau et al. [119]-[120] tested a 12-week adaptive artificial pancreas where the ICR and the basal delivery were adapted every 4 weeks and one week, respectively. They

demonstrated a decrease in time in hypoglycemia (from 2% to 1.9%) and time in range (76.7% to 72.6%) after the 12th week. Toffanin et al. [121] proposed an adaptive run-to-run approach in which the basal rate was adjusted based on the patient's clinical performance during the last 24 hours. If time in hypoglycemia was observed, their algorithm reduced the basal rate. If time in hyperglycemia was observed, their algorithm increased basal rate accordingly. They tested their algorithm on 100 virtual patients using the UVA/Padova simulator. They showed that time in hypoglycemia was reduced from 8.3% to 1.5% after 8 days. Their algorithm treated non-meal and meal hypo/hyper events equivalently. In a recent paper by the same group, Toffanin et al. [122] adapted basal rates based on performance during non-meal/ overnight periods and they adjusted pre-meal boluses using the same run-to-run structure. While time in range improved, there was not a change in hypoglycemia based on this approach to adaptation. Ruiz et al. [66] integrated an insulin feedback method in a proportional-integral-derivative controller, preventing possible hypoglycemic events induced by the delay between the infused insulin and glucose level. They found no postprandial hypoglycemia across four participants. Turksoy et al. [123] developed a hypoglycemia early alert system, embedded in an AP, enabling the prediction of hypoglycemia 25 minutes in the future. For each hypoglycemia alert, a 15-gram carbohydrate (CHO) was delivered. They tested their algorithm across three AP experiments with random

meal size and found 13 hypoglycemic events occurred. Time in hypoglycemia reduced to zero and time in hyperglycemia increased to 47% from 38% when the hypoglycemia alert system was not enabled. In a different study, Galati et al. [124] developed a hierarchical diagram to diagnose and prevent postprandial hypoglycemia. Their method required measuring C-peptide, insulin, β-hydroxybutyrate, insulin antibodies and sulfonylurea screen to prevent hypoglycemia. Herrero et al. [113] described an adaptive algorithm to modify ICR for a meal bolus calculator in a hybrid AP. This algorithm improved time in range and did not change postprandial hypoglycemia. Like Toffanin et al. [122], they did not focus on adapting postprandial basal insulin, which may be necessary for avoiding hypoglycemia as we show in the current paper.

The current paper presents two approaches to postprandial hypoglycemia prevention using a new Adaptive Learning Postprandial Hypoglycemia-prevention Algorithm (ALPHA), designed to be used in hybrid AP insulin therapy. In one implementation, ALPHA modifies the aggressiveness of the basal rate of postprandial insulin (ALPHA-BR) and in the second implementation, ALPHA adjusts the aggressiveness of the pre-meal bolus insulin by modifying the ICR which is a similar approach to Toffanin et al. [122] and Herrero et al. 2017 [113]. The objective of the comparison was to determine whether adapting pre-meal vs. postprandial basal insulin was

optimal in preventing postprandial hypoglycemia. In addition, we demonstrate how the ALPHA algorithm can be used to tune the post-prandial insulin delivery aggressiveness factor for any AP control algorithm using an in-silico virtual patient population.

ALPHA-BR and ALPHA-ICR were evaluated by a series of in-silico simulations conducted under closed loop control across four days on 99 virtual patients that are further described below. Each virtual patient was given 20 real-world meal scenarios acquired during real-world AP studies. Performance of ALPHA-BR and ALPHA-ICR was compared while using the current version of the OHSU Fading Memory Proportional Derivative controller (FMPD), described further in [20, 22], which does not have postprandial meal adaptation. We also evaluated the ALPHA algorithm using a model predictive control (MPC) algorithm [49, 125] to demonstrate that ALPHA is algorithm agnostic and can work on various types of AP control methodologies.

The primary contributions of the paper are as follows. First, we introduce a method for adapting aggressiveness of insulin dosing after meals. Second, we introduce a method for adapting aggressiveness of carbohydrate ratios for dosing insulin prior to meals. Third, we show that adapting postprandial insulin is significantly more effective than adapting carbohydrate ratios when it is necessary to address problems

of postprandial hypoglycemia in patients.

3.3 Material and Methods

A virtual T1D patient population was generated based on a glucoregulatory model consisting of insulin kinetics and dynamics models and a glucose kinetics model. The parameters of insulin dynamics model were statistically sampled to build a virtual population with different insulin sensitivities as described further in the Supplementary Material.

3.3.1 ALPHA-BR Description

ALPHA-BR is an algorithm that adapts postprandial insulin delivery to achieve a certain target range. In other words, it adjusts postprandial basal insulin delivery if postprandial glucose following prior meals is outside of a target range. If post-prandial hypoglycemia occurs, ALPHA-BR will reduce postprandial insulin for the next meal. The factor by which postprandial insulin is decreased is determined by an aggressiveness factor (A_f). The initial postprandial insulin infusion rate calculated by the AP, called IIR_{orig} (i.e. before aggressiveness factor is applied). Smooth adaptation was realized by averaging A_f values from prior meals to give A_f^{Avg}. The value of A_f^{Avg} is between 0 and 1 and is re-calculated after each meal.

$$A_f^{Avg}(k) = \frac{A_f(k) + A_f^{Avg}(k-1) + A_f^{Avg}(k-2)}{3} \quad (1)$$

where, the variable k denotes the meal event and t is the time of day. The new postprandial insulin infusion rate (IIR_{adapt}) is calculated according to equation 2. The aggressiveness factor is applied from the time that the meal starts (t_{meal}) through a window of time ($t_{agg\text{-}win}$).

$$IIR_{adapt}(t)\Big|_{t_{meal}}^{t_{meal}+t_{agg-win}} = A_f^{Avg}(k) \times IIR_{orig}(t)\Big|_{t_{meal}}^{t_{meal}+t_{agg-win}} \quad (2)$$

$A_f(k)$ is adjusted using a piece-wise linear adjustment that is a function of the minimum glucose measured within an observation time-window after the last meal (G_{min}) whereby the window begins at t_{start} and ends at t_{stop} relative to $t_{meal}(k\text{-}1)$. Figure 3.1 and equation 3 show how $A_f(k)$ is modified based on G_{min} and A_f^{Avg}.

$$A_f(k) = \begin{cases} 0, & 0 \le G_{min} \le G_{hypo} \\ \dfrac{G_{min} - G_{hypo}}{G_{eug-lower} - G_{hypo}} \times A_f^{Avg}(k-1), & G_{hypo} \le G_{min} \le G_{eug-lower} \\ A_f^{Avg}(k-1), & G_{eug-lower} \le G_{min} \le G_{eug-upper} \\ \dfrac{G_{min} - G_{hyper}}{G_{hyper} - G_{eug-upper}} \times \left(1 - A_f^{Avg}(k-1)\right) + 1, & G_{eug-upper} \le G_{min} \le G_{hyper} \\ 1, & G_{hyper} \le G_{min} \end{cases} \quad (3)$$

If G_{min} is within a euglycemic range of $G_{eug\text{-}lower}$ = 90 to $G_{eug\text{-}upper}$=140 mg/dl, then the aggressiveness factor does not change and $A_f = A_f^{Avg}$. However, if G_{min} drops

below $G_{eug\text{-}lower}$, the aggressiveness factor, A_f, is reduced proportionally down to a hypoglycemic threshold of G_{hypo} (70 mg/dl in Figure 3.1). Below the hypo threshold (G_{hypo}), $A_f = 0$ meaning that insulin being delivered during $t_{agg\text{-}win}$ for the next meal is the least aggressive since A_f is zero in Equation 1. The aggressiveness factor is likewise increased if G_{min} is above the upper limit of euglycemia ($G_{eug\text{-}upper}$). Again, the aggressiveness factor is increased proportionally with respect to G_{min} until G_{min} exceeds the hyperglycemic threshold (G_{hyper}). Above G_{hyper}, the value of IIR_{adapt} is closer to the original AP-calculated postprandial basal rate insulin (IIR_{orig}) since A_f is set to one in equation 1.

Figure 3.2 shows graphically every example from the piecewise linear function to demonstrate how A_f adapts with respect to prior postprandial glycemic responses. Prior to adaptation, $A_f(1)$ is 1 for the first meal. For the second meal, $A_f(2)$ was reduced since glucose dropped below $G_{eug\text{-}lower}$ after the first meal. For the third meal, $A_f(3)=A_f(2)$ as the glucose fell within the euglycemic range after the second meal. After the third meal, glucose never dropped into/below the euglycemic range, so $A_f(4)$ was increased. After the fourth meal, hypoglycemia occurred so $A_f(5)=0$. After the fifth meal, glucose never fell below the hyperglycemic limit, and so $A_f(6)=1$.

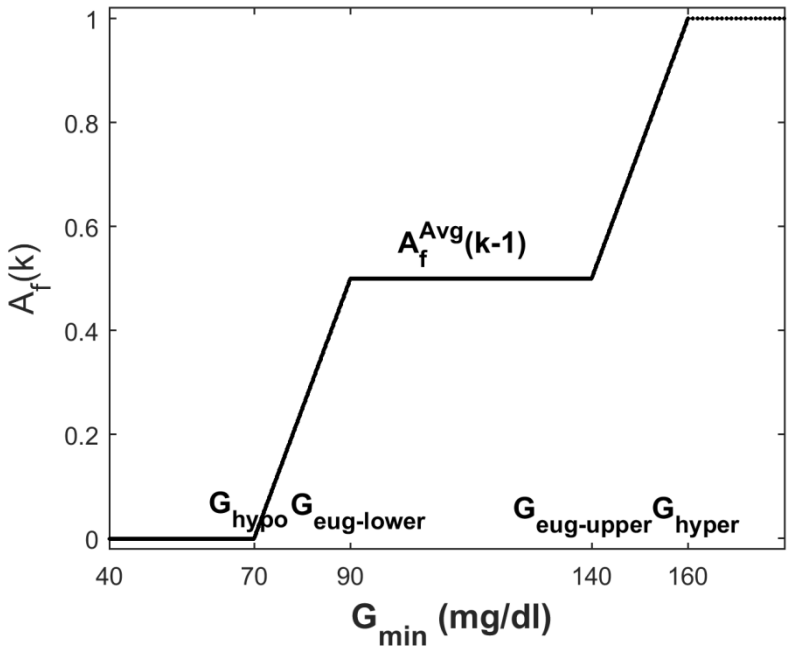

Figure 3.1 $A_f(k)$ as a function of minimum postprandial glucose excursion

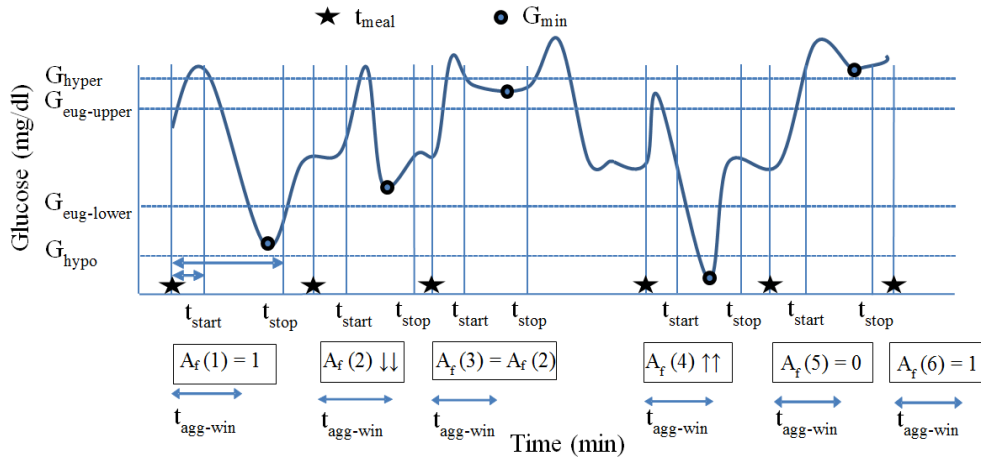

Figure 3.2 Changes of $A_f(k)$ with respect to G_{min} values over meal events for the ALPHA-BR

A special exception to the above rules is if a subsequent meal, snack or exercise event occurs during the postprandial observation time window (i.e. between t_{start} and

ends at t_{stop}). If this occurs, the observation end time (t_{stop}), is the time of the subsequent meal, snack, or exercise event. Adaptation of A_f proceeds as described above using the shorter observation window, but A_f is only changed if it is determined that hypoglycemia has occurred and A_f needs to be decreased. This is to avoid adaptively increasing A_f in response to observation periods that are too soon after a meal has occurred when postprandial hyperglycemia is still likely and acceptable.

3.3.2 ALPHA-ICR

ALPHA-ICR, like ALPHA-BR, is also an adaptive algorithm that adapts to a target range. However, rather than adjusting the postprandial basal insulin, ALPHA-ICR adjusts the ICR if postprandial glucose from a prior meal is outside of a target range. The pre-meal bolus prior to adaptation is a function of CHO, ICR, and the percentage of the insulin bolus given prior to the meal (I_p). The ICR is defined as $\text{ICR} = \frac{1}{3} \times \frac{1700}{\text{TDIR}}$ [111].

$$Bolus(k) = I_p^{Avg}(k) \times \frac{CHO}{ICR} \tag{4}$$

$$I_p^{Avg}(k) = \frac{I_p(k) + I_p^{Avg}(k-1) + I_p^{Avg}(k-2)}{3} \tag{5}$$

The ALPHA-ICR works similarly to ALPHA-BR except that it is the I_p which adapts based on postprandial hypoglycemia rather than the postprandial A_f. I_P is computed according to a similar piecewise linear equation given in equation 6. The same relationship can be shown as is given in Figure 3.1 except that the y-axis is for I_P, which has an upper and lower range of pre-meal insulin (I_P) on the y-axis set to 40% to 100%.

$$I_P(k) = \begin{cases} 0.4, & 0 \le G_{min} \le G_{hypo} \\ \dfrac{G_{min} - G_{hypo}}{G_{eug-lower} - G_{hypo}} \times I_P^{Avg}(k\text{-}1), & G_{hypo} \le G_{min} \le G_{eug-lower} \\ I_P^{Avg}(k\text{-}1), & G_{eug-lower} \le G_{min} \le G_{eug-upper} \\ \dfrac{G_{min} - G_{hyper}}{G_{hyper} - G_{eug-upper}} \times \left(1 - I_P^{Avg}(k\text{-}1)\right) + 1, & G_{eug-upper} \le G_{min} \le G_{hyper} \\ 1, & G_{hyper} \le G_{min} \end{cases} \quad (6)$$

3.3.3 Tuning parameters

ALPHA-BR has seven parameters to be determined. These parameters are G_{hypo}, $G_{eug\text{-}lower}$, $G_{eug\text{-}upper}$, G_{hyper}, t_{start}, t_{stop} and $t_{agg\text{-}win}$. ALPHA-ICR has the same parameters as ALPHA-BR except $t_{agg\text{-}win}$ is unnecessary since only the pre-meal bolus is adjusted and there is no window of postprandial adjustment. Changing G_{hypo} affects how gradually the adaptation occurs when postprandial hypoglycemia is observed. Changing $G_{eug\text{-}lower}$ affects the euglycemic range over which adaptation does not occur. Likewise, changing the G_{hyper} parameter will affect how rapidly adaptation

occurs when postprandial hyperglycemia is observed and $G_{eug\text{-}upper}$ affects the upper range of euglycemia when no adaptation occurs.

We determined ad-hoc that three parameters were most sensitive for preventing hypoglycemia and optimizing time in euglycemia: G_{hypo}, $G_{eug\text{-}upper}$ and $t_{agg\text{-}win}$. Other parameters were fixed based on ad-hoc experimentation. The beginning of the postprandial observation window, t_{start} was fixed at 60 min to provide adequate time for glucose to peak following a meal [117]. The end of the postprandial observation window, t_{stop}, was fixed at 240 min. $G_{eug\text{-}lower}$, was fixed at 90 mg/dl and G_{hyper} was fixed to 160 mg/dl. To tune the parameters we compared performance outcome metrics (percent time less than 70 mg/dl, percent time between 70 and 180 mg/dl, and percent time greater than 180 mg/dl) as we varied the parameters. We varied G_{hypo} between 40 and 80 mg/dl, $t_{agg\text{-}win}$ between 0.5 hr to 3 hr, and $G_{eug\text{-}upper}$ between 110 and 140 mg/dl. Under the results section, we show how performance varied with respect to the different combinations of these tuned parameters.

3.3.4 Testing under real-world meal scenario

A. Background on FMPD control algorithm used in testing

For the evaluation of the ALPHA algorithm, we used a control algorithm on which we have previously reported. The OHSU FMPD controller is a classical fading memory proportional derivative controller that considers both the proportional error

(i.e. distance from a glucose target) as well as the derivative error (i.e. how rapidly the glucose is changing with respect to time). The glucose target was set to 130 mg/dL and the derivative error was calculated using the slope of the glucose curve measured over the prior 15 minutes in time. The fading memory aspect of the controller is implemented by including exponentially weighted prior proportional and derivative error components in the control estimation of insulin. In addition to utilizing the proportional error and derivative error, there is a steady-state basal insulin delivered to the patient that is calculated using the patient's total daily insulin requirement. We have published extensively on the FMPD algorithm both on in-silico evaluations and in human clinical trials [20, 22, 28].

B. Background on MPC control algorithm used in testing

While ALPHA was tuned and evaluated primarily on the FMPD control algorithm, we did additional preliminary analysis of the ALPHA algorithm using the OHSU model predictive control algorithm (MPC) described under [49]. The OHSU MPC uses a physical model of the glucoregulatory system including a model of insulin kinetics, insulin dynamics, carbohydrate absorption kinetics, and a model for exercise to predict future glucose trajectories across a prediction horizon and selects an optimal dosing schedule for insulin [36, 52]. It then delivers the current insulin dose. The optimization is carried out every 5 minutes when new CGM data arrives

at the controller. The analysis on the MPC algorithm was not as extensive as the analysis and tuning done on the FMPD algorithm. The purpose of doing additional analysis on the MPC algorithm was do demonstrate that ALPHA can be used on different control algorithms.

C. Evaluation of ALPHA using FMPD and real-world meal scenarios

Twenty real-world meal scenarios were acquired from a 4-day outpatient AP study [64]. Each virtual patient was given each of the 20 meal scenarios while the patients' glucose was controlled using (1) the OHSU FMPD controller [20, 22, 28] (called AP), (2) the OHSU FMPD + ALPHA-BR (called ALPHA-BR), and (3) the OHSU FMPD + ALPHA-ICR (called ALPHA- ICR). The system was further challenged by introducing a randomly selected -30% to 30% meal uncertainty that was applied to each carbohydrate intake in each meal scenario as has been done in other in-silico trials of postprandial meal adaptation [113]. Circadian variability of insulin sensitivity was introduced to the insulin parameter S_{f1}, S_{f2} and S_{f3} by varying these parameters with respect to time of day using equation 7 [113]:

$$S_{fi}(t)=S_{fi}^{*}\times(1+0.3\sin(\frac{2\pi}{24\times60/Ts}\times t+2\pi\times RND),\ i=1,2,3 \tag{7}$$

where, RND is a random variable generated from a uniform distribution between 0 and 1; Ts is the sampling interval (5 minutes). Sfi* in equation 7 denotes the nominal

value of each of the insulin sensitivity factors. Notice that, in this paper, we have not changed ICR throughout a day. The AP system is designed to compensate for the intra-day variability of the ICR value. Our AP delivers 80% of the meal insulin at the time of the meal and then allows the controller to deliver the additional meal insulin during the hours following the meal. This approach has also been implemented and described in [113]. Notice also that the AP algorithms used in this work and the in-silico virtual patient population models are designed to work with rapid-acting insulin; the AP systems presented in this paper are not designed to be used with long-acting insulin.

3.3.5 Evaluation metrics and statistical analysis

We evaluated the performance of ALPHA-BR and ALPHA-ICR on the 23 patients from the in-silico population who experienced greater than 1% time in hypoglycemia. The primary outcome measure for the experiment was percent time in hypoglycemia (<70mg/dl). Secondary outcome measures were percent time in hyperglycemia (>180mg/dl), percent time in range (70-180 mg/dl), number of times rescue carbs were required, low blood glucose index (LBGI) and high blood glucose index (HBGI). The Wilcoxon rank-sum test was used to test statistical difference between AP, AP+ALPHA-BR and AP+ALPHA-ICR with significance level set to 0.05. In addition to showing adaption results on the 23 patients who experienced

greater than 1% time in hypoglycemia (Table X), we also show results on all 99 of the virtual patients (Table XI).

3.4 Results

3.4.1 Determining $G_{min\text{-}lower}$ and $t_{agg\text{-}win}$

Figure 3.3 and Figure 3.4 show how the performance comparisons between AP and ALPHA-BR across different parameters that were tuned for the subjects with greater than 1% time in hypoglycemia. Figure 3.3 shows a substantial reduction in percent time in hypoglycemia when comparing AP with the ALPHA-BR and the improvement is greater for larger $t_{agg\text{-}win}$ sizes. This makes sense since if $t_{agg\text{-}win}$ is larger, it means that the postprandial insulin dosing is changed over a longer period of time. The optimal time for applying the aggressiveness factor is for $t_{agg\text{-}win}$ = 1.5 hr, after which there is not a significant improvement. There is also a reduction in percent time in hypoglycemia by increasing G_{hypo} with minimal hypoglycemia observed when G_{hypo} = 80 mg/dl. Figure 3.4 shows how adjusting $t_{agg\text{-}win}$ and G_{hypo} affected percent time in hyperglycemia and time in range for $G_{eug\text{-}upper}$ fixed to 140 mg/dl. We selected a G_{hypo} of 70 mg/dl based on the consideration that there was not a significant difference in time in hypoglycemia between 70 and 80 mg/dl ($p = .46$), but there was less time in hyperglycemia when G_{hypo} was set to 70 mg/dl as shown in Figure 3.4. When we varied $G_{eug\text{-}upper}$ between 90 and 140 mg/dl with G_{hypo}=70 mg/dl

and $t_{agg\text{-}win}$=1.5 hr, we observed marginally increased time in range for smaller values of $G_{eug\text{-}upper}$. However, to maintain a stable target glycemic range during which the system did not adapt (see Figure 3.1), we set Geug-upper to 140 mg/dl. Time in hypoglycemia was lowest (0.54%) with the ALPHA-BR for the optimized $t_{agg\text{-}win}$ = 1.5 hr and G_{hypo}=70 mg/dl, compared to AP (1.92%). However, time in hyperglycemia increased slightly from 13.5% to 15.6%.

The ALPHA parameters were also tuned for ALPHA-ICR. The ALPHA-ICR implementation was far less sensitive to the parameters than ALPHA-BR. For example, when we varied G_{hypo} from 40 to 80 mg/dl with $G_{eug\text{-}upper}$=140 mg/dl, it only changed the percent time in hypoglycemia from 1.92% to 1.77% and the difference was not significant (p=.72). Similarly, when we varied the $G_{eug\text{-}upper}$ from 90 to 140 mg/dl with G_{hypo}=80 mg/dl, we saw no change in percent time in range and hypoglycemia (p=.73). Therefore, we used the same $G_{eug\text{-}upper}$ and G_{hypo} parameters in the ALPHA-ICR implementation that we used in the ALPHA-BR implementation. Table IX shows the final values of the ALPHA-BR and ALPHA-ICR parameters. Table X shows improvement in glycemic control for subjects who experienced high hypoglycemia under the AP condition (>1%). Comparable glycemic outcomes were observed across all the in-silico subjects as shown in Table XI.

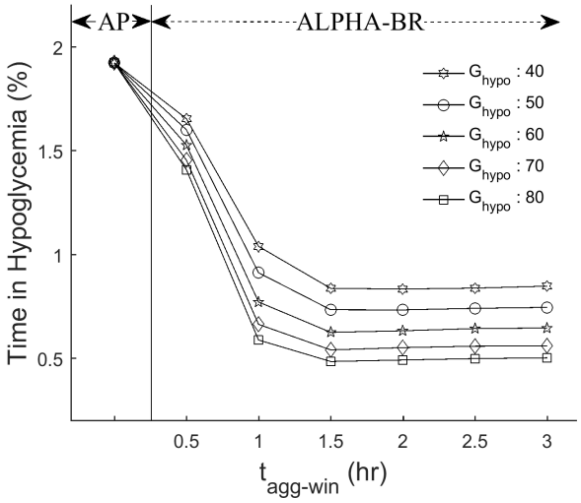

Figure 3.3 Percent time in hypoglycemia across different $t_{agg\text{-}win}$ and G_{hypo}, for $G_{eug\text{-}upper}$ fixed at 140 mg/dl.

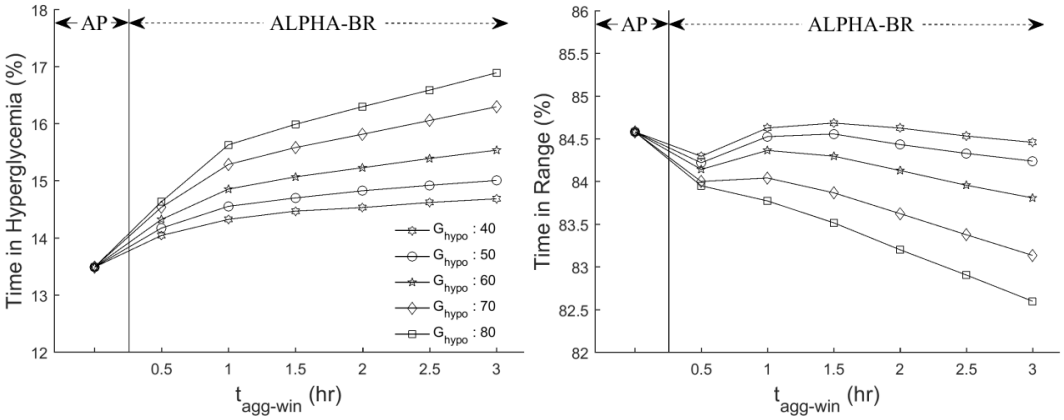

Figure 3.4 Percent time in hyperglycemia (left) and euglycemia (right) across different parameter settings

Table IX The optimal parameters of ALPHA-BR and ALPHA-ICR

G_{hypo} [mg/dl]	$G_{eug\text{-}lower}$ [mg/dl]	$G_{eug\text{-}upper}$ [mg/dl]	G_{hyper} [mg/dl]	t_{start} [min]	t_{stop} [min]	$t_{agg\text{-}win}$ [hr]
70	90	140	160	60	240	1.5

3.4.2 Comparison of adaptive AP vs. non-adaptive AP

Overall, the ALPHA-BR implementation was successful in reducing post-prandial hypoglycemia while ALPHA-ICR reduced hypoglycemia, but not as significantly. The comparison between the performance of ALPHA-BR, ALPHA-ICR and AP across all meal scenarios for subjects with higher hypoglycemia (>1%) is shown in Table X. ALPHA-BR significantly reduced time in hypoglycemia compared with AP (0.54% vs. 1.92%, $p<0.001$) whereas ALPHA-ICR reduced time in hypoglycemia slightly and the difference was not significant (1.77%, $p=.41$). ALPHA-BR also reduced average rescue carbs per day (0.36 vs. 1.29, $p<0.001$). However, ALPHA-BR resulted in modest increase in time in hyperglycemia (15.6% vs. 13.5%, $p=.06$) and an increased average glucose level (147.3 vs. 142.1 mg/dl, $p<0.001$) compared with AP.

Table XI shows the outcome measures for all virtual subjects. Time in hypoglycemia was significantly reduced with ALPHA-BR compared to AP whereas this reduction was not significant with ALPHA-ICR. ALPHA-BR resulted in increased time in hyperglycemia and HBGI compared with AP, but these differences were not significant. ALPHA-BR did result in a small increase in average glucose compared to AP (153.5 vs. 150.9 mg/dl, $p=0.04$).

Table X Comparison between AP, ALPHA-BR, ALPHA-ICR across the meal scenarios for subjects with hypoglycemia greater than 1%

$\mu \pm \sigma$	AP	ALPHA-BR	ALPHA-ICR
Time in Hypoglycemia [%]	1.92 ± 0.74	0.54 ± 0.3*	1.77 ± 0.8
rescue carbs [event/day/patient]	1.29 ± 0.47	0.36 ± 0.19*	1.19 ± 0.52
Time in Euglycemia [%]	84.6 ± 4.4	83.9 ± 4.6	83 ± 4.4
Time in Hyperglycemia [%]	13.5 ± 4.2	15.6 ± 4.4	15.3 ± 4.1
Average glucose [mg/dl]	142.1 ± 5.2	147.3 ± 5.47*	144.6 ± 5.2*
HBGI	4.6 ± 0.9	4.8 ± 1.1	5 ± 1
LBGI	2.73 ± 0.44	1.74 ± 0.28*	2.7 ± 0.5

*) shows significance compared to AP (p-value < 0.05)

Table XI Comparison between AP, ALPHA-BR, ALPHA-ICR across the meal scenarios for all virtual patients

$\mu \pm \sigma$	AP	ALPHA-BR	ALPHA-ICR
Time in Hypoglycemia [%]	0.57 ± 0.86	0.17 ± 0.27*	0.53 ± 0.83
rescue carbs [event/day/patient]	0.38 ± 0.57	0.11 ± 0.18*	0.35 ± 0.55
Time in Euglycemia [%]	80.9 ± 6.9	80.1 ± 6.9	80.3 ± 6.7
Time in Hyperglycemia [%]	18.5 ± 7.2	19.7 ± 6.9	19.2 ± 6.8
Average glucose [mg/dl]	150.9 ± 11	153.5 ± 11*	151.8 ± 10.7
HBGI	5.3 ± 1.9	5.5 ± 1.9	5.4 ± 1.9
LBGI	1.46 ± 0.94	1.09 ± 0.56*	1.45 ± 0.93

*) shows significance compared to AP (p-value < 0.05)

Table XII Convergence at each meal scenario in ALPHA-BR

Meal Scenario	Mean carbs and std	# meals to converge	Final A_f^{Avg}
1	40.2 ± 9.9	2	0.77 ± 0.08
2	72.8 ± 36.6	5	0.65 ± 0.09
3	45.1 ± 8.7	7	0.6 ± 0.09
4	42.6 ± 30.1	2	0.74 ± 0.11
5	42.8 ± 28.7	8	0.67 ± 0.05
6	47.4 ± 21.9	1	0.79 ± 0.13
7	46.4 ± 15.5	2	0.73 ± 0.11
8	32.6 ± 18.9	2	0.79 ± 0.11
9	40.2 ± 34.7	3	0.75 ± 0.09
10	38.9 ± 20	2	0.75 ± 0.1
11	45.1 ± 25.4	3	0.67 ± 0.12
12	31.6 ± 16.9	2	0.75 ± 0.1
13	40.4 ± 30.4	5	0.63 ± 0.07
14	55.8 ± 35.2	2	0.79 ± 0.1
15	57.2 ± 15.9	7	0.62 ± 0.09
16	33.9 ± 21.6	2	0.75 ± 0.09
17	48.4 ± 24.8	2	0.74 ± 0.11
18	32.2 ± 11.1	2	0.75 ± 0.08
19	40.9 ± 21.7	5	0.65 ± 0.12
20	38.9 ± 2.6	2	0.71 ± 0.1

Average	43.7 ± 9.7	3.3 ± 2.1	0.72 ± 0.06

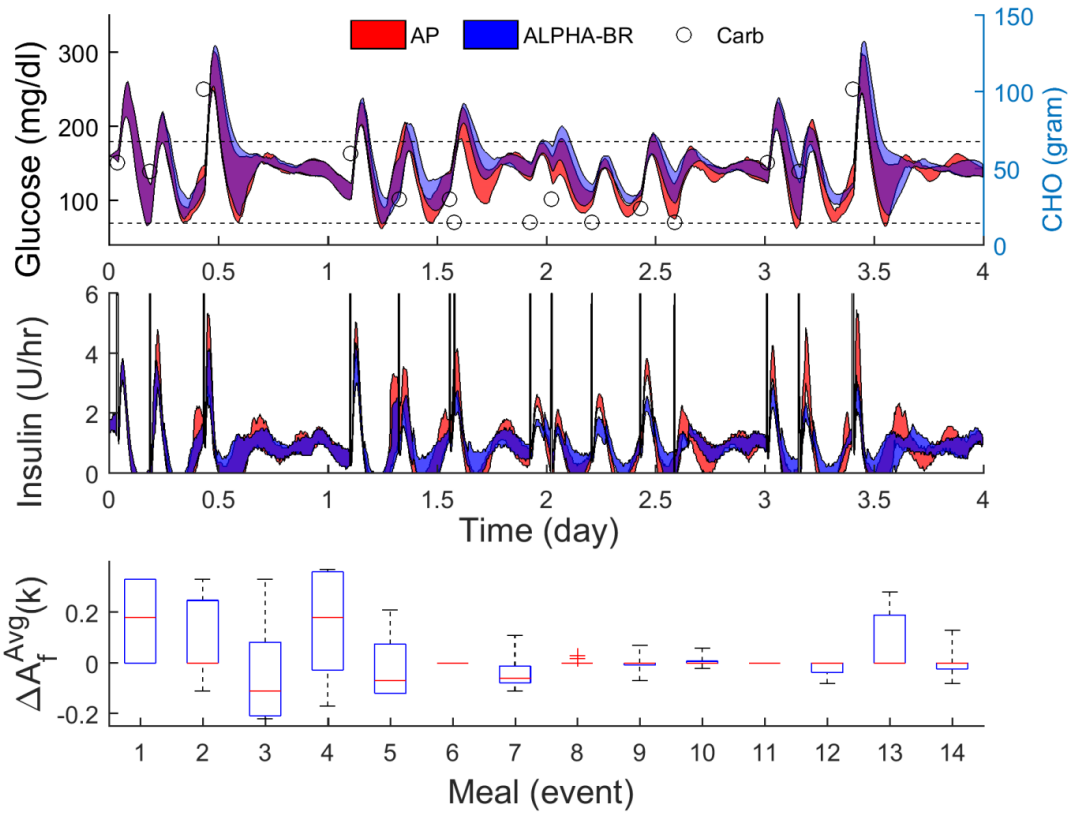

Figure 3.5 Interquartile range of the glucose profile and the box-plot of the changes of the A_f^{Avg} over the meal events across the virtual patients for the 5th meal scenario

Figure 3.5 compares the performance of AP and ALPHA-BR with the optimized ALPHA-BR parameters for the 5th meal scenario. The adaptation of the A_f^{Avg} over the meal events is shown in the lower subplot. The aggressiveness factor started at a value of 1 and then converged over time to a final value. ALPHA-BR gradually began reducing hypoglycemia after the first day. We defined convergence of A_f to be

the meal number when A_f changed less than 5% from the median of the next three A_f values. Notice that for this example scenario in Figure 3.5, A_f converged after 8 meals. Table XII shows the convergence number for each of the meal scenarios across the subjects with hypoglycemia greater than 1%.

A natural alternative to the ALPHA algorithm could be to simply increase the glucose target of the control algorithm. The performance of ALPHA-BR was compared with the FMPD algorithm when the target for the FMPD algorithm was increased from 115 mg/dl to 130 mg/dl. By increasing the target value to 130 mg/dl, time in hypoglycemia was reduced; however, this reduction was not as significant compared to ALPHA-BR, which used a target of 115 mg/dL. In addition, by increasing the target value, the time in hyperglycemia increased more than ALPHA-BR. And the time in hyperglycemia significantly increased with the higher target value. Table XII summarizes these results. From this analysis, we concluded that using ALPHA was more effective at reducing postprandial hypoglycemia than simply raising the glucose target of the control algorithm.

Table XIII Comparison between AP with higher target value and ALPHA-BR across the meal scenarios for all virtual subjects

$\mu \pm \sigma$	AP $_{(TGT = 115\ mg/dl)}$	AP $_{(TGT = 130\ mg/dl)}$	ALPHA-BR
Time in Hypoglycemia [%]	0.57 ± 0.86	0.38 ± 0.67	0.17 ± 0.27*

rescue carbs [event/day/patient]	0.38 ± 0.57	0.26 ± 0.45	0.11 ± 0.18*
Time in Euglycemia [%]	80.9 ± 6.9	78.1 ± 7.2*	80.1 ± 6.9
Time in Hyperglycemia [%]	18.5 ± 7.2	21.5 ± 7.4*	19.7 ± 6.9
Average glucose [mg/dl]	150.9 ± 11	156.4 ± 11.4*	153.5 ± 11*
HBGI	5.3 ± 1.9	5.9 ± 2*	5.5 ± 1.9
LBGI	1.46 ± 0.94	1.31 ± 0.95	1.09 ± 0.56*

*) shows significance compared to AP. (p-value < 0.05)

3.5 Discussion and Conclusion

We describe here an adaptive AP algorithm to reduce postprandial hypoglycemia by adjusting either postprandial basal insulin (ALPHA-BR) or pre-meal bolus insulin (ALPHA-ICR). Both implementations reduced time in hypoglycemia; however, ALPHA-BR reduced hypoglycemia further and was selected as the better implementation. For the 23 subjects with hypoglycemia greater than 1%, ALPHA-BR was able to significantly reduce time in hypoglycemia from 1.92% to 0.54% while ALPHA-ICR only reduced hypoglycemia to 1.77% (Table X).

To demonstrate whether ALPHA-BR is effective on an algorithm different than the OHSU FMPD algorithm, we evaluated ALPHA-BR on the OHSU single-hormone

MPC algorithm [49]. ALPHA-BR significantly reduced percent time in hypoglycemia compared with MPC from 0.55% to 0.19% ($p < 0.001$) in the same virtual patient population and same meal scenarios. ALPHA-BR also significantly reduced average rescue carbohydrates needed per day from 0.42 [S.D. 0.41] to 0.16 [S.D. 0.21] ($p < 0.001$). For the MPC algorithm without ALPHA-BR, the percent time in range (70-180 mg/dL) was 84.39% while time in range was lower at 81.27% with MPC plus ALPHA-BR ($p<0.001$). The percent time in hyperglycemia for MPC was 15.08% while the MPC plus ALPHA-BR had time in hyperglycemia of 18.54% ($p < 0.001$). These results are summarized in a Supplemental Table XV in the supplementary section.

To further evaluate across alternative in-silico simulators, we tested the ALPHA-BR across 10 virtual adults of the single hormone UVa/Padova simulator [31] using the OHSU-FMPD controller. However, we did not observe any postprandial hypoglycemia using this simulator with the non-adaptive OHSU-FMPD algorithm. Therefore, we were unable to evaluate the ALPHA-BR and ALPHA-ICR algorithms using this simulator.

A major finding of this paper is that adapting post-prandial basal insulin is more effective at influencing post-prandial hypoglycemia than adaptively changing pre-meal insulin. In addition, ALPHA-BR demonstrates that the average aggressiveness

factor should be reduced after each meal for 1.5 hours to gain substantial reduction in time in hypoglycemia. The ALPHA-BR algorithm can be used to initialize the postprandial insulin dosing based on in-silico testing. For example, for the FMPD algorithm evaluated here, we determined that the postprandial insulin should be reduced by 28 percent from the typical insulin dosing (i.e. not after a meal). ALPHA-BR can also be used to adapt to each individual during usage as that patient's insulin sensitivity, diet and behavior change with time.

The ALPHA-BR adaptation converged on average after approximately 3 meals (Table XII), showing the feasibility of the ALPHA-BR in real-time applications. Other papers have also presented adaptive algorithms to improve glycemic control in people with T1D and these algorithms typically require about a week to converge. Toffanin *et al*. (2017) [122] developed a run-to-run algorithm for use within an AP study with fixed amount of meals at specific times (40, 80 and 60 grams for breakfast, lunch and dinner, respectively). They adjusted nighttime basal insulin and daytime bolus insulin adaptively to reduce time in hypoglycemia and increase time in range. The algorithm was tested in two different scenarios across 100 virtual patients of the UVA/Padova simulator using a model predictive control algorithm. In one scenario, a random ±30% variation was added to the nominal insulin sensitivity for 8 weeks and in the other, the random variation was added gradually from ±10%

to ±30% during 4 weeks. In the 1st scenario, time in range improved from 86% after week 1 to 90.86% and 91.35% after week 4 and 8. Time in hypoglycemia was reported as 0.66%, 0.17%, 0.91% for week 1, 4 and 8 respectively. In the 2nd scenario, time in hypoglycemia was reported as 0.52% and 0.65% after week 1 and 4, respectively. The convergence rate of their algorithm exceeded one week. In another run-to-run study by Herrero *et al*. (2017) [113], only meal bolus insulin was adaptively changed to improve glycemic controls. They also used fixed pattern of carbs dose intake (60, 100 and 80 grams for breakfast, lunch, dinner, respectively) and incorporated inter-day and intra-day insulin sensitivity and meal variabilities to their simulations. They evaluated their algorithm across 11 adolescences and 11 adults within the UVA/Padova simulator using their developed controller, Imperial College Artificial Pancreas. After a 3-month simulation, time in range was improved from 82% to 89.5% whereas time in hypoglycemia did not change (0.21%) among 11 adults. A major difference between these studies and the current study is that the meal scenarios presented to our virtual patients were taken from real-world meals consumed by patients in an AP study. The meal times and amounts were sporadic both in times and amounts. ALPHA can robustly manage this variability and convergence still occurred rapidly across all 20 real-world meal scenarios.

A limitation of the ALPHA algorithm is that it treats all meals equivalently, which may not be appropriate if insulin sensitivities change throughout the day. We considered using a case-based-reasoning approach similar to Herrero et al.'s approach [113], to handle difference in meal times. However, we found that even with insulin sensitivity varying +/- 30% throughout the day and incorporating real-world sporadic meals into our simulations, convergence of the adaptation was rapid without the need for separately accounting for time-of-day or case-based meals. Another limitation of this study is that it was only done on an in-silico virtual patient population. While real-world meals were used from real-world AP studies, the results are still based on a glucoregulatory model. In the future, we plan to evaluate ALPHA-BR within a clinical hybrid AP study. The preliminary analyses of ALPHA-BR across study participants demonstrated that the initial aggressiveness factor of 0.7 (also shown in table XI) could reduce time in hypoglycemia substantially. For our new clinical studies, we start all subjects with an aggressiveness factor of 0.7, and then allowing the aggressiveness factor to range from 0 to 1. In this way, the ALPHA algorithm can be used to increase or decrease the postprandial insulin from a starting value.

3.6 Conclusion

This paper has shown that adaptation is important within an AP as the physiology differences amongst people with T1D can be challenging for an AP to handle. If post-prandial hypoglycemia is observed, the best way to handle this is through post-prandial basal adjustments. Adjustments of pre-meal bolus on postprandial hypoglycemia had minimal benefit.

3.7 Acknowledgments

The guarantor of this research is Peter G. Jacobs who takes responsibility for the contents of this article. NR and PGJ designed the ALPHA algorithm, did the data analysis, and wrote the manuscript. JEY, RR, and JC contributed to the manuscript writing and data interpretation. This work was supported by grants from the National Institutes of Health (grant 1DP3DK101044). JRC and PGJ have a financial interest in Pacific Diabetes Technologies Inc., a company that may have a commercial interest in the results of this research and technology.

3.8 Supplementary Materials: In-silico patient population description

3.8.1 Glucoregulatory Model

The insulin kinetic model, which represents the pathway of absorption for short-acting insulin, was introduced as outlined in [36, 49]:

$$\dot{S_1} = u_I - \frac{S_1}{t_{max}}$$
$$\dot{S_2} = \frac{S_1}{t_{max}} - \frac{S_2}{t_{max}} \quad (8)$$
$$\dot{I} = \frac{S_2}{t_{max} V_I} - k_e I$$

where S_1 and S_2 represent the masses of insulin [mU/kg] in two subcutaneous compartments, u_I represents the rate of insulin infusion [mU/kg/min], I represents the plasma insulin concentration [mU/L], and t_{max}, V_I and k_e are the time to maximum absorption [min], distribution volume [L/kg] and elimination rate [min^{-1}] of insulin. The insulin dynamic model, which describes the action of plasma insulin on glucose, was presented as described in [36] and [125]:

$$\dot{X_1} = -k_{a1} X_1 + S_{f1} k_{a1} I$$
$$\dot{X_2} = -k_{a2} X_2 + S_{f2} k_{a2} I \quad (9)$$
$$\dot{X_3} = -k_{a3} X_3 + S_{f3} k_{a3} I$$

where x_1 [min^{-1}], x_2 [min^{-1}] and x_3 [unitless] represent the effect of insulin on glucose distribution, disposal and suppression of endogenous glucose production. S_{f1} [min^{-1} per mU/L], S_{f2} [min^{-1} per mU/L] and S_{f3} [per mU/L] are the insulin sensitivity factors. These factors vary significantly between individuals with T1D and are therefore of importance during the creation of the virtual population. k_{a1}, k_{a2} and k_{a3} [min^{-1}] are used as both entry rates of insulin into the action compartments as well as clearance rates of the insulin effect. The glucose kinetic model, which estimates the

glucose levels with respect to insulin and non-insulin mediated effects, was presented as in [36]:

$$\dot{Q_1} = -X_1 Q_1 - F_{01}^c - F_R + k_{12} Q_2 + U_G + EGP_0(1 - X_3)$$
$$\dot{Q_2} = X_1 Q_1 - k_{12} Q_2 - X_2 Q_2 \quad (10)$$

where Q_1 and Q_2 are the masses of glucose in the accessible (plasma) and non-accessible (rapidly-equilibrating interstitial) compartments, respectively [mmol/kg]. EGP_0 is the basal endogenous glucose production at a theoretical zero insulin concentration [mmol/kg/min]. F_{01}^c and F_R are the non-insulin mediated glucose uptake and the renal glucose clearance rate, respectively [mmol/kg/min]. U_G represents the glucose absorption rate from meals [mmol/kg/min] [36]:

$$U_G = \frac{D_G A_G (t - t_0) e^{-\frac{t - t_0}{t_{max,G}}}}{t_{max,G}^2} \quad (11)$$

where, $t_{max,G}$ is the time to maximum appearance rate of glucose in Q_1 [min], A_G is the carbohydrate bioavailability [unitless], t_0 is the meal announcement time [min] and D_G is the estimated carbohydrate intake (mmol/kg). Note that, in the in-silico simulations, D_G is converted from grams to mmol/kg to be compatible with the variables of the glucose kinetic model.

3.8.2 Virtual Patient Population

A virtual patient population, compatible with the characteristics of people with T1D, was generated for the in-silico simulations. Since the original glucoregulatory model was developed for people without diabetes [36] and [126], S_{f1}, S_{f2} and S_{f3} were modified to represent the sensitivity of insulin for people with T1D. A series of sensitivity composite (Sc) ranging from 0.1 to 2 was multiplied to the nominal values of S_{f1}, S_{f2} and S_{f3} in equation 9. The basal insulin rate at each Sc was computed at the steady state for a target level of 115 mg/dl. And, the total daily insulin requirement (TDIR) was estimated. Finally, the best Sc that the estimated TDIR was the closest to the mean clinical TDIR was selected. Based on the mean clinical TDIR of approximately 45 units/day, an Sc of 0.4 was chosen as the insulin sensitivity modifier across T1Ds. Then, the nominal insulin sensitivity factors were reduced by 60% for this T1D virtual population relative to people without diabetes. A similar relationship between the insulin sensitivity of people with and without T1D was investigated by Rickels et al. [112] in a euglycemic clamp study.

Next, virtual T1D individuals were created by statistically sampling from the distributions of the updated insulin sensitivity factors given an ad-hoc 75% correlation between S_{f1} and S_{f2}, and 25% correlation between S_{f2} and S_{f3}. After sampling the parameters of each virtual patient, the physiologic feasibility of each virtual patient was evaluated through two tests:

A) Steady-state glucose levels – in the absence of insulin, glucose should exceed 300 mg/dl.

B) Delivery of high-dose insulin (15 units/hr) should result in a low steady-state glucose level (typically less than 100 mg/dl from the baseline steady-state glucose).

Ninety-nine virtual individuals out of 100 passed the above criteria. Figure 3.6 shows the histogram of the TDIR values of the virtual population.

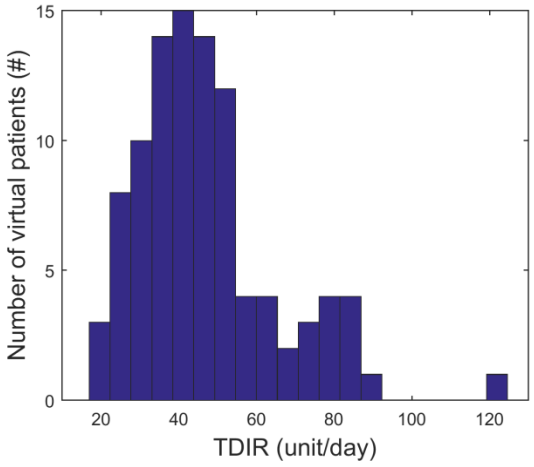

Figure 3.6 Histogram of the TDIR values of the virtual patients

The virtual patient population was evaluated with the above clinical dataset. Virtual patients were matched to clinical study participants by closest match of TDIR and weight. This approach was repeated for all 20 actual patients from each clinical study trial and the 20 closest virtual patients were identified. The same AP algorithm was used to control the glucose levels of each of the 20 virtual patients. The glucose profiles of the virtual patients were compared with the related actual glucose profiles

controlled by the same algorithm during the in-vivo trial (Table XIV). For all outcome measures, the virtual population was not statistically different from the true population. The time spent in hyperglycemia was slightly underestimated by the virtual population, which was not significant but was trending towards significant.

Table XIV Outcome metrics of the virtual population across the selected virtual patients

Outcome Metrics	Clinical Results	Simulated Results	*p*-value
Time in hypoglycemia (%)	2.8 ± 1.7	3.4 ± 1.3	0.23
Time in hyperglycemia (%)	22.9 ± 8.8	18.4 ± 5.3	0.08
Time in range (%)	74.3 ± 8.1	78.1 ± 5.1	0.11
LBGI	3.1 ± 1	3.5 ± 0.9	0.24
HBGI	6.2 ± 1.7	5.9 ± 1.2	0.47

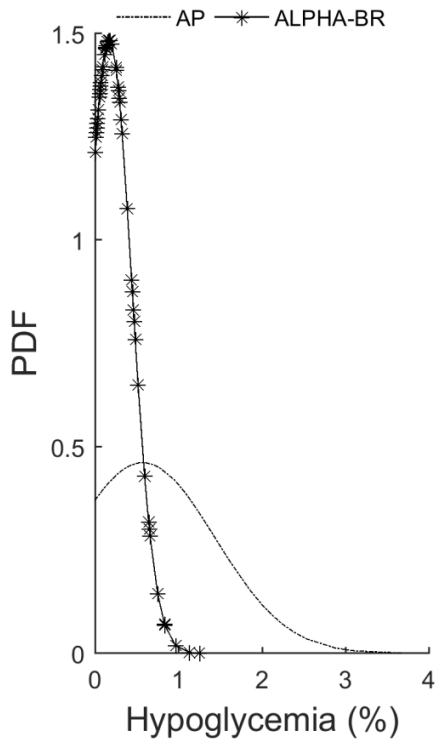
AP
ALPHA-BR
PDF
Hypoglycemia (%)

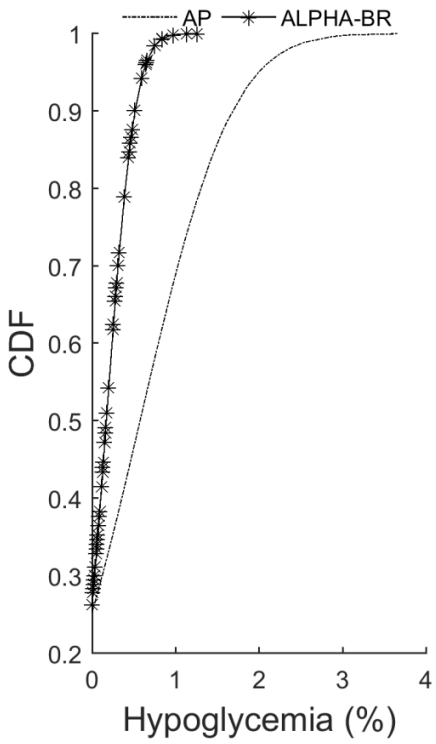
AP
ALPHA-BR
CDF
Hypoglycemia (%)

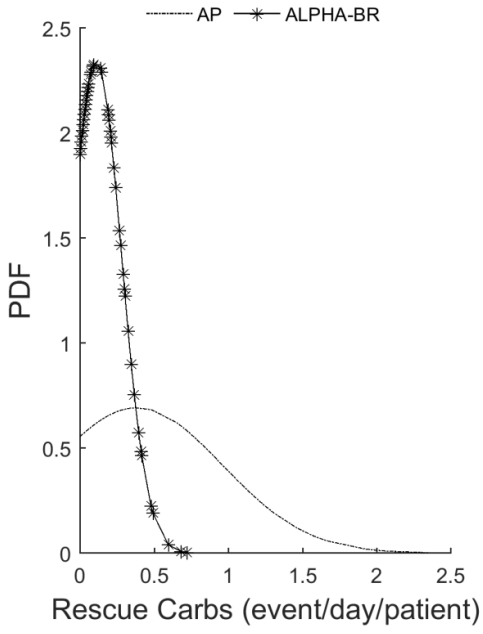
AP
ALPHA-BR
PDF
Rescue Carbs (event/day/patient)

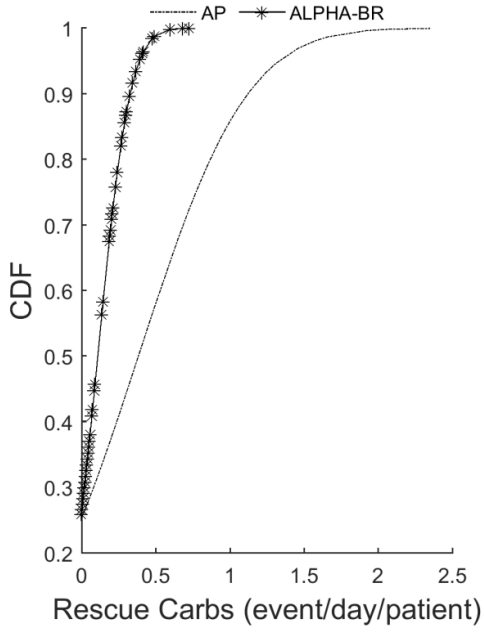
AP
ALPHA-BR
CDF
Rescue Carbs (event/day/patient)

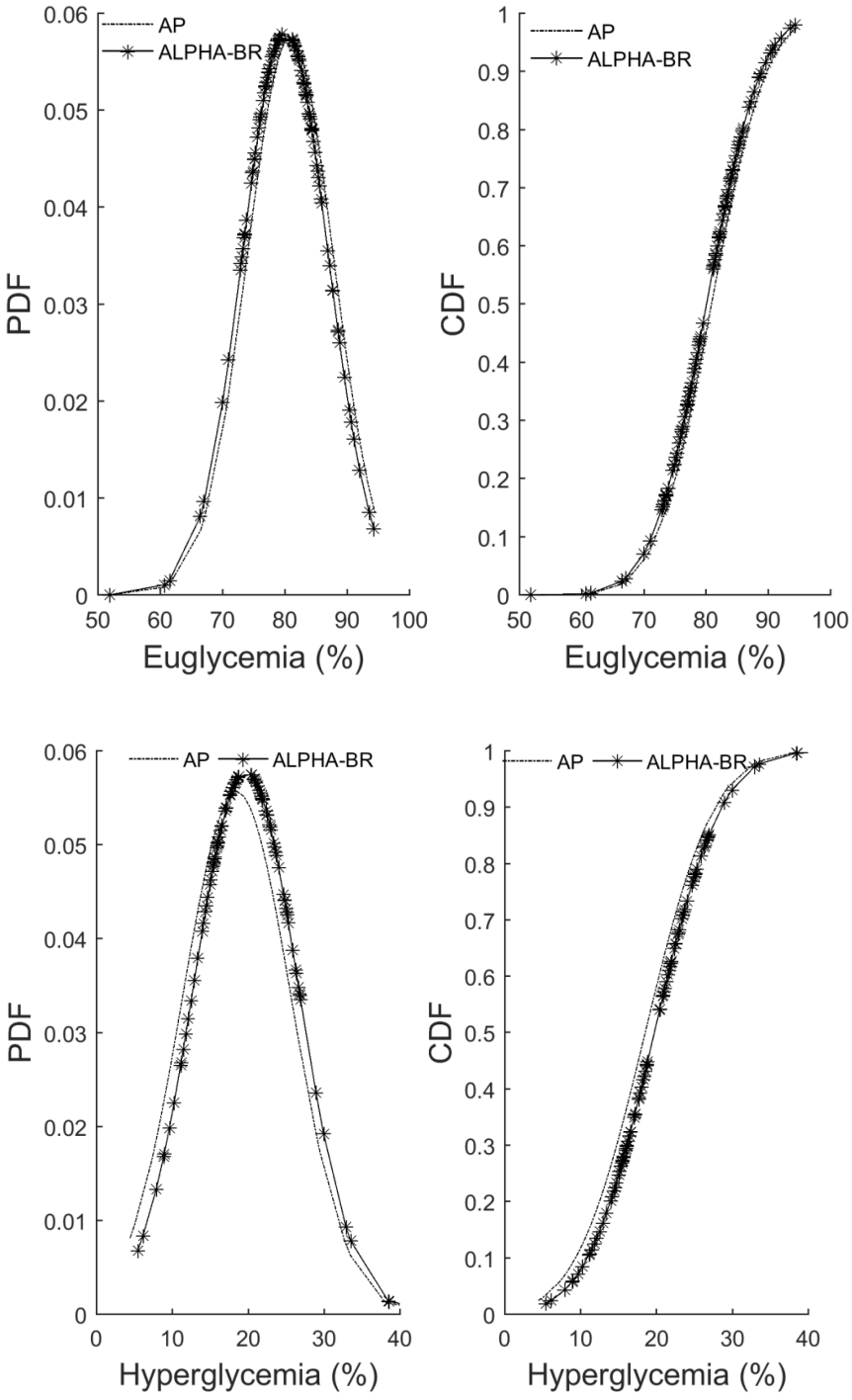
AP
ALPHA-BR
PDF
Euglycemia (%)
CDF
Euglycemia (%)
Hyperglycemia (%)
Hyperglycemia (%)

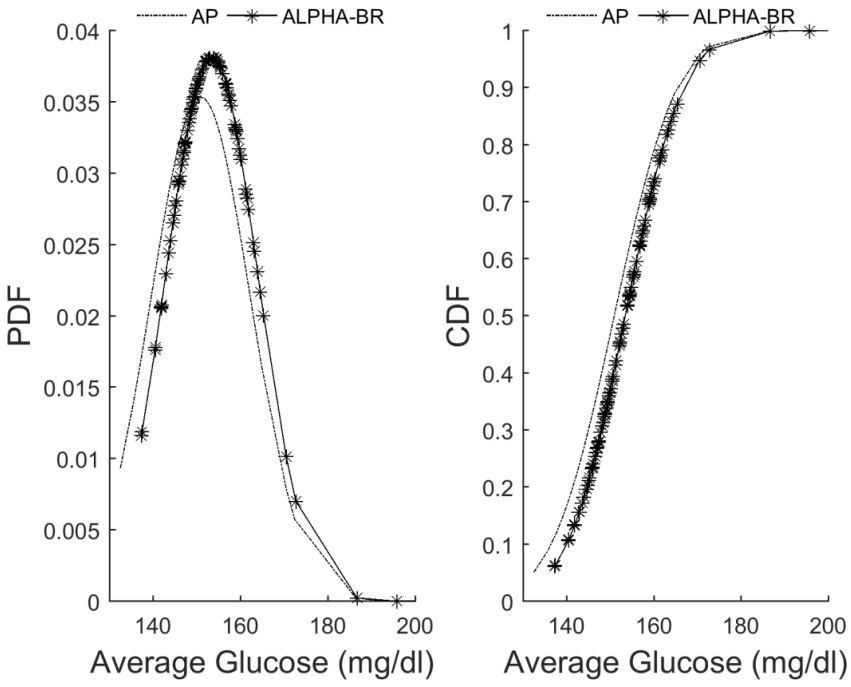
AP
ALPHA-BR
PDF
Average Glucose (mg/dl)
CDF
Average Glucose (mg/dl)

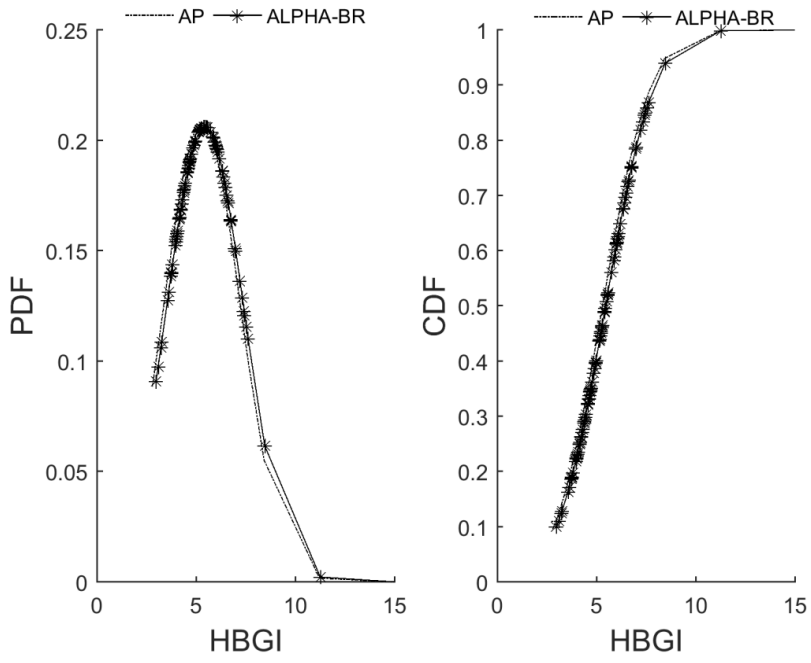
AP
ALPHA-BR
PDF
HBGI
CDF
HBGI

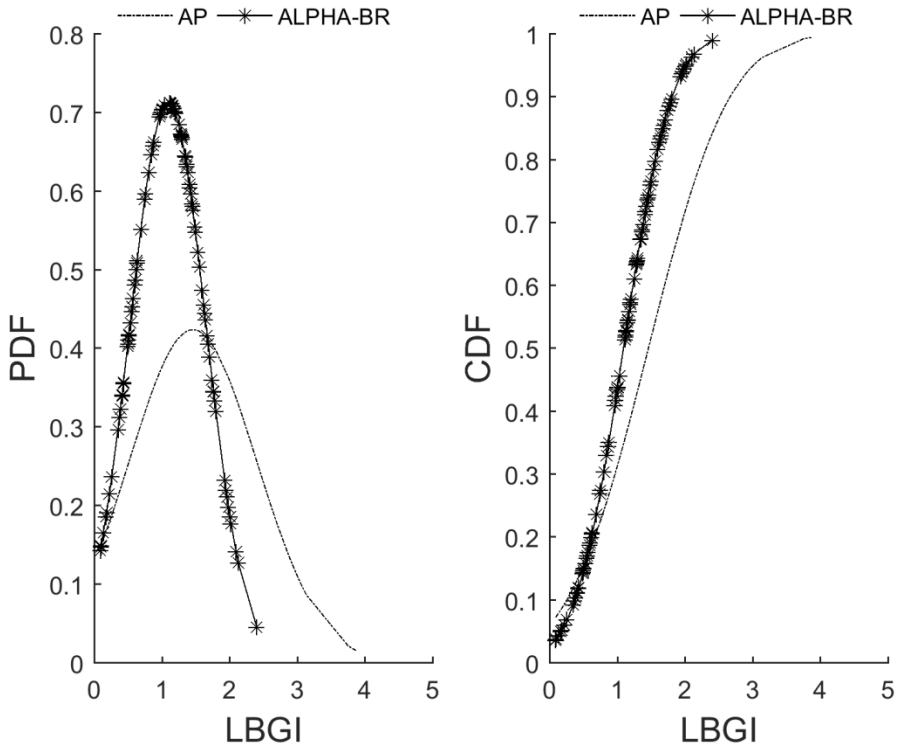

Figure 3.7 Cumulative distribution plots showing impact of ALPHA-BR on outcome measures

Table XV Performance of ALPHA on OHSU-MPC algorithm

$\mu \pm \sigma$	AP	ALPHA-BR
Time in Hypoglycemia [%]	0.55	0.19*
rescue carbs [event/day/patient]	0.42	0.16*
Time in Euglycemia [%]	84.39	81.27*
Time in Hyperglycemia [%]	15.08	18.54*

*) shows significance compared to AP. (p-value < 0.05)

3.8.3 ALPHA-BR evaluation using the UVA/Padova simulator

The performance of the ALPHA-BR was further evaluated using another virtual patient population, the UVA/Padova simulator. The UVA/Padova simulator consists of 100 T1D virtual adults, 100 T1D virtual adolescents and 100 T1D virtual children. In this section, we have tested the ALPHA-BR across the adult patients. Each of the 20 meal scenarios described above was given to the patients, and the clinical metrics were computed across all the patients and are shown in Table XVI. The results showed 40% reduction of time spent in hypoglycemia with the ALPHA-BR ($p = .063$) and small increase in time in hyperglycemia ($p = .66$).

Table XVI Comparison between AP and ALPHA-BR across the meal scenarios for all the UVA/Padova virtual subjects

$\mu \pm \sigma$	AP	ALPHA-BR
Time in Hypoglycemia [%]	1.48 ± 1.66	0.88 ± 1.1
rescue carbs [event/day/patient]	0.43 ± 0.5	0.25 ± 0.3
Time in Euglycemia [%]	86 ± 9.4	85.5 ± 9.6
Time in Hyperglycemia [%]	12.5 ± 8.9	13.6 ± 9.1
Average glucose [mg/dl]	141 ± 9 8	144.3 ± 7.8*
HBGI	4.1 ± 1.8	4.3 ± 1.8
LBGI	2.1 ± 1.7	1.7 ± 1.3
*) shows significance compared to AP (p-value < 0.05)		

4 Design of a Dual-Hormone Model Predictive Control for Artificial Pancreas with Exercise Model

Many studies have shown the importance of using a dual-hormone artificial pancreas to further reduce time in hypoglycemia. In dual-hormone APs, glucagon is injected when glucose is low, preventing severe glucose drops by increasing glucose production in liver. As there is no published dual-hormone AP with the MPC algorithm, a dual-hormone MPC is developed in this chapter.

Chapter Summary:

- A dual-hormone (DH) MPC is developed for dual-hormone AP analysis.
- A single-hormone (SH) MPC is developed to compare and evaluate the performance of the dual-hormone MPC.
- Both MPC algorithms are less complex, linearized, and compatible with subcutaneous insulin delivery and validated with meal events.
- We further extended both MPCs by integrating an exercise model.
- Results show that time in hypoglycemia is less with DH-MPC. Also, both MPC designs with an integrated exercise model reduced exercise-induced hypoglycemia more significantly compared to no exercise integration.

This work was originally published in 2016:

N. Resalat, R. Reddy, J. El Youssef, and P. G. Jacobs, "Design of a Dual-Hormone Model Predictive Control for Artificial Pancreas with Exercise Model" in 38th Annual International Conference of the IEEE Engineering in Medicine and Biology Society, Orlando, FL, 2016, pp. 2270-2273, Reprinted with Permission from IEEE.

4.1 Abstract

The Artificial Pancreas (AP) is a new technology for helping people with type 1 diabetes to better control their glucose levels through automated delivery of insulin and optionally glucagon in response to sensed glucose levels. In a dual hormone AP, insulin and glucagon are delivered automatically to the body based on glucose sensor measurements using a control algorithm that calculates the amount of hormones to be infused. A dual-hormone MPC may deliver insulin continuously; however, it must avoid continuous delivery of glucagon because nausea can occur from too much glucagon. In this section, we propose a novel dual-hormone (SH) switching model predictive control and compare it with a single-hormone (SH) MPC. We extended both MPCs by integrating an exercise model and compared performance with and without the exercise model included. Results were obtained on a virtual patient population undergoing a simulated exercise event using a mathematical glucoregulatory model that includes exercise. Time spent in hypoglycemia is

significantly less with the DH-MPC than the SH-MPC ($p= 0.0022$). Additionally, including the exercise model in the DH-MPC can help prevent hypoglycemia ($p < 0.001$).

4.2 Introduction

Diabetes mellitus is a physiological disorder where the body either is resistant to or does not sufficiently secrete insulin. Type 1 diabetes is the less prevalent but more challenging type of diabetes mellitus in which the pancreas fails to produce insulin for glucose regulation. Without insulin, glucose cannot be absorbed into tissues, and blood glucose (BG) levels increase, resulting in hyperglycemia (BG > 180 mg/dl). Difficulty controlling glucose is compounded by meals which require additional insulin. On the contrary, when glucose utilization is high, for example during physical activity, tissues absorb glucose more rapidly, and the BG can fall very steeply. The American Diabetes Association identifies a lower boundary of 70 mg/dl for the BG, below which is defined hypoglycemia, where severe symptoms may occur if untreated for even short periods [127]. The replacement of insulin in type 1 diabetes requires both basal insulin delivery, either with long-acting insulin or by continuous infusion of fast-acting insulin, and bolus insulin doses for meals with fast-acting insulin.

Insulin pump therapy (open-loop therapy) is a common method for people with type 1 diabetes to maintain euglycemia; the patient can use the insulin pump to infuse basal insulin and can also deliver boluses prior to meals [16]. For closed-loop insulin delivery, also known as the artificial pancreas (AP), insulin delivery is automatically adjusted based on sensed glucose levels and a control algorithm. In single hormone AP systems, only insulin is dosed whereas in dual hormone APs, glucagon is also dosed [19]. A number of closed loop algorithms utilize a proportional integral derivative controller [128], [129]. Our group has previously described variations of PID or PD AP control algorithm [22]. We also have described an exercise detection and dosing adjustment algorithm that can be incorporated [28]. Other groups have described single-hormone MPC including Hovorka et al. [108], Magni et al. [42] used a SH-MPC in the presence of three daily meals. Although they got good results, they did not account for low blood glucose especially during exercise. It may be necessary to include glucagon within a DH-MPC in order to prevent hypoglycemia, especially during exercise periods. Boiroux et al. [130] used a DH-MPC for blood glucose regulations during a day with three meals. They used a switching algorithm for each hormone's delivery. Although glucagon was mainly used to correct for postprandial hypoglycemia due to the injected insulin boluses, there was no glucagon delivery due to increased insulin sensitivity during exercise.

In this chapter, we introduce a DH-MPC approach that can switch between dual hormone and single hormone operation based on the sensed glucose level of the patient. Our DH-MPC algorithm includes a model for exercise, such that if exercise is detected or if a user announces an exercise event to the controller, the algorithm can respond appropriately. We test the feasibility of the algorithm in the presence of moderate exercise. We also compared the effect of including versus not including the exercise model in the MPC. We linearize the non-linear equations within the process model to reduce the processing time in the controller.

4.3 Material and Method

4.3.1 Process Model

The prediction of BG in our MPC algorithm is achieved using a glucoregulatory model, consisting of a glucose kinetics model, insulin kinetics and dynamics models, and glucagon kinetics and dynamics models. The model describes the relationship between subcutaneously delivered insulin and glucagon and blood glucose concentration. The glucose kinetics model defines the effect of the insulin and glucagon actions on the blood glucose, as follows [36]:

$$\dot{Q_1} = -X_1 Q_1 - F_{01}^c - F_R + k_{12} Q_2 + U_G + EGP_0(1 - X_3 + Y + k_{g3}\dot{Y})$$

$$\dot{Q_2} = X_1 Q_1 - k_{12} Q_2 - X_2 Q_2 \quad (1)$$

where Q1 and Q2 are the masses of glucose in the accessible and non-accessible compartments respectively, in mmol/L. F_{01}^{c} and FR represent non-insulin mediated glucose uptake and renal glucose clearance respectively, in mmol/L/min. U_G represents gut absorption rate in mmol/L/min, which is considered zero in this study. EGP0 is the basal endogenous glucose production in mmol/L/min at a theoretical zero insulin concentration [36]. The source of non-linearity in these equations comes from the interactions between the effect of the insulin on EGP, distribution and disposal within the measurable and non-measurable glucose compartments. These nonlinear equations are linearized based on a Taylor series expansion at each time point, where the higher order terms are excluded. The insulin kinetics model, which represents the insulin absorption rate from the short-acting insulin administration, as shown below [131]:

$$\begin{aligned}
\dot{Q_{1a}} &= ku_I - k_{a1}Q_{1a} - \frac{V_{max}Q_{1a}}{k_m + Q_{1a}} \\
\dot{Q_{1b}} &= (1-k)u_I - k_{a2}Q_{1b} - \frac{V_{max}Q_{1b}}{k_m + Q_{1b}} \\
\dot{Q_2} &= k_{a1}Q_{1a} - k_{a1}Q_2 \\
\dot{Q_3} &= k_{a1}Q_2 + k_{a2}Q_{1b} - k_eQ_3 \\
I &= \frac{Q_3}{V_I}
\end{aligned} \tag{2}$$

where Q_{1a} and Q_2 represent the insulin mass through the slow absorption pathway, and Q_{1b} represents a faster channel for insulin absorption. Q_3 represents plasma insulin mass [131]. All insulin masses are in mU/kg. The sources of nonlinearity in these equations come from the local degradation of insulin at the injection site. These non-linear equations are linearized using a Taylor series. The insulin dynamics model is based on a study from [36].

$$\begin{aligned}
\dot{X_1} &= -k_{a1}X_1 + k_{b1}\frac{Q_3}{V_{d_IN}} \\
\dot{X_2} &= -k_{a2}X_2 + k_{b2}\frac{Q_3}{V_{d_IN}} \\
\dot{X_3} &= -k_{a3}X_3 + k_{b3}\frac{Q_3}{V_{d_IN}}
\end{aligned} \tag{3}$$

where x_1 (min^{-1}), x_2 (min^{-1}) and x_3 (unitless) represent the effect of insulin on glucose distribution, glucose disposal and suppression of endogenous glucose production, respectively [36]. The glucagon kinetics model, which represents the absorption rate of subcutaneously injected glucagon, is reported based on a study from Lv et al. [109].

$$\begin{aligned}
\dot{X_{1g}} &= -(k_{1g} + k_{ge1})X_{1g} + u_g \\
\dot{X_{2g}} &= k_{1g}X_{1g} - k_{2g}X_{2g} \\
\dot{X_{3g}} &= k_{2g}X_{2g} - k_{ge2}X_{3g}
\end{aligned} \tag{4}$$

where x_{1g} and x_{2g} represent subcutaneous glucagon mass compartments and x_{3g} is plasma glucagon mass, all measured in mg/kg. The nominal values of the parameters for the glucagon kinetics model used in this chapter have been provided from Lv et al. [109]. The glucagon dynamic model, which describes the interaction between the glucagon and the glucose concentration, was developed from our published study [28].

$$\begin{aligned}\dot{Y} &= \frac{10^6 \times \dot{k}_c \times S_{fGG}}{V_{dGG}} X_{3g} - k_c Y = k_g - k_c Y \\ \dot{Y} &= Z \\ \dot{Z} &= k_g k_{2g} X_{2g} - k_g k_{ge2} X_{3g} - k_c Z\end{aligned} \tag{5}$$

Y represents the effect of glucagon on endogenous glucose production. Since the change on Y has an effect on EGP, we introduce a new variable Z as another state, which is used in the MPC algorithm. The values of the parameters of the glucagon kinetics are described previously [28]. These values change per subject and make a virtual patient population.

4.3.2 Model Predictive Controller

Model predictive control is an optimization based control algorithm, which considers the dynamic model of the plant. Unlike PID controllers, MPC is able to predict the future outputs and optimize the inputs to the plant accordingly.

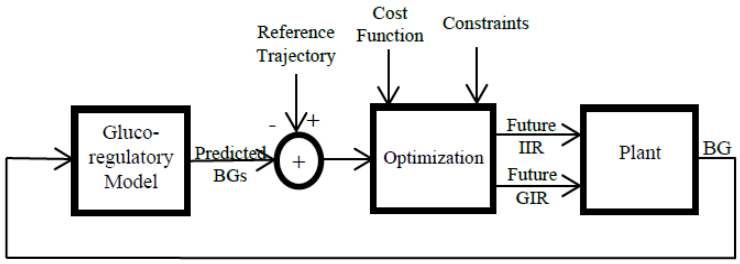

Figure 4.1 MPC Schematic

Figure 4.1 shows the structure of the MPC algorithm. The glucoregulatory model is the MPC process model. Typically, the plant would be the patient using the device. In our simulations, the structure of the plant is the same as the glucoregulatory model for the in-silico simulation; however, while the process model parameters are kept constant, the plant model parameters vary based on each individual virtual subject tested during simulation.

There are 13 state variables, which includes two state variables from the glucose kinetics model, four from the insulin kinetics model, three from the insulin dynamic models, three from the glucagon kinetics model and two from the glucagon dynamic model. Since the derivative of the glucagon concentration also affects the glucose concentration (equation 1), we define the second glucagon dynamic model state variable (variable Z in equation 5) for this effect. The final linearized form of the MPC equations is as follows:

$$x_m(k+1) = A_m x_m(k) + B_m u(k) + d_m(k);$$
$$y(k) = C_m x_m(k); \tag{6}$$

$x_m(k)$ is the state vector, u(k) is the 2-dimensional input vector (insulin and glucagon) and d(k) includes the constant terms resulting from the linearization. Since the controller requires a history of the output for future predictions, it is essential to relate the input vector to the output. We define a new vector as follows $x(k) = [\Delta x_m(k)^T \; y(k)]^T$ and the augmented state equations after some computations are re-arranged for the MPC algorithm as below:

$$\underbrace{\begin{bmatrix} \Delta x_m(k+1) \\ y(k+1) \end{bmatrix}}_{x(k+1)} = \underbrace{\begin{bmatrix} A_m & 0_m^T \\ C_m A_m & 1 \end{bmatrix}}_{A} \underbrace{\begin{bmatrix} \Delta x_m(k) \\ y(k) \end{bmatrix}}_{x(k)} + \underbrace{\begin{bmatrix} B_m \\ C_m B_m \end{bmatrix}}_{B} \Delta u(k) + \underbrace{\begin{bmatrix} 1 \\ C_m \end{bmatrix}}_{D} \Delta d_m(k);$$
$$y(k) = \underbrace{\begin{bmatrix} 0_m & 1 \end{bmatrix}}_{C} \begin{bmatrix} \Delta x_m(k) \\ y(k) \end{bmatrix}; \tag{7}$$

Therefore, the predicted outputs are calculated using equation 8.

$$Y_P = Fx(k) + \Phi \Delta U + \Psi \Delta D \tag{8}$$

where the matrices F, Φ and Ψ are presented in [132] and

$$Y_P = [y(k+1) \; y(k+2) \; \cdots \; y(k+N_p)]^T,$$
$$\Delta U = [\Delta u(k) \; \Delta u(k+1) \; \cdots \; \Delta u(k+N_c - 1)]^T,$$
$$\Delta D = [\Delta d_m(k) \; \Delta d_m(k+1) \; \cdots \; \Delta d_m(k+N_c - 1)]^T,$$

We chose a 300-minute prediction horizon as the action of insulin is several hours [36]. We chose a 20-minute control horizon as the results did not change substantially with a longer horizon. The cost function is defined in equation 9, which includes the reference trajectory (Rs) and the predicted outputs, and the tuning the control parameter ($\overline{R}$).

$$J = (R_s - Y_P)^T (R_s - Y_P) + \Delta U^T R_W \Delta U, \tag{9}$$

We can now compute the output of the optimizer (future inputs) by setting the derivative of the cost function with respect to ΔU zero and; after some calculations, the optimal ΔU is defined in equation 10.

$$\Delta U = (\Phi^T \Phi + \overline{R}_w)^{-1} \Phi^T (R_s - Fx(k) - \Psi \Delta D) \tag{10}$$

At the next step, we impose some constraints on the insulin and glucagon delivery. We set the maximum amount of insulin infusion rate (IIR) and glucagon infusion rate (GIR) to 15 Unit per hour and 50 microgram per hour, respectively. In this chapter, we show the performance of (1) a single hormone MPC algorithm (SH-MPC) in which the insulin is the only hormone used for blood glucose regulation, and (2) a dual hormone algorithm (DH-MPC). For the dual-hormone, we consider different ways of switching between single hormone and dual hormone operation. One option (DH-Thr) is to use a SH-MPC when glucose levels are greater than a

threshold (85 mg/dl) and then use DH-MPC when glucose levels drop below this threshold. A second option (DH-Pred) is to use SH-MPC when glucose levels are predicted to be above 70 mg/dl during the prediction horizon, otherwise switch to DH-MPC.

4.3.3 Exercise Model

Exercise can have profound effects on glucose levels in a person with type 1 diabetes, causing hypoglycemia if dosing is not adjusted. We incorporated an exercise model described by Hernandez et al. [73] into our process model. The exercise model affects the influence of insulin on glucose transport and disposal, and endogenous glucose production and causes increased insulin sensitivity by influencing equations 3 (k_{b1}, k_{b2} and k_{b3}) as follows:

$$\begin{aligned} k_{b1}^{*} &= M_{PGU} \times M_{PIU} \times k_{b1} \\ k_{b2}^{*} &= M_{PGU} \times M_{PIU} \times k_{b2} \\ k_{b3}^{*} &= M_{HGP} \times k_{b3} \end{aligned} \tag{11}$$

The model parameters (k_{b1}, k_{b2} and k_{b3}) are updated during the exercise period according to equation 12.

$$
\begin{aligned}
M_{PGU} &= 1 + \frac{\Gamma_{PGUA} \times PAMM}{35\ \text{mg/min}}; \\
M_{PIU} &= 1 + 2.4 \times PAMM; \\
M_{HGP} &= 1 + \frac{\Gamma_{HGPA} \times PAMM}{155\ \text{mg/min}};
\end{aligned}
\tag{12}
$$

where Γ_{PGUA} and Γ_{HGPA}, which are related to the percent of maximum oxygen consumption (PVO_{2max}), are calculated based on a dynamic model that is explained further in [73]. PAMM is the percent of active muscular mass.

4.3.4 Virtual patient population

We defined a virtual patient population for our in-silico simulations. We changed the most sensitive inter-subject parameters (EGP_0, k_{b1}, k_{b2}, k_{b3}, S_{fGG}, k_c and k_{g3}) of the process model across each subject. First, we produced a normal distribution based on the information of each parameter, given prior studies [36], [28], and then randomly selected samples, using a random number generator that is weighted by the parameter distribution, in order to generate the virtual population. Each parameter set was then subjected to a battery of tests to determine the physiologic feasibility. If a virtual subject did not pass each of the following 4 criteria, they were excluded from further testing. A total of 163 out of 400 virtual subjects passed the below criteria and were selected for our in-silico simulations.

A) Steady-state glucose levels; in the absence of insulin, glucose should exceeds 300 mg/dl.

B) Delivery of high-dose insulin (15 U/hr) should result in a low steady-state glucose level (typically less than 100 mg/dl).

C) Delivery of high-dose glucagon (20 mcg/kg) should result in a significant rise in glucose within 2 hours of the dose, greater than 50 mg/dl above the baseline steady-state glucose.

D) Delivery of a small dose of glucagon (0.2 mcg/kg) should not result in a response greater than 100 mg/dl above baseline steady-state glucose.

4.3.5 Test scenario and statistical analysis

All virtual subjects completed the following scenario. First, their glucose levels were brought to a steady state value of 160 mg/dl at time t=0. Next, subjects completed the equivalent of 45 minutes of exercise starting at time t=10 minutes at 60% PVO_{2max} and 80% PAMM. We compared the performance of our proposed methods in terms of the average time spent in hypo/hyperglycemia and the average blood glucose across the virtual subjects. We used the Student's t-test and the Wilcoxon rank-sum test to compare the average blood glucose and the time spent in

hypo-/hyperglycemia, respectively, across different process model configurations. The significance level was set to 5%.

4.3.6 Results and Discussion

Figure 4.2 shows the benefit of using DH compared with SH. Some subjects within the 25%-75% interquartile range using the SH process model crossed the hypoglycemia threshold interquartile range, whereas subjects using the DH model generally did not go hypoglycemic (only the lower 2.5% of subjects went hypoglycemic under DH). The time the virtual subjects spent in hypoglycemia was significantly less for the DH (p-value = 0.0022). In DH, the glucagon delivery not only prevented more subjects from becoming hypoglycemic, but also increased the median blood glucose across the subjects. Preventing hypoglycemia and reducing time spent in hypoglycemia can prevent symptoms related to hypoglycemia including nervousness, shakiness, dizziness and nausea. It is important to note that both the SH and DH process models included exercise in these results.

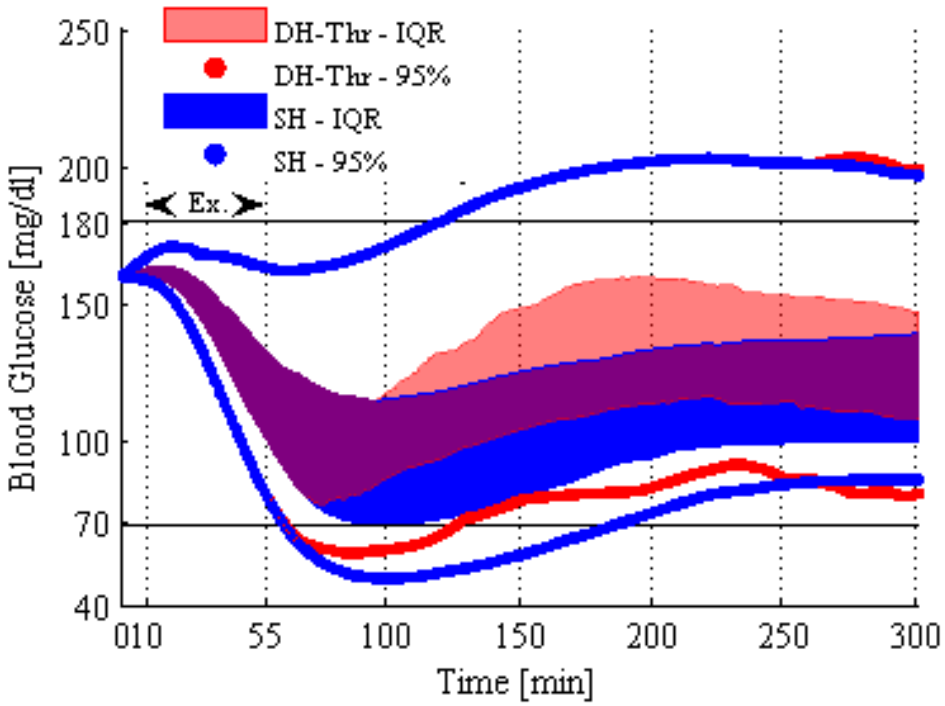

Figure 4.2 SH-MPC vs DH-MPC performance. Interquartile range along with the 95% intervals of the blood glucose across the virtual subjects are shown for DH-Thr (red line) and SH (blue line) methods with the exercise model included

Figure 4.3 shows the importance of including the exercise model in the process model. When the exercise model is not included, hypoglycemia occurs, whereas when it is included, hypoglycemia is generally avoided. When the exercise model is not included, the algorithm cannot anticipate forthcoming hypoglycemia and thereby turn off insulin and increase glucagon dosing as shown in the insulin and glucagon delivery panels of Figure 3. The time spent in hypoglycemia was significantly less when exercise was included (p-value < 0.001). This makes intuitive sense. Exercise can cause rapid drops in glucose levels because insulin sensitivity increases during

exercise. If the process model is not aware of this sensitivity change, and dosing is not adjusted, then hypoglycemia results.

There was a difference in performance when the process model switched between DH and SH based on a fixed glucose threshold (DH-Thr) compared with a predicted drop below 70 mg/dl (DH-Pred). DH-Pred resulted in some post-exercise hyperglycemia. While time spent in hypoglycemia with the DH-Pred approach did not change significantly in comparison to the DH-Thr approach (p-value = 0.011), the time spent in hyperglycemia, as well as the median blood glucose, were significantly higher for DH-Pred (p-value < 0.001). Results here indicate that DH-Thr is optimal for controlling glucose during exercise. A limitation of this study is that the exercise model only models the effect of aerobic exercise on the glucoregulatory system. Furthermore, the exercise model was static for all subjects, whereas we know that different people respond differently to exercise. In the future, we plan to integrate anaerobic exercise and high intensity interval training into the exercise model. In conclusion, the threshold-based dual-hormone MPC with exercise in the process model outperformed the other controlling approaches. It was critical to include exercise in the controller process model so that the time spent in hypoglycemia would be reduced substantially. Also, we plan to include a meal

model to the process model (U_G would not be zero in equation 1) and evaluate in human subjects.

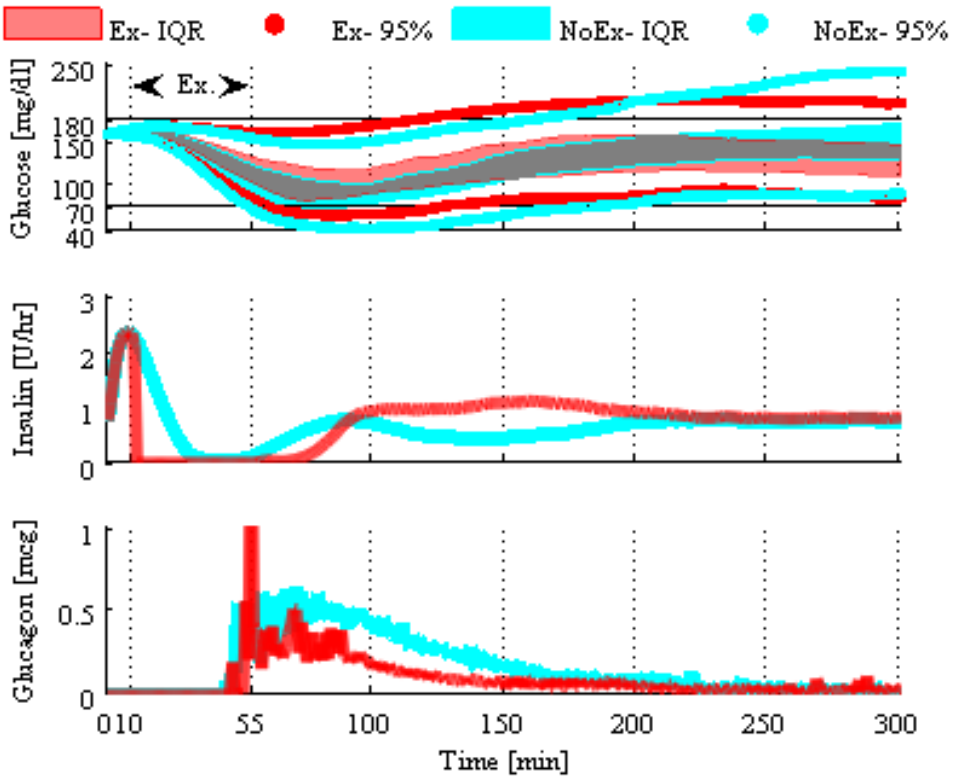

Figure 4.3 DH-MPC performance with/without exercise model. Interquartile ranges along with the 95% intervals of the blood glucose across the virtual subjects are shown for the DH-Thr with exercise model (red line) and DH-Thr without exercise model (cyan line)

5 Evaluation of model complexity in model predictive control within an exercise-enabled artificial pancreas

In this chapter, we evaluate the feasibility of the MPC algorithm for the in-vivo study. In clinical studies, the plant structure is always more complex than the MPC's process model. We investigate less complex MPC's process models against the more complex plant structure. Then, the best MPC design is selected for the in-vivo trials.

Chapter Summary:

- Four single-hormone MPC algorithms are designed with different complexities.
- Two insulin kinetics models defined by either 2 or 3 differential equations are used. Two glucose kinetics models defined by either 1 or 2 differential equations are used. The insulin dynamics model with 1 differential equations is identical for all the four MPC designs.
- Each of the four models, consisting of 4, 5, 5 and 6 differential equations, is tested against a more complex plant defined by eight differential equations.
- Results show that the glucose kinetics model defined by 3 equations works better than the other glucose kinetics model, and no significant difference is observed regarding the complexity of the insulin kinetics models.

- The best less-complex MPC design, consisting of five differential equations, is selected and is used to investigate the exercise effect.
- Results show that time in hypoglycemia is reduced by 40 minutes by incorporating the exercise model.

This work was originally published in 2017:

Navid Resalat, Joseph El Youssef, Ravi Reddy, Peter G. Jacobs, "Evaluation of model complexity in model predictive control within an exercise-enabled artificial pancreas", IFAC-PapersOnLine, vol. 50, no. 1, pp. 7756-7761, 2017, Reprinted with permission from Elsevier.

5.1 Abstract

Model predictive control (MPC) algorithms have been used often within artificial pancreas control systems both in-silico and in clinical studies. Increasingly complex models in the controller can more accurately predict the glycemic response, but they introduce increased computational complexity which can be challenging to implement especially within an embedded environment where computational resources are limited. Less complex models are also preferable in that they can be evaluated in silico against more complex plant models. There has not yet been an evaluation of how the complexity of models used within an MPC impacts

performance within an artificial pancreas. A model within an artificial pancreas MPC algorithm should be as complex as necessary to accurately predict a glycemic response to meals, exercise, stress, and other disturbances, but not overly complex. In this paper, we evaluate four glucoregulatory models used within an MPC, starting with a 4-state model and increasing in complexity up to six states. We evaluate the complexity using an in-silico population derived from a more complex glucoregulatory model (9 state variables). We assess how complexity of the model impacts performance both in terms of standard control metrics such as settling time and overshoot as well as clinically relevant metrics such as percent time in euglycemia (glucose between 70 and 180 mg/dl), percent time in hypoglycemia (<70 mg/dl) and percent time in hyperglycemia (>180 mg/dl). We find that model complexity matters far less than how well the model parameters match the individual subjects. When the simplest model is used, but fit to an individual subject's data, it performed comparably with more complex models. We selected a middle-complexity model and integrated it into our previously published exercise-enabled MPC model and evaluated it in a virtual patient population both with and without the exercise model present. We found that increasing complexity by modeling exercise is critical to help enable early insulin shut-off by the controller to avoid hypoglycemia.

5.2 Introduction

Model predictive control (MPC) is a control strategy whereby a model is used to predict the response of a system to a receding horizon of inputs. MPC uses the model to predict how the system will respond to current and future inputs and selects an optimal control output based on how well the predicted output of the system matches an optimal control trajectory. MPC uses the model to predict the system's response over a prediction horizon (Np) based on a given set of control outputs (Nc). Typically, the control horizon is much less than the prediction horizon (Nc<<Np). Other control strategies such as proportional-integrative-derivative controllers (PID) choose a control output based on the input including how far the input is from the target, how fast the input is moving towards or away from the target, or how long the input has been distant from the target. The power of MPC is in its predictive ability such that systems, which have a very long response time, can be modelled to avoid over or under-delivery of control outputs of the system to the plant which thereby lead to instability.

An artificial pancreas (AP) is a control system that must control a plant with a long response time. A dual-hormone AP controls blood glucose in people with type 1 diabetes (T1D) through the automated delivery of the hormones insulin and glucagon. There are also single-hormone AP systems that only deliver insulin. A

continuous glucose sensor is a subcutaneous, amperometric device that connects to the control algorithm and is used to determine a person's glucose level. If the glucose is too high or rising rapidly, insulin is dosed. If it is too low or falling rapidly, insulin is shut off and glucagon may be dosed in a dual-hormone AP. The kinetics and dynamics of insulin can be very long (90 minutes for peak action of currently available "fast-acting" analogs). This long time constant makes it challenging to control insulin and glucagon with a classical PID controller. Our group has implemented a fading memory proportional-derivative controller (FMPD) for use within a dual-hormone AP control system which has been evaluated both in-silico and in a clinical study [22]. We updated this algorithm to include adjustments of dosing during exercise [28] and have shown that this can help prevent hypoglycemia. While this algorithm performs well, we are now exploring whether MPC is a better alternative. We are specifically interested in whether model-based approaches can improve performance during disturbances such as meals and exercise events.

While there is an ongoing debate regarding the benefits of MPC vs. PID control strategies [133, 134], both approaches have been shown to be successful in-silico and in clinical studies. An early paper describing an approach to MPC using a glucoregulatory model was Hovorka et al. [108]. This group has gone on to use MPC within their single-hormone control system, which has been evaluated clinically

[135]. The group at University of Virginia developed an MPC for use within an AP [42] and they have published results on this algorithm within a multi-center trial [136]. The Padova group has also done work on MPC algorithms within an AP including an algorithm that uses an auto-regressive model that adapts over time called a run-to-run algorithm [43].

Despite the many publications on MPC within an AP, there has not yet been an assessment of the impact on model complexity on control performance. In theory, a more complex model may be more accurate in predicting how a plant will respond to a set of control inputs, thereby improving the optimization of matching an optimal control trajectory. However, adding complexity to the model increases the opportunity for error if a model is not properly identified. Also, a more complex model requires more time to run an MPC algorithm, increasing processing time, which may negatively impact implementation on an embedded system. This study explores different glucoregulatory models of varying complexity to determine the impact on control in a single-hormone MPC.

Recently, we described a new algorithm that uses a glucoregulatory model within an MPC framework to integrate exercise/physical activity directly into the control strategy [52]. This model was evaluated within a virtual patient population that was derived from a relatively complex glucoregulatory model comprised of 9 states that

describe both insulin and glucose homeostasis in type 1 diabetes [36], [131]. A model of equal complexity was used within the controller and the plant, making it challenging to assess in-silico how well the algorithm would perform within a maximally complex plant (e.g. a human). In this chapter, we assess models within the controller that are of lower complexity than the plant and evaluate these models of order 4, 5, and 6 both for general control performance as well as performance based on clinical outcome measures. Lastly, we consider whether the added complexity of including a model for exercise within the controller adds benefit, specifically in preventing exercise-induced hypoglycemia.

5.3 Material and Methods

5.3.1 Model Predictive Control

The controller contains a glucoregulatory model, as does the plant, but preferably the plant's model of higher complexity than the controller so as to match the physiologic test conditions whereby the human body will always be more complex than the model used in the controller. In this paper, we will switch the controller glucoregulatory model to determine the impact of model complexity on performance.

Within MPC there is a cost function consisting of 1) the error between the predicted glucose output (Yp) and the reference glucose trajectory (R_t) and 2) a tuning

parameter, r_w ($\bar{R}_W = r_w I_{N_C \times N_C}$, where I is the identity matrix) for input variability restricting the size of input changes (1). The reference glucose trajectory is how we optimally expect the glucose to reach a target level (G_t = 120 mg/dl) across a period defined as the prediction horizon. Optimization is done by minimizing the derivative of the cost function with respect to the changes in the output of the controller, in this case insulin (ΔU).

$$J = (R_t - Y_P)^T (R_t - Y_P) + \Delta U^T \bar{R}_w \Delta U \quad (1)$$

The reference trajectory that we used is depicted in Figure 5.1. In this chapter, r_w was empirically set to 1, and the maximum amount of permissible injected insulin to the plant was 15 units/hr due to restrictions on insulin pumps.

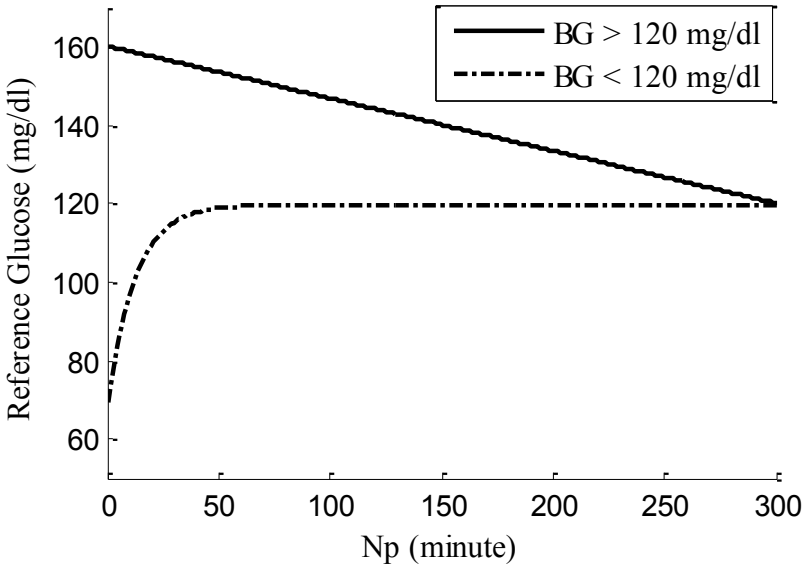

Figure 5.1 Reference Glucose Trajectory. For blood glucose (BG) greater than 120 mg/dl, the predicted values follow a linear moving trajectory during Np. For BG less than 120 mg/dl, the trajectory follows an exponential trend with a time constant of approximately 15 minutes.

5.3.2 Glucoregulatory Models and Virtual Patient Population

In this paper, we used a 9-compartment model for our plant to generate our in-silico virtual patient population. We then considered four less complex compartment models and evaluated them within the controller. The plant model along with each of the controller models are described below.

The glucoregulatory model of the plant consists of 9 differential equations. Four equations represent the insulin kinetic model reported by [131]. Three equations represent the insulin dynamic model, and two equations describe the glucose kinetic model, which was introduced by [108]. The results of this study were obtained on a

virtual patient population. In Resalat et al. [137] we describe how the virtual patient population was generated from the plant by adjusting the insulin sensitivity and endogenous glucose production (EGP) of each subject.

5.3.3 1-Compartment Minimal Model (1CMM)

This model consists of one glucose kinetics model and one insulin dynamics model. It describes the impact of glucose effectiveness and the effect of insulin on blood glucose. This model is presented by Bergman et al. [138] as follows:

$$\begin{aligned} \dot{G} &= -\{P_1 + X_{(t)}\} \times G_{(t)} + P_1 G_b \\ \dot{X} &= P_3 \times I(t) - P_2 X(t) \end{aligned} \tag{2}$$

P_1 (also known as S_G in some studies) is glucose effectiveness [min^{-1}]; X(t) is the effect of insulin in remote compartment [min^{-1}]; G(t) is plasma glucose (mg/dl); G_b is basal plasma glucose [mg/dl]; I(t) is plasma insulin concentration [mU/L]. The ratio between P_3 [min^{-2} per mU/L] and P_2 [min^{-1}] represents insulin sensitivity [138].

5.3.4 2-Compartment Minimal Model (2CMM)

This model consists of two equations representing the glucose kinetics model, and one equation representing the insulin dynamics model. The additional equation captures the variations of glucose in the non-accessible compartment [139]. This model is presented as follows:

$$\dot{Q}_1(t) = -(P_1 + k_{21} + X(t))Q_1(t) + k_{12}Q_2 + P_1Q_{1b}$$
$$\dot{Q}_2(t) = k_{21}Q_1(t) - k_{12}Q_2(t) \quad (3)$$
$$\dot{X}(t) = -P_2X(t) + P_3(I(t) - I_b)$$

where, Q_1 and Q_2 are glucose masses in accessible and non-accessible compartments, respectively [mg/kg], and X is the effect of insulin on blood glucose in interstitial fluid [min^{-1}]. Q_{1b} and I_b are basal plasma glucose and insulin, respectively.

5.3.5 1-Compartment Insulin Kinetic Model (1CIKM)

This model represents the relationship between plasma insulin concentration and subcutaneously infused insulin with two equations [140]. This insulin kinetic model is presented as follows:

$$\dot{X}_I(t) = -k_aX_I(t) + u_I(t - \tau)$$
$$\dot{I}(t) = -k_eI(t) + \frac{k_a}{V_d}X_I(t) \quad (4)$$

where, $x_I(t)$ is the amount of insulin in the subcutaneous depot [mU/kg], I(t) is plasma insulin concentration [mU/L] and $u_I(t)$ is subcutaneous injected insulin [mU/kg/min]. k_e is the elimination rate of insulin (min^{-1}), k_a is the absorption rate of insulin [min^{-1}], V_d is the insulin volume of distribution [L/kg] and τ is the time delay for injected insulin to be effective in the interstitial fluid [min], which was set to zero.

5.3.6 2-Compartment Insulin Kinetic Model (2CIKM)

This model consists of two equations representing the effect of subcutaneously injected insulin in interstitial fluid, as well as one equation to show its impact on plasma insulin concentration. This model is presented in equation (1) and is re-shown in equation (21) for better comparison with 1CIKM, where, S_1 and S_2 represent the absorption of subcutaneously infused insulin [mU/kg]. u_I is the insulin infusion rate [mU/kg/min]. k_e is the elimination rate of insulin [min^{-1}]. t_{max} is the maximal absorption time of insulin [min]. V_I is the volume of insulin distribution [L/kg] [108].

$$\begin{aligned} \dot{S_1} &= u_I - \frac{S_1}{t_{max}} \\ \dot{S_2} &= \frac{S_1}{t_{max}} - \frac{S_2}{t_{max}} \\ \dot{I} &= \frac{S_2}{t_{max} V_I} - k_e I \end{aligned} \tag{5}$$

5.3.7 Evaluation of Models of Varying Complexity

We combined the above models in various ways to create four glucoregulatory models of differing levels of complexity to be used within the controller of our MPC.

Model 1: The first model is the least complex model with 4 compartments total and is comprised of the 1CMM and 1CIKM models (Least Complex Model).

Model 2: The second model has 5 compartments total and is comprised of the 1CMM and 2CIKM models.

Model 3: The third model also has 5 compartments and is comprised of the 2CMM and 1CIKM models.

Model 4: This model has 6 compartments and is comprised of the 2CMM and 2CIKM models (most complex).

These models are ranked based on their differential equations from the least (Model 1) to the most complex model (Model 4). Moreover, the plant includes 9 differential equations and is therefore more complex than each of the controller models.

5.3.8 Fitting Models to Virtual Patient Population Data to Overcome Plant/Controller Model Mismatch

When examining the impact of model complexity on performance in an MPC framework, we must consider that each of the models published and used here were developed using different physiologic data. For example, if Model 1 was not able to accurately predict the output of the plant compared with Model 2, it may not be caused by complexity differences between Models 1 and 2, but may instead be due to differences in the physiology of the human data used to fit the model parameters for each of these models.

To overcome this problem so that we can attempt to understand the impact of complexity specifically, we first fit all models to the same virtual patient population data set using an insulin step-response scenario. The step response was done such that each of the subjects was brought to a steady-state glucose level of 160 mg/dl. Then their basal rate was increased to bring them down to 120 mg/dl. The model parameters for each of Models 1-4 were adjusted to fit the response of the plant to this scenario.

5.3.9 Selection of Initial Model Parameters and Ranges

Prior to fitting, we needed to select the initial model parameter values and the range of the parameters to search. We could not simply use the published model parameters and the published standard deviations. This is because the glucoregulatory models referenced in these papers were originally built for people who did not have T1D. These models needed to be modified to match insulin sensitivities of people with T1D. Furthermore, these models were published many years ago and there have since been further studies on these models indicating that their model parameters needed to be adjusted to better reflect the true physiology of normal healthy subjects.

Step 1: Update models to fit physiology of people without T1D: We modified the 1CMM by decreasing glucose effectiveness (S_G) by 60% and by increasing insulin

sensitivity (S_I) by 35% to match recent physiology data on healthy people based on the study by Friis-Jenson which demonstrated 60% overestimation of S_G and 35% underestimation of S_I with the Bergman's minimal model.

Step 2: Update models to represent people with T1D: We then reduced the modified S_I by 70% and reduced the modified S_G by 38% to make the 1CMM representative of people with T1D. We did this because the S_I and S_G are different between healthy people and people with T1D. Ward et al. [141] published the difference in insulin sensitivity and glucose effectiveness between people with T1D and the healthy subjects and showed 70% reduced mean insulin sensitivity for T1D as well as 38% reduced mean glucose effectiveness compared with people without diabetes. Other groups have also discussed the importance of reducing the insulin sensitivity in models to better represent people with T1D [142, 143].

For the 2CMM, we modified S_I and S_G to match the 1CMM. We did this by reducing the 2CMM S_I by 40% and the S_G by 50% to get them to match. We could not find any prior publications comparing the insulin sensitivity and the glucose effectiveness of people with T1D relative to healthy subjects for the 2CMM. To set appropriate modified values for this model, we made the 1CMM and 2CMM similar to each other such that the insulin sensitivity and glucose effectiveness for these two models were the same

The insulin volume of distribution of the 1CIKM also needed to be adjusted. The plasma insulin concentration of 1CIKM is 64% less than 2CIKM Model. To make the models equivalent, we reduced the insulin volume of distribution of the 1CIKM by 36%. In Table XVII, we list the original published parameters as well as the parameters that were modified (changes on bold).

Table XVII Published vs. modified parameters

	Published model parameters		Modified model parameters to match T1D	
Glucose Kinetic Model	1CMM	2CMM	1CMM	2CMM
	P_1: 0.049, P_2: 0.091 P_3:8.96×10^{-5}, G_b: 80	P_1: 0.024, k_{12}: 0.0885, k_{21}: 0.058, P_2: 0.035, P_3: 2.46×10^{-5}, Q_{1b}: 103	P_1: 0.012, P_2: 0.091, P_3: 3.66×10^{-5}, G_b: 225	P_1: 0.012, k_{12}: 0.0885, k_{21}: 0.058, P_2: 0.035, P_3:1.45×10^{-5}, Q_{1b}: 290, I_b: 0
Insulin Kinetic Model	1CIKM	2CIKM	1CIKM	2CIKM
	k_a: 0.026, k_e: 0.013, V_d: 1.99	t_{max}: 55, k_e: 0.138, V_I: 0.12	k_a: 0.026, k_e: 0.013, V_d: 1.27	t_{max}: 55, k_e: 0.138, V_I: 0.12

Step 3: Model fitting. The modified model parameters given in the left two columns of Table XVII were used as the initial parameters of the models prior to fitting to the in-silico virtual patient population. Model fitting was done to match all four models to the same physiologic data set - the virtual patient population. During fitting, model

parameters were permitted to vary by two standard deviations relative to the mean values in Table XVII. Model fitting was done by fitting the models to the virtual patients during a step response of insulin. Each subject started at a steady state glucose level of 160 mg/dl and was then given additional insulin to bring the glucose level down to 120 mg/dl. The mean values of each model's parameters after fitting are shown in Table XVIII. By fitting each of the models to the same virtual patient population, we can ensure that each model has been tuned to match the same physiologic data. This allows us to look at the impact of model complexity independent of model-plant mismatch that may be due to model identification issues.

Table XVIII Final mean model parameters after fitting

μ	1CIKM	2CIKM
1CMM	Model 1 P_1: 0.0127, P_3: 2.89×10^{-5}, G_b: 262.7	Model 2 P_1: 0.0134, P_3: 2.89×10^{-5}, G_b: 255.5
2CMM	Model 3 P_1: 0.0122, P_3: 1.25×10^{-5}, Q_{1b}: 355.8	Model 4 P_1: 0.0126, P_3: 1.25×10^{-5}, Q_{1b}: 349.8

5.3.10 Incorporating Exercise Information

In addition to evaluating the glucoregulatory model complexity, we also consider the benefit of adding a model for exercise into one of the controller's glucoregulatory

models to help avoid exercise-induced hypoglycemia. In this analysis, we evaluated one of Models 1-4 (based on the controller and clinical outcome performance measures described above) and integrated an exercise model into the controller. As described in detail in [52], the exercise information was incorporated into the model by increasing the model's insulin sensitivity factor ($S_I = P_3/P_2$) in response to exercise using an approach described by Hernandez et al. [73]. Two exercise coefficients were used to indicate the intensity of exercise: percent of active muscle mass (PAMM) and the percent of maximum oxygen consumption (PVO_2^{max}). PAMM and PVO_2^{max} were set to 80% and 60%, respectively, for a fixed 45- minute period, 30 minutes following the second meal. The insulin sensitivity was adjusted during exercise by modifying P_3, we call this P_{3Ex} as defined in equation (22).

$$P_{3Ex} = M_{PGU} \times M_{PIU} \times P_3, \tag{6}$$

where, M_{PGU} and M_{PIU} are greater than one and represent a percentage increment of peripheral insulin uptake and peripheral glucose uptake, respectively. Exercise was integrated into the plant model by applying M_{PGU} and M_{PIU} as well as M_{HGP} to the plant's insulin sensitivity factors (equation 8). In both 1CMM and 2CMM, the parameter X(t) was the only parameter representing the effect of insulin on glucose uptake and insulin utilization. Therefore, we used M_{PGU} and M_{PIU} to adjust X(t) for Models 1-4.

5.4 Control Performance

Here we evaluate settling time (t_s), rising (falling) time (t_r) and overshoot (undershoot) of each of the controllers. To calculate these metrics, we first brought the virtual subjects in the plant to the steady state value of 300 mg/dl and then ran a 24-hour simulation without any meal or exercise disturbances to determine how each controller brings the glucose down within the target range of euglycemia. Therefore, settling time shows the time required for the system to be settled within the euglycemic region (70-180 mg/dl). Rising time represents how fast the controller can reach euglycemia. Undershoot (Us) is the difference between the minimum value of a signal and the target value representing a distortion in the signal. These metrics should be as small as possible under optimal control. Table XIX shows these controllers' performance metrics. In this table, undershoot values are reported based on percentage undershoot relative to the G_t. Notice that generally, the more complex models have smaller response times, and undershoot. Model 3 actually outperformed Model 4 despite being less complex. However, overall, the performance is comparable between the four models.

Table XIX Control Metrics Across Models

$\mu \pm \sigma$	1CIKM	2CIKM
1CMM	Model 1 $t_r = 246.6 \pm 47.5$,	Model 2 $t_r = 251.8 \pm 47.8$,

	t_s = 313.8 ± 111.4, % Us = 22.4 ± 6.2	t_s = 318.2 ± 111.5, % Us = 22.4 ± 6.1
2CMM	Model 3 t_r = **204.1** ± **64.9**, t_s = 243.4 ± 70.8, % Us = **7.5** ± **4.6**	Model 4 t_r = 207.5 ± 66.1, t_s = 246.3 ± 71.8, % Us = 7.7 ± 4.5

5.4.1 Clinical Performance

All virtual subjects completed the following scenario. Their glucose levels were brought to a steady state value of 160 mg/dl at time t = 0. An overnight period of 8 hours was at the beginning of the simulation. Following this overnight period, three meals of 20, 40 and 60 grams were given to subjects 8, 12 and 18 hours from the start of the simulation. The meal information was added as an input into the controller models.

We report the time in euglycemia and time in hypoglycemia for each of the four models (Figure 5.2). Percent time in hypoglycemia was comparable across the models with the lowest mean time in Model 3 (0.1%).

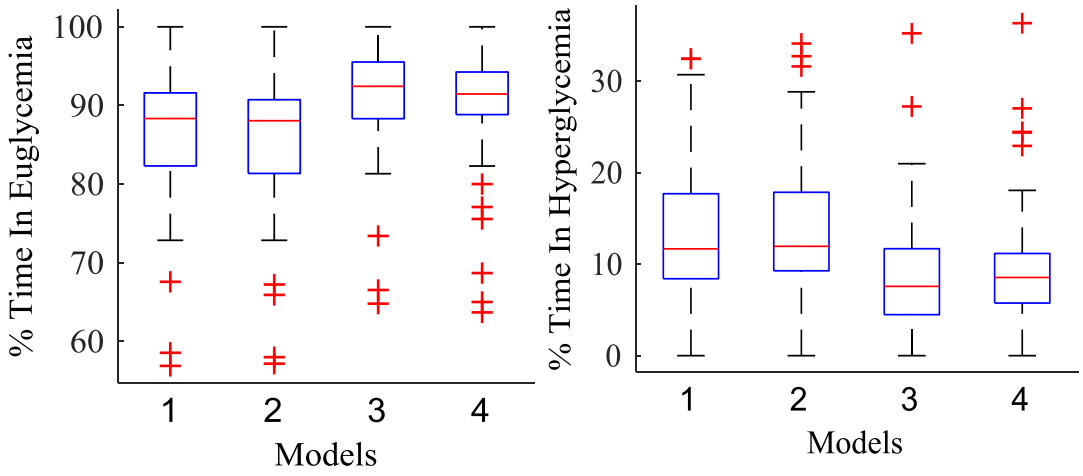

Figure 5.2 Percent time in euglycemia (left) and hyperglycemia (right) for each of the four models

While the percent time in euglycemia was higher and percent time in hyperglycemia was lower for models with higher complexity as we expected, the difference was not significant, and overall all models performed well. This result indicates that model complexity may not be as important as the fitting of the data to the patient. While not shown here, using the published model parameters, the percent time in euglycemia was significantly lower and the time in hyperglycemia was higher than after the models were fit to the virtual patient population.

5.4.2 Model-Plant mismatch evaluation

A more complex model should be able to better estimate a maximally complex plant model. Here we evaluated how well each controller model estimated the plat at each control step and calculated the root mean square error between the controller model

and the plant model when both were given the same inputs (insulin infusion and meals). Figure 5.3 shows the RMSE for all the models. As model complexity increased, the RMSE was lower. The 6-state model (Model 4) was the best estimate of the 9-state plant model. However, the differences between RMSE for each model again were not significant and all models generally performed well in estimating the plant.

5.4.3 Results of incorporating exercise in the process model

In this section, we show the result of incorporating exercise information in the process model and compare it with the situation where exercise is not announced to the model. We used Model 3 as the best model because according to Figure 5.2 and Figure 5.3, it seemed to be the best balance between performance and complexity. Figure 5.4 shows the effect of incorporating exercise information. As a result, the insulin rate is shut off to zero during the exercise period, resulting in less hypoglycemia (≈ 40 minutes less time below 70 mg/dl).

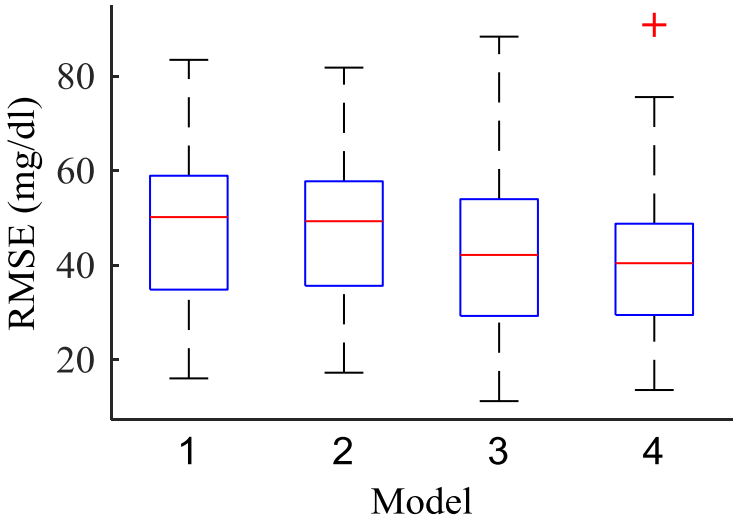

Figure 5.3 RMS between model and plant for each model

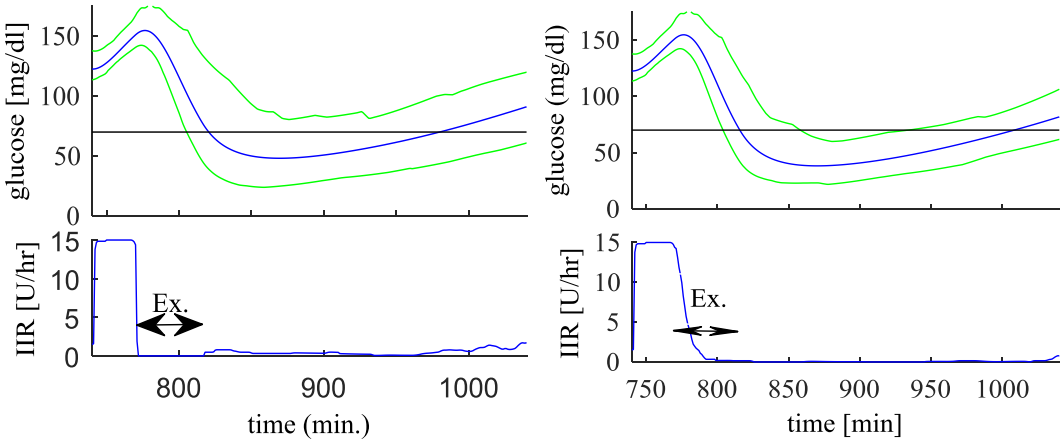

Figure 5.4 Effect of incorporating exercise on the process model. Glucose profile (top) and insulin infusion rate (IIR) (bottom) after the second meal and during exercise (left) with and (right) without exercise model integrated into Model 3. Green lines represent 95th percentile range for glucose.

6 Adaptive Control of an Artificial Pancreas using Model Identification and Adaptive Postprandial Insulin Delivery and Exercise

Adaptive control for type 1 diabetes is an emerging control algorithm where the design and structure of AP systems are modified based on new glucose measurements. In the OHSU-MPC design, the insulin sensitivity factor is updated adaptively based on glucose data. Insulin sensitivity is the fundamental parameter in the MPC algorithm which describes the body's reaction to insulin.

Chapter Summary:

- A single hormone MPC with the best process model introduced in the previous chapter is used.
- An insulin sensitivity adaptation (ISA) algorithm is designed to update the insulin sensitivity factor defined in the process model at each non-meal event.
- The performance of the ISA was compared with the ALPHA algorithm introduced in chapter 3.
- Results show that the ISA algorithm reduces average glucose and time spent in hyperglycemia significantly. ALPHA reduced postprandial hypoglycemia significantly.

• A combination of ALPHA and ISA (ALPHA-ISA) yields better glycemic outcomes.
Navid Resalat, Joseph El Youssef, Nichole Tyler, Jessica Castle and Peter G. Jacobs, "Adaptive Control of an Artificial Pancreas using Model Identification and Adaptive Postprandial Insulin Delivery", Journal of process control, under revisions.

6.1 Abstract

Background: People with type 1 diabetes (T1D) have varying sensitivity to insulin and also varying responses to meals and exercise. We introduce an adaptive run-to-run model predictive control (MPC) algorithm that can be used to help people with T1D better manage their glucose levels using an artificial pancreas (AP). The algorithm adapts to individuals' different insulin sensitivity, glycemic response to meals, and adjustment during exercise as a continuous input during free-living conditions. *Methods:* An insulin sensitivity adaptation (ISA) algorithm is presented that updates during non-meal periods to reduce the error between the actual glucose levels and the process model. We further demonstrate how an adaptive learning post-prandial hypoglycemia-prevention algorithm (ALPHA) presented in previous work can complement the ISA algorithm, and the algorithm can adapt in several days. We show that if physical activity is incorporated as a continuous input (heart rate and

accelerometry) performance is improved. *Results:* Incorporating ALPHA, ISA and physical activity into the MPC improved glycemic outcome measures. ALPHA combined with ISA significantly reduced time spent in hypoglycemia by 55.5% and the total number of rescue carbs by 52.3% to 0.2 events/day/patient. ISA significantly reduced model-actual mismatch by 17.5% compared to an AP without ISA. Incorporating physical activity as a continuous input modestly improved time in range (70-180 mg/dL) during high physical activity days from 80.7% to 81.5% and reduced time in hypoglycemia from 0.52% to 0.43%. *Conclusion:* Adapting postprandial insulin delivery, insulin sensitivity, and adapting to physical exercise in an MPC-based AP systems can improve glycemic outcomes.

6.2 Introduction

Closed loop control for type 1 diabetes also known as the artificial pancreas (AP) is an emerging control technology. The insulin delivery rate at each time-interval is calculated using a control algorithm that considers current and past continuous glucose measurements (CGM) [22]. A number of studies have shown that model predictive controller (MPC) is an effective control strategy because it models delayed insulin kinetics [42, 50, 144]. The first MPC algorithm for diabetes management was introduced by Parker et al. [34]. MPC was further developed for single-hormone and dual-hormone APs with alternative mathematical models and

different insulin delivery methods and timing intervals [4, 35, 43, 49, 52]. MPC performs optimally if the parameters of the mathematical models are defined accurately and are consistent with the characteristics of the person with T1D or plant. Model-plant mismatch can be a problem because the model parameters derived and used in the MPC are typically obtained from a population model or average across many patients. This mismatch can degrade the performance of the controller. A number of factors can cause the model-plant mismatch. First, the mathematical model in an MPC is inherently less complex than a human or a plant model that is designed to represent a human's glucoregulatory system. Second, the MPC's controller model does not have accurate knowledge of the process noise or the measurement noise. Boiroux et al. [4, 145] incorporated the measurement noise and a time-varying filtered process noise into MPC's mathematical model for reducing the mismatch. Furthermore, the physiology of each patient changes over time whereas the model in an MPC is fixed, thereby creating further mismatch between the model and the plant.

In this paper, we extended the MPC developed by Resalat et al. [49, 52] to make it adaptive and patient-specific to minimize the model-plant mismatch. We show how the algorithm can respond to free-living changes in physical activity by incorporating heart rate and accelerometry data into the control algorithm. We introduce the

Insulin Sensitivity Adaption (ISA) algorithm, which updates the insulin sensitivity factor (ISF) within the MPC controller model at each non-meal period. The ISF defined in the mathematical model of the MPC is used to calculate insulin amounts. If the ISF is initialized to a value that is too high for a patient, the MPC will presume that the patient needs less insulin and hyperglycemia can occur. Conversely, if the ISF is initialized to be lower than the patient's ISF, then too much insulin will be dosed to the patient and hypoglycemia can occur. Enabling the ISF within the MPC to adapt based on the patient's response to insulin is hypothesized to reduce the model-plant mismatch and optimize the performance of MPC.

Laguna Sanz et al. [146] defined a trust index that indicated how closely the MPC model was able to predict prior glucose values based on the residuals across a prediction horizon. They updated the cost function of the MPC by adaptively changing an aggressiveness factor to change insulin dosing. They found that when implemented in a zone MPC, there was not a significant change in time in target range, but there was decreased time in hypoglycemia when using the adaptive algorithm. Toffanin et al. [147] also introduced a run-to-run adaptive algorithm. They adaptively changed the bolus insulin and overnight basal insulin in a run-to-run design with MPC. They modified overnight basal insulin and daytime bolus insulin at each run showing increased time in range of 11.39%. Toffanin et al. adapted the

insulin-to-carbohydrate ratio in response to postprandial glucose excursions. We have shown previously [116] that adapting postprandial insulin is more effective than adapting carbohydrate ratios when using an algorithm called adaptive learning postprandial hypoglycemia-prevention algorithm (ALPHA).

Other work has been done to adapt the AP to exercise. Turksoy and Cinar showed that using an autoregressive model-based controller with exercise could be included as an input to the controller [71, 148]. Breton et al. showed that incorporating heart rate into an AP, the rate of decline of glucose during exercise could be reduced [149]. Our group has also shown that incorporating automated exercise detection into both a single-hormone and dual-hormone AP can help reduce time in hypoglycemia [20, 64]. For these prior studies, however, exercise levels above 4 METs was detected and an exercise adjustment algorithm was executed that turned off insulin and increased glucagon, but only during and shortly after the detected exercise event [28]. In the current paper, we show the benefit of including exercise as a continuous input into an AP system during free-living conditions as well as during scheduled exercise. And we show the benefit of using both ISA and ALPHA to adapt to patient-specific physiologies and improve time in target glucose ranges.

6.3 Material and Methods

6.3.1 Controller Design

The schematic of the MPC used in this study is shown in Figure 6.1. The MPC consists of a process model (i.e. mathematical model), a reference trajectory and an optimization tool to calculate the next insulin delivery rate. The process model is a mathematical description of glucose and insulin metabolism. It is defined by five differential equations in this study and is further described in [49]. The ISA algorithm updates the insulin sensitivity factor of the process model in the MPC during non-meal periods. The ALPHA algorithm adapts postprandial insulin to help prevent meal-based excursions. The ALPHA algorithm can be used with any type of control algorithm, not just MPC. It only uses glycemic excursion information from prior meal events to adjust the postprandial insulin delivery using an adaptive aggressiveness factor. We used the OHSU virtual patient population to represent patients with T1D (i.e. the plant) [36, 52]. In general, the complexity of the process model should be less than the plant for better representing real-world control scenarios whereby the human is substantially more complex than the MPC process model. The plant in the OHSU virtual patient population is represented by 8 differential equations, making it more complex than the MPC process model.

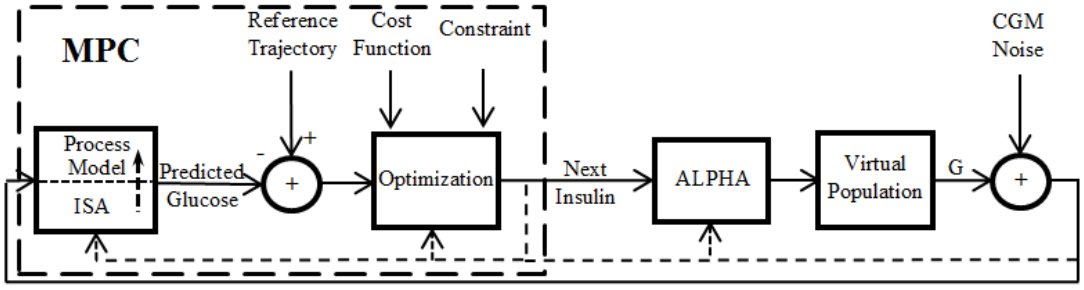

Figure 6.1 The schematic of the MPC. ALPHA modifies basal insulin during meal periods. ISA modifies basal insulin by updating insulin sensitivity factor of the process model during non-meal periods.

The process model of the MPC consists of an insulin kinetics model [140], an insulin dynamics model and a glucose kinetics model [139], described in Resalat et al. [49]. It is presented with the following equations:

$$\begin{aligned}
\dot{Q}_1(t) &= -(P_1 + k_{21} + X(t))Q_1(t) + k_{12}Q_2 + P_1Q_{1b} \\
\dot{Q}_2(t) &= k_{21}Q_1(t) - k_{12}Q_2(t) \\
\dot{X}(t) &= -P_2X(t) + P_3(I(t) - I_b) \\
\dot{X}_I(t) &= -k_aX_I(t) + u_I(t-\tau) \\
\dot{I}(t) &= -k_eI(t) + \frac{k_a}{V_d}X_I(t)
\end{aligned} \tag{1}$$

where, Q_1 and Q_2 are glucose masses in accessible and non-accessible compartments, respectively (mg/kg), and X is the effect of insulin on blood glucose in interstitial fluid (min^{-1}). Q_{1b} and I_b are basal plasma glucose and insulin, respectively. $x_I(t)$ is the amount of insulin in the subcutaneous depot (mU/kg), I(t) is plasma insulin concentration (mU/L) and u(t) is subcutaneous infused insulin (mU/kg/min). k_e is the

elimination rate of insulin (min^{-1}), k_a is the absorption rate of insulin (min^{-1}), V_d is the insulin volume of distribution (L/kg) and τ is the time delay for injected insulin to be effective in the interstitial fluid (min), which was set to zero [49].

The process model determines the predicted glucose levels over the prediction horizon (N_P) which are compared with the reference trajectory. For glucose levels greater than the target value (G_t = 115 mg/dl), reference glucose trajectory linearly approach the target wile for glucose levels less than the target, they exponentially approach the target as shown in [49]. The time constant of the exponential term is comparably low to shut off insulin faster for low glucose levels. The constraint of basal delivery was set to 80 unit/hr, enabling more aggressive basal control for high glucose levels.

6.3.2 Incorporating exercise into the model

We have previously described how we incorporate an exercise model into the MPC [49, 52, 116]. This is briefly described in the Supplemental Material.

6.3.3 Adapting insulin sensitivity

The insulin sensitivity factor (ISF = $\frac{P_3}{P_2}$, in (1)) was updated at each non-meal period as follows. A polynomial function (P(k)) of order 6 was fit to the insulin levels during the non-meal periods using the least-square method and was set as the input

(u(t)) in (1). A function (@Fun_G) describing the relationship between the u(t) and $Q_1(t)$ in (1) was determined (Q1(t) = Fun_G(u(t))) and was set as the fit-function. The ISF was updated using glucose data (G(k)), P(k) and Fun_G. This approach was also performed using the least square method. Finally, the new ISF was calculated as the average of the last three updated insulin sensitivity factors ($ISF^{Avg}(k)$).

6.3.4 Adapting postprandial insulin

We have previously developed an adaptive learning postprandial hypoglycemia-prevention algorithm (ALPHA) that can be used to adapt postprandial insulin dosing to improve glycemic control. ALPHA modifies the aggressiveness of the postprandial insulin delivery as follows. If postprandial glucose levels fall below 90 mg/dl, postprandial insulin delivery after the subsequent meal is reduced proportional to the difference between the minimum glucose level and 70 mg/dl. If glucose levels drop below 70 mg/dl, ALPHA shuts off postprandial insulin delivery. ALPHA modifies insulin delivery for 90 minutes after the meal announcement. ALPHA is further described in [116].

6.3.5 Evaluating ISA and Alpha under real-world meal scenarios

We used twenty meal scenarios from a 4-day outpatient AP study [64]. Each meal scenario was extended to 28 days by duplicating the original meal scenarios. This

was done to investigate the convergence rate of the insulin sensitivity factor in the ISA. Then, each meal scenario was given to the virtual patients who were then subjected to the following conditions: (1) the OHSU MPC controller (called AP), (2) the AP + ISA (called ISA), (3) the AP + ALPHA (called ALPHA) and (4) ALPHA + ISA (called ALPHA-ISA). We challenged the simulations by introducing a randomly selected -30% to 30% meal uncertainty that was applied to each carbohydrate intake as done by other groups [113]. We introduced 30% circadian variability of insulin sensitivity factors for each virtual patient to represent intra-day variability of the insulin sensitivity [113].

6.3.6 Evaluating physical activity as a continuous input using real-world exercise data

We used the same 4-day real-world meal and exercise scenarios acquired from a prior AP study as described above [64] to evaluate physical activity as a continuous input to the AP system. During this study, participants continuously wore a Zephyr patch that acquired heart rate and accelerometry data. We converted this data to METs using a method previously described by Zakeri et al. [110]. And METs was used as an input to the AP as described above under the Supplemental Materials. Using the physical activity and meal data acquired from these study participants with T1D, we evaluated the performance of the exercise-enabled MPC algorithm

compared with the non-exercise-enabled MPC algorithm during the entire study duration that included free-living, non-structured exercise periods of time and also during structured exercise periods of time (i.e. start of exercise until 4 hours after the exercise or until first meal).

6.3.7 Evaluation metrics and statistical analysis

We evaluated percent time in target range (70-180 mg/dL) and percent time in hypoglycemia (<70 mg/dL) as the primary outcome measures. Secondary outcome measures were percent time in hyperglycemia (>180mg/dl), root mean square error (RMSE) of the MPC model predicted output relative to the plant output, total number of rescue carbohydrates required per day, low blood glucose index (LBGI) and high blood glucose index (HBGI). The statistical two-sample t-test was used to test statistical difference between AP, ISA, ALPHA and ALPHA-ISA with significance level set to 0.05.

6.4 Results

6.4.1 Adapting postprandial insulin and insulin sensitivity factor

We found overall that the ALPHA algorithm was effective at reducing time in hypoglycemia by 55.5% relative to the AP without ALPHA as shown in Table XX. However, this was at the expense of also reducing time in range from 84.4% to

81.3%. By including the ISA algorithm in combination with ALPHA, we were able to both reduce the time in hypoglycemia with less impact on time in range. As shown in Table XX, the number of rescue carbohydrates per day was reduced by 52% when using ALPHA-ISA (0.24 / day) compared with AP (0.54 / day). Time in range changed from 84.4% (AP) to 82.2% (ALPHA-ISA).

The ISA algorithm was effective at reducing the model-plant mismatch, specifically during the overnight periods when the insulin sensitivity was adapted to each patient. Figure 6.2 shows how the ISA algorithm reduces model-plant mismatch during non-meal periods. ALPHA-ISA reduces the RMSE for the non-meal periods overnight from 12.7 to 4.9 mg/dl, compared to AP. The RMSE values across all the meal scenarios and subjects are shown in Table XX. It also shows the comparison between AP, ISA, ALPHA and ALPHA-ISA over the virtual patients and meal scenarios for the entire experiment including meal and non-meal periods. ISA+ALPHA significantly reduced the RMSE during meal and non-meal periods from 19.4 mg/dL (AP) to 17.3 mg/dL (ALPHA + ISA) as shown in Table XX.

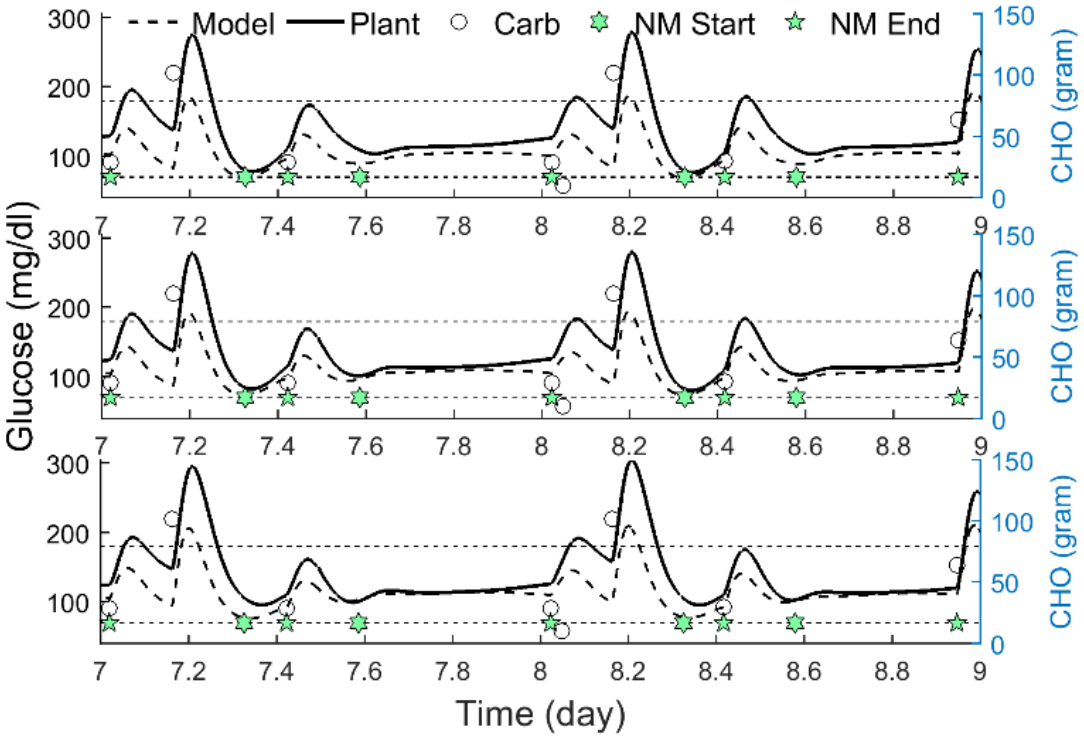

Figure 6.2 Performance of AP(top), ISA(middle) and ALPHA-ISA(bottom) for a representative subject in a representative meal scenario. Start time (NM start) and end time (NM End) of the non-meal periods are shown with hexagon and pentagon symbols, respectively.

Table XX Comparison between AP, ISA, ALPHA AND ALPHA-ISA over the meal scenarios

$\mu \pm \sigma$	AP	ISA	ALPHA	ALPHA-ISA
Time in Hypoglycemia [%]	0.54 ± 0.56	0.73 ± 0.5*	0.19 ± 0.25*	0.24 ± 0.25*
Rescue Carbs [event/day/patient]	0.42 ± 0.42	0.56 ± 0.38*	0.16 ± 0.21*	0.2 ± 0.21*
Time in range [%]	84.4 ± 5.9	86 ± 4.5*	81.3 ± 5.7*	82.2 ± 4.9*
Time in Hyperglycemia [%]	15.1 ± 5.9	13.3 ± 4.4*	18.54 ± 5.6*	17.5 ± 4.7*
Average glucose [mg/dl]	140.2 ± 9.7	136.5 ± 6.9*	146.1 ± 8.1*	143.8 ± 6.3*$^{\#}$
HBGI	4 ± 1.5	3.8 ± 1.2	4.7 ± 1.6*	4.5 ± 1.5*

LBGI	1.5 ± 0.43	1.8 ± 0.27*	1.18 ± 0.32*	1.35 ± 0.28*[#]
RMSE	19.4 ± 0.7	16 ± 0.4*	20.7 ± 1*	17.3 ± 0.6*[#]

*) shows significance compared to AP (p-value < .05)

[#]) shows significance compared to ALPHA (p-value < .05)

Figure 6.3 compares the performance of AP with ALPHA-ISA over the virtual patients for one representative meal scenario. The lower panel shows the adaptation of IS_f^{Avg} over the non-meal events. The glucose control was tighter during the non-meal periods, specifically during nighttime after the first 4 days, showing that the model-plant mismatch was reduced with the ISA. Table XXI shows the convergence rate at each meal scenario for ALPHA-ISA. The average convergence rate over the meal scenarios was 3.4.

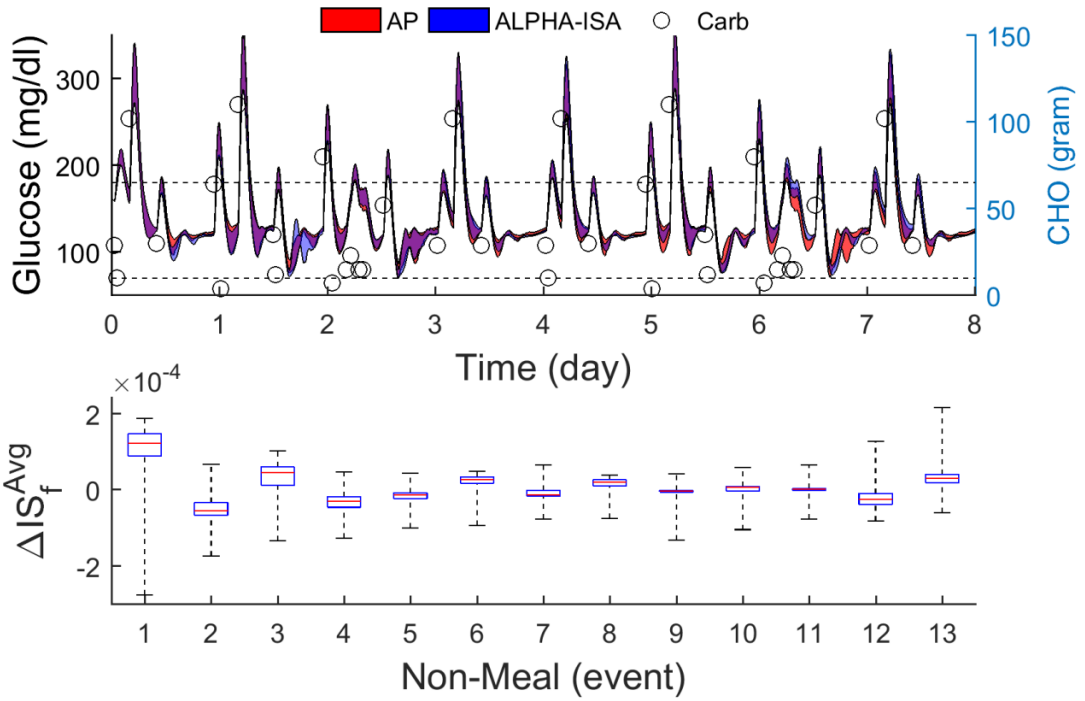

Figure 6.3 Interquartile range of the glucose profile and the boxplot of the changes of IS_f^{Avg} over the non-meal periods across the virtual patients for one representative meal scenario. 'o' denotes the amount of CHO. Dashed lines represent hypoglycemia and hyperglycemia thresholds.

Table XXI Convergence at each meal scenario

Meal Scenario	Mean carbs and std	# Non-meal periods to converge	
		ALPHA-ISA	Final IS_f^{Avg} ($\times 10^{-4}$) min^{-1} per (mU/L)
1	40.2 ± 9.9	2	9.36 ± 3.1
2	72.8 ± 36.6	5	9.63 ± 3.3
3	45.1 ± 8.7	4	9.26 ± 3
4	42.6 ± 30.1	4	8.93 ± 3.1
5	42.8 ± 28.7	1	10 ± 3.4

6	47.4 ± 21.9	1	10 ± 3.1
7	46.4 ± 15.5	1	10 ± 3.51
8	32.6 ± 18.9	2	9.41 ± 2.9
9	40.2 ± 34.7	4	9.96 ± 4.1
10	38.9 ± 20	4	9.7 ± 3.4
11	45.1 ± 25.4	4	9.6 ± 3.3
12	31.6 ± 16.9	1	9.82 ± 3.4
13	40.4 ± 30.4	4	9.6 ± 3.6
14	55.8 ± 35.2	4	9.12 ± 3.2
15	57.2 ± 15.9	5	8.87 ± 2.9
16	33.9 ± 21.6	5	9.1 ± 3
17	48.4 ± 24.8	4	9.88 ± 3.3
18	32.2 ± 11.1	4	9.43 ± 3.4
19	40.9 ± 21.7	5	9.05 ± 3.1
20	38.9 ± 2.6	4	8.95 ± 2.9
Average	43.7 ± 9.7	3.4 ± 1.5	9.48 ± 0.39

6.4.2 Results of adapting to exercise

Including exercise as a continuous input to the AP controller led to a 17% reduction in time in hypoglycemia and 17% reduction of number of rescue carbohydrates and led to a small but statistically significant increase of time in target range (80.7% to

81.5%) as shown in Table XXII. These results indicate that including exercise as a continuous input to the AP system results in better glycemic outcome measures.

Table XXII Comparison between an exercise-enabled (AP-Ex) with non-exercise enabled (AP)

$\mu \pm \sigma$	AP	AP-Ex
Time in Hypoglycemia [%]	0.52	0.43 *
Rescue Carbs [event/day/patient]	0.47	0.39 *
Time in range [%]	80.70	81.50 *
Time in Hyperglycemia [%]	18.80	18.10 *
Average glucose [mg/dl]	149.10	147.80 *
HBGI	5.47	5.26
LBGI	1.36	1.20 *

*) shows significance compared to AP (p-value < .05)

**) shows significance compared to AP (p-value < .001)

6.5 Discussion

In this paper, we have demonstrated how adaptation of postprandial insulin, adaption of insulin sensitivity, and adaptation to physical activity and exercise as an input into an AP can yield improvements in glycemic outcomes in automated insulin delivery. As shown in a prior publication [116], we have shown that incorporating adaptive

postprandial insulin delivery using ALPHA can reduce hypoglycemia and the need for rescue carbohydrates, but at the cost of reducing time in target range. By simultaneously incorporating an adaptive insulin sensitivity measure that adapts to each patient during non-meal periods, we can still observe a substantial reduction in time in hypoglycemia while minimizing the reduction of time in target range.

While prior studies have shown a benefit of incorporating physical activity measures as an input to AP systems [20, 52, 64, 71, 148, 149], there has not yet been a study showing how physical activity incorporated as a metric during *free-living* (i.e. *non-scheduled* exercise) can yield improvements in glycemic outcomes compared with not including physical activity. These prior studies have shown that if insulin can be shut off early and also that optionally glucagon can be given in response to or in anticipation of exercise, exercise-induced hypoglycemia can be avoided. We were able to show that physical activity metrics (heart rate and accelerometry) may be incorporated as an additional input under *free-living* as well as *scheduled* exercise periods of time to yield improvements in glycemic control including moderate but statistically significant reduction of time in hypoglycemia, number of rescue carbohydrates, increased time in target range, reduction of time in hyperglycemia, and improvements in LBGI and HBGI. In the future, we plan to evaluate these

adaptive control algorithms in a clinical study on people with type 1 diabetes over longer-term in-home studies to demonstrate the benefit of adaptation over time.

The primary limitation of this study is that it was done in-silico. We purposely designed the MPC control model to be less complex than the plant model in the virtual patient population, making it more challenging for the MPC to adapt over time to match the plant. However, the human body is substantially more complex than the plant model in our virtual patient population. When adaptation is done in actual humans, the insulin sensitivity parameter in the MPC will adapt to account for all discrepancies between the human physiology and the MPC model. The model for exercise in the plant model is similar to the model for exercise in the MPC controller, and the model was designed for aerobic exercise. In the future, we will need to incorporate models for other types of exercise including resistance training and moderate/high intensity interval training.

6.6 Conclusions

This paper showed that incorporating exercise as a continuous input as well as adapting insulin sensitivity and postprandial insulin delivery in a MPC design can be helpful for improving glycemic outcomes.

Acknowledgements

The guarantor of this research is Peter G. Jacobs who takes responsibility for the contents of this article. NR and PGJ developed the MPC design, the study design, wrote the manuscript, and supported the data collections. WH contributed to the tuning of the MPC model parameters and did the exercise analysis. NT and WH contributed to the in-silico simulations. JRC, and JEY contributed to the writing, study design, data collection, data analysis, and data interpretation. This work was supported by grants from the National Institutes of Health (grant 1DP3DK101044) and by Oregon Clinical and Translational Research Institute UL1TR002369 from the National Center for Advancing Translational Sciences at the NIH. JRC and PGJ have a financial interest in Pacific Diabetes Technologies Inc., a company that may have a commercial interest in the results of this research and technology.

6.7 Supplemental Material

6.7.1 Integrating exercise into the glucoregulatory model

We used a model presented by Hernandez-Ordonez et al. [73]. The insulin sensitivity factor in Equation 1 is represented by the factors P_3/P_2. We model the impact of exercise as an increase in insulin sensitivity according to Equation 2 whereby P_3 in Equation 1 is replaced by P_{3Ex}.

$$P_{3Ex} = M_{PGU} \times M_{PIU} \times P_3 \quad (2)$$

M_{PGU} represents a gain factor related to peripheral glucose uptake while M_{PIU} represents a gain factor related to peripheral insulin uptake. These parameters are a function of both percent active muscle mass (PAMM) during exercise as well as the percent of maximal VO_2 (PVO_{2max}) during exercise which is a function of metabolic expenditure (MET).

$$M_{PGU} = 1 + \frac{\Gamma_{PGUA} \times PAMM}{35} \tag{3}$$

$$M_{PIU} = 1 + 2.4 \times PAMM$$

The Γ_{PGUA} represents the percent glucose uptake by active muscle mass and is represented by a differential equation.

$$\dot{\Gamma_{PGUA}} = -\frac{1}{30}\Gamma_{PGUA} + \frac{1}{30}\Gamma_{\overline{PGUA}} \tag{4}$$

The $\Gamma_{\overline{PGUA}}$ is a function of PVO_{2max}, is a function of MET which is given in Equation 5.

$$\Gamma_{\overline{PGUA}} = 0.006(PVO_{2max})^2 + 1.2264(PVO_{2max}) - 10.1958$$

$$PVO_{2max} = \frac{MET}{MET_{max}} \tag{5}$$

MET can be derived using heart rate and accelerometry data as given in [110]. In our studies, we collect this data using a Zephyr biopatch.

6.7.2 Mathematical representation of the MPC

The mathematical representation of the MPC is shown in the supplemental materials.

Design of the MPC

The state space representation of the MPC process model is represented in equation 6.

$$\begin{aligned} x_m(k+1) &= A_m x_m(k) + B_m u(k) + d_m(k) \\ y(k) &= C_m x_m(k) \end{aligned} \tag{6}$$

$x_m(k)$ is the state vector, u(k) is the input vector (insulin) and d(k) is the constant terms resulted after the linearization. Because MPC predicts future glucose levels (y(k)) during N_P by varying future insulin levels (u(k) in (6)) during the control horizon (N_c), The changes of insulin are first linked to glucose levels. We defined a new vector, $x(k) = [\Delta x_m(k)^T \; y(k)]^T$, and re-arranged the state equations shown below.

$$\begin{bmatrix} \Delta x_m(k+1) \\ y(k+1) \end{bmatrix} = \begin{bmatrix} A_m & 0_m^T \\ C_m A_m & 1 \end{bmatrix} \begin{bmatrix} \Delta x_m(k) \\ y(k) \end{bmatrix} + \begin{bmatrix} B_m \\ C_m B_m \end{bmatrix} \Delta u(k) + \begin{bmatrix} 1 \\ C_m \end{bmatrix} \Delta d_m(k)$$

$$y(k) = \begin{bmatrix} 0_m & 1 \end{bmatrix} \begin{bmatrix} \Delta x_m(k) \\ y(k) \end{bmatrix}$$

$$\Rightarrow \begin{cases} x(k+1) = Ax(k) + B\Delta u(k) + D\Delta d_m(k) \\ y(k) = Cx(k) \end{cases} \tag{7}$$

where, 0_m denotes a vector of zeros whose dimension is the number of the states. The predicted outputs (Y_p) are then calculated in equation 8.

$$Y_P = Fx(k) + \Phi\Delta U + \Psi\Delta D \tag{8}$$

where ΔU and ΔD denote the changes of the input vector, and the constant terms, respectively. The matrices F, Φ and Ψ, which are related to A, B, C and D matrices in equation 3, are presented in appendix and

$$Y_P = [\,y(k+1)\ y(k+2)\ \cdots\ y(k+N_p)]^T,$$
$$\Delta U = [\Delta u(k)\ \Delta u(k+1)\ \cdots\ \Delta u(k+N_c\text{-}1)]^T,$$
$$\Delta D = [\Delta d_m(k)\ \Delta d_m(k+1)\ \cdots\ \Delta d_m(k+N_c\text{-}1)]^T,$$

The prediction horizon was set to 300 minutes ($N_P = \frac{300}{T_s} = 60$ samples; Ts = 5min was the sampling interval) because the peak effect of the short-acting insulin is several hours [36] and the control horizon was set to 20 minutes ($N_c = \frac{20}{T_s} =$ 4 samples) [52]. We empirically found that longer control horizons did not impact the glycemic outcomes and we chose 20 minutes to have less computational burden and faster MPC control. The cost function, defined in (9), consists of an error term and an input-controllable term. The error term measures the discrepancy between the predicted glucose output (Y_P) and the reference glucose trajectory (R_s). The input-

controllable term restricts the size of the input changes by a tuning parameter ($R_w = r_w \times I_{N_c \times N_c}$, where I is the identity matrix).

$$J = (R_s - Y_P)^T (R_s - Y_P) + \Delta U^T R_W \Delta U \tag{9}$$

The MPC optimization's step was done by minimizing the derivative of the cost function with respect to the input changes shown in (10).

$$\begin{cases} \dfrac{\partial J}{\partial \Delta U} = 0 \Rightarrow \Delta U = (\Phi^T \Phi + \bar{R}_w)^{-1} \Phi^T (R_s - Fx(k) - \Psi \Delta D) \\ 0 < u_I < 80 \text{ units/hr} \end{cases} \tag{10}$$

The optimal ΔU vector contains Δu(k), Δu(k + 1),…, Δu(k + N_c – 1) however only the first element (i.e. Δu(k)), according to the receding horizon control principle, is given to the plant. Therefore, next insulin delivery, is calculated below:

$$u(k+1) = u(k) + \overbrace{[1 \quad 0 \quad \cdots \quad 0]}^{N_C} \Delta U \tag{11}$$

In the MPC implementation of this study, we employed an observer using a Kalman filter. It compensates the difference between the plant's and the model's output during the entire simulation time including meal and non-meal periods. The meal period was defined as a 4-hour period following a meal event and the non-meal period was defined as a period starting 4 hours after the meal event up to the next

one. The non-meal period covered both overnight periods and the periods between meals excluding the meal periods. The observer is shown in (12).

$$\begin{aligned} x_m(k+1) &= A_m x_m(k) + B_m u(k) + d_m(k) + K_{ob}(G(k) - C_m x_m(k)) \\ y(k) &= C_m x_m(k) \end{aligned} \tag{12}$$

where, G is the glucose level and K_{ob} is the Kalman gain. For calculating K_{ob}, we assumed that the mean and the covariance of the discrepancy between the plant's and model's outputs (model-plant mismatch) were 0 mg/dl and 100^2 $(mg/dl)^2$, respectively. In addition, we set the mean and the covariance of the process noise to 0 mg/dl and 1 $(mg/dl)^2$. We also assumed that there was no correlation between the process noise and the model-plant mismatch. To quantify the model-plant mismatch, average root mean square error over non-meal periods was used.

$$RMSE = \frac{1}{P} \times \sum_{i=1}^{P} \sqrt{\frac{1}{N} \times \sum_{k=1}^{N} (G(k) - y(k))^2}, i = 1, 2, \ldots \tag{13}$$

where, N is the number of samples in a non-meal period and P is the total number of non-meal periods in a glucose signal for one virtual patient.

The mathematical representation of the predicted glucose levels (Y_P) at each time-interval is shown below.

$$x(k+1) = Ax(k) + B\Delta u(k) + D\Delta d_m(k)$$

$$x(k+2) = Ax(k+1) + B\Delta u(k+1) + D\Delta d_m(k+1) =$$
$$A(Ax(k) + B\Delta u(k) + D\Delta d_m(k)) + B\Delta u(k+1) + D\Delta d_m(k+1) =$$
$$A^2x(k) + AB\Delta u(k) + AD\Delta d_m(k) + B\Delta u(k+1) + D\Delta d_m(k+1)$$
$$x(k+N_p) = A^{N_p}x(k) + A^{N_p-1}B\Delta u(k) + A^{N_p-1}D\Delta d_m(k) + A^{N_p-2}B\Delta u(k+1) +$$
$$A^{N_p-2}D\Delta d_m(k+1) + A^{N_p-3}B\Delta u(k+2) + A^{N_p-3}D\Delta d_m(k+2) + \cdots$$
$$A^{N_p-N_c+1}B\Delta u(k+N_c-2) + A^{N_p-N_c+1}D\Delta d_m(k+N_c-2) +$$
$$A^{N_p-N_c}B\Delta u(k+N_c-1) + A^{N_p-N_c}D\Delta d_m(k+N_c-1)$$

$$y(k+1) = Cx(k+1) = C(Ax(k) + B\Delta u(k) + D\Delta d_m(k)) =$$
$$CAx(k) + CB\Delta u(k) + CD\Delta d_m(k)$$

$$y(k+2) = Cx(k+2) =$$
$$C(A^2x(k) + AB\Delta u(k) + AD\Delta d_m(k) + B\Delta u(k+1) + D\Delta d_m(k+1)) =$$
$$CA^2x(k) + CAB\Delta u(k) + CAD\Delta d_m(k) + CB\Delta u(k+1) + CD\Delta d_m(k+1)$$
$$y(k+N_p) = Cx(k+N_p) =$$
$$CA^{N_p}x(k) + CA^{N_p-1}B\Delta u(k) + CA^{N_p-1}D\Delta d_m(k) +$$
$$CA^{N_p-2}B\Delta u(k+1) + CA^{N_p-2}D\Delta d_m(k+1) + \cdots$$
$$CA^{N_p-N_c}B\Delta u(k+N_c-1) + CA^{N_p-N_c}D\Delta d_m(k+N_c-1)$$

$$Y_P = [y(k+1)\ y(k+2)\ \cdots \qquad \text{N}_p)]^T;$$
$$\Delta U = [\Delta u(k)\ \Delta u(\text{k+1})\ \cdots \qquad \text{N}_c\text{-1})]^T;$$
$$\Delta D = [\Delta d_m(k)\ \Delta d_m(k+1)\ \cdots \qquad +\text{N}_c\text{-1})]^T;$$

$$\Rightarrow Y_P = Fx(k) + \Phi\Delta U + \Psi\Delta D$$

$$F = \begin{bmatrix} CA \\ CA^2 \\ CA^3 \\ \vdots \\ CA^{N_p} \end{bmatrix}$$

$$\Phi = \begin{bmatrix} CB & 0 & 0 & \cdots & \\ CAB & CB & 0 & \cdots & \\ CA^2B & CAB & CB & \cdots & \\ \vdots & \vdots & \vdots & \vdots & \vdots \\ CA^{N_p-1}B & CA^{N_p-2}B & CA^{N_p-3}B & \cdots & {}^{-N_c}B \end{bmatrix}$$

$$\Psi = \begin{bmatrix} CD & 0 & 0 & \cdots & \\ CAD & CD & 0 & \cdots & \\ CA^2D & CAD & CD & \cdots & \\ \vdots & \vdots & \vdots & \vdots & \vdots \\ CA^{N_p-1}D & CA^{N_p-2}D & CA^{N_p-3}D & \cdots & {}^{-N_c}D \end{bmatrix}$$

7 Future Directions

In this thesis, three main contributions to the field of diabetes were drawn. These contributions were related to the exercise component, in-silico type 1 diabetes simulator, personalized postprandial insulin adjustments, development of linearized and fast single and dual hormone controllers.

The exercise model incorporated in this thesis was based on a study that was conducted under aerobic exercise. For each exercise type, in real-time applications, the percentage increment of the basal peripheral glucose uptake, as well as peripheral insulin uptake and basal hepatic glucose production, were likely to differ. Therefore, in future research, a separate exercise model should be designed considering the changes of glucose fluxes.

In addition to exercise type, exercise intensity must also be considered. Exercise intensity can be modeled using accelerometry and heart rate data for modeling the PVO2max. The accelerometry data changes substantially at each exercise type. For example, in anaerobic exercise, the frequency of acceleration data is less than aerobic exercise. The frequency and the amplitude components, as well as the exercise bout, can be used to model the PVO2max. In addition, a thorough study should be conducted to determine the percentage of active muscular mass (PAMM) for different exercise types and intensity levels. Afterwards, the updated PAMM and

PVO2max can be used in equation 10 from chapter two to take different exercise types and levels into account. Currently, there is no study in the field to address the PAMM values at different exercise bouts.

The single and dual hormone simulators developed in chapter two showed consistency compared to the clinical data. The models still need to be modified with respect to the insulin kinetics model, glucose kinetics model and the meal model -- all of which are subject-dependent and were treated similarly in this dissertation. For example, the insulin absorption rate and glucose effectiveness change differently for each subject. In addition, the amount of the meals along with the meals' composition affect the glucose levels differently, as well. Whether the meals consist of carbohydrates, protein or fat and whether the amounts are large, medium or small, glucose fluxes change substantially across the subjects.

Considering the current setting of the MPC controller, the most optimum and individualized MPC would first fit the process model of the MPC to the glucose data of the subjects, and then calculate the parameters of the model separately. One approach could be to start with the Markov Chain Monte Carlo sampling method, where the model will be fit to the data using the likelihood function and the priori knowledge of the parameters. Then, the individualized model can be used during the control and update after each day of glucose data. In the future, to get more advanced

and accurate model predictive control, deep neural networks such as recurrent neural network can be used as the process model.

References

[1] S. Kalra, J. J. Mukherjee, S. Venkataraman, G. Bantwal, S. Shaikh, B. Saboo, A. K. Das, and A. Ramachandran, "Hypoglycemia: The neglected complication," *Indian Journal of Endocrinology and Metabolism,* vol. 17, no. 5, pp. 819-834, Sep-Oct, 2013.

[2] "Investments in Type 1 Diabetes Research," *American Diabetes Association*, 2017.

[3] "Statistics About Diabetes," *American Diabetes Association*, 2017.

[4] D. Boiroux, A. K. Duun-Henriksen, S. Schmidt, K. Nørgaard, S. Madsbad, O. Skyggebjerg, P. R. Jensen, N. K. Poulsen, H. Madsen, and J. B. Jørgensen, "Overnight Control of Blood Glucose in People with Type 1 Diabetes," *IFAC Proceedings Volumes,* vol. 45, no. 18, pp. 73-78, 2012/01/01/, 2012.

[5] A. Rovlias, and S. Kotsou, "The influence of hyperglycemia on neurological outcome in patients with severe head injury," *Neurosurgery,* vol. 46, no. 2, pp. 335-42; discussion 342-3, Feb, 2000.

[6] A. Bur, H. Herkner, C. Woisetschlager, M. Vlcek, U. Derhaschnig, and M. M. Hirschl, "Is fasting blood glucose a reliable parameter for screening for diabetes in hypertension?," *Am J Hypertens,* vol. 16, no. 4, pp. 297-301, Apr, 2003.

[7] P. J. Phillips, "Oral glucose tolerance testing," *Aust Fam Physician,* vol. 41, no. 6, pp. 391-3, Jun, 2012.

[8] D. M. Nathan, J. B. Buse, M. B. Davidson, R. J. Heine, R. R. Holman, R. Sherwin, and B. Zinman, "Management of Hyperglycemia in Type 2 Diabetes: A Consensus Algorithm for the Initiation and Adjustment of Therapy," *A consensus statement from the American Diabetes Association and the European Association for the Study of Diabetes,* vol. 29, no. 8, pp. 1963-1972, 2006.

[9] L. Yu, D. C. Boulware, C. A. Beam, J. C. Hutton, J. M. Wenzlau, C. J. Greenbaum, P. J. Bingley, J. P. Krischer, J. M. Sosenko, J. S. Skyler, G. S.

Eisenbarth, and J. L. Mahon, "Zinc Transporter-8 Autoantibodies Improve Prediction of Type 1 Diabetes in Relatives Positive for the Standard Biochemical Autoantibodies," *Diabetes Care,* vol. 35, no. 6, pp. 1213-1218, 2012.

[10] K. F. B. Gomes, C. Semzezem, R. Batista, R. T. Fukui, A. S. Santos, M. R. Correia, M. R. Passos-Bueno, and M. E. R. d. Silva, "Importance of Zinc Transporter 8 Autoantibody in the Diagnosis of Type 1 Diabetes in Latin Americans," *Scientific Reports,* vol. 7, no. 1, pp. 207, 2017/03/16, 2017.

[11] B. Fensom, C. Harris, S. E. Thompson, M. Al Mehthel, and D. M. Thompson, "Islet cell transplantation improves nerve conduction velocity in type 1 diabetes compared with intensive medical therapy over six years," *Diabetes Res Clin Pract,* vol. 122, pp. 101-105, Dec, 2016.

[12] S. C. Conrad, M. T. McGrath, and S. E. Gitelman, "Transition from multiple daily injections to continuous subcutaneous insulin infusion in type 1 diabetes mellitus," *J Pediatr,* vol. 140, no. 2, pp. 235-40, Feb, 2002.

[13] J. D. C. www.joslin.org, "Joslin Diabetes Center | Different Types of Insulin," 2017.

[14] P. Karagianni, C. Sampanis, C. Katsoulis, G. Miserlis, S. Polyzos, I. Zografou, S. Stergiopoulos, I. Douloumbakas, and C. Zamboulis, "Continuous subcutaneous insulin infusion versus multiple daily injections," *Hippokratia,* vol. 13, no. 2, pp. 93-96, Apr-Jun, 2009.

[15] R. Retnakaran, J. Hochman, J. H. DeVries, H. Hanaire-Broutin, R. J. Heine, V. Melki, and B. Zinman, "Continuous Subcutaneous Insulin Infusion Versus Multiple Daily Injections," *The impact of baseline A1c,* vol. 27, no. 11, pp. 2590-2596, 2004.

[16] R. M. Bergenstal, W. V. Tamborlane, A. Ahmann, J. B. Buse, G. Dailey, S. N. Davis, C. Joyce, T. Peoples, B. A. Perkins, J. B. Welsh, S. M. Willi, and M. A. Wood, "Effectiveness of sensor-augmented insulin-pump therapy in type 1 diabetes," *N Engl J Med,* vol. 363, no. 4, pp. 311-20, Jul 22, 2010.

[17] A. Tumminia, L. Sciacca, L. Frittitta, S. Squatrito, R. Vigneri, R. Le Moli, and L. Tomaselli, "Integrated insulin pump therapy with continuous glucose monitoring for improved adherence: technology update," *Patient Prefer Adherence,* vol. 9, pp. 1263-70, 2015.

[18] S. Rosenlund, T. W. Hansen, P. Rossing, and S. Andersen, "Effect of Sensor-Augmented Pump Treatment Versus Multiple Daily Injections on

Albuminuria: A 1-Year Randomized Study," *J Clin Endocrinol Metab,* vol. 100, no. 11, pp. 4181-8, Nov, 2015.

[19] A. Haidar, L. Legault, V. Messier, T. M. Mitre, C. Leroux, and R. Rabasa-Lhoret, "Comparison of dual-hormone artificial pancreas, single-hormone artificial pancreas, and conventional insulin pump therapy for glycaemic control in patients with type 1 diabetes: an open-label randomised controlled crossover trial," *Lancet Diabetes Endocrinol,* vol. 3, no. 1, pp. 17-26, Jan, 2015.

[20] P. G. Jacobs, J. El Youssef, R. Reddy, N. Resalat, D. Branigan, J. Condon, N. Preiser, K. Ramsey, M. Jones, C. Edwards, K. Kuehl, J. Leitschuh, U. Rajhbeharrysingh, and J. R. Castle, "Randomized trial of a dual-hormone artificial pancreas with dosing adjustment during exercise compared with no adjustment and sensor-augmented pump therapy," *Diabetes Obes Metab,* vol. 18, no. 11, pp. 1110-1119, Nov, 2016.

[21] B. A. Buckingham, D. Raghinaru, F. Cameron, B. W. Bequette, H. P. Chase, D. M. Maahs, R. Slover, R. P. Wadwa, D. M. Wilson, T. Ly, T. Aye, I. Hramiak, C. Clarson, R. Stein, P. H. Gallego, J. Lum, J. Sibayan, C. Kollman, and R. W. Beck, "Predictive Low-Glucose Insulin Suspension Reduces Duration of Nocturnal Hypoglycemia in Children Without Increasing Ketosis," *Diabetes Care,* vol. 38, no. 7, pp. 1197-204, Jul, 2015.

[22] P. G. Jacobs, J. El Youssef, J. Castle, P. Bakhtiani, D. Branigan, M. Breen, D. Bauer, N. Preiser, G. Leonard, T. Stonex, and W. K. Ward, "Automated control of an adaptive bihormonal, dual-sensor artificial pancreas and evaluation during inpatient studies," *IEEE Trans Biomed Eng,* vol. 61, no. 10, pp. 2569-81, Oct, 2014.

[23] R. R. Little, and D. B. Sacks, "HbA1c: how do we measure it and what does it mean?," *Current Opinion in Endocrinology, Diabetes and Obesity,* vol. 16, no. 2, pp. 113-118, 2009.

[24] R. M. Bergenstal, Y. Li, T. K. B. Porter, C. Weaver, and J. Han, "Exenatide once weekly improved glycaemic control, cardiometabolic risk factors and a composite index of an HbA1c < 7%, without weight gain or hypoglycaemia, over 52 weeks," *Diabetes, Obesity and Metabolism,* vol. 15, no. 3, pp. 264-271, 2013.

[25] A. L. McCall, D. J. Cox, R. Brodows, J. Crean, D. Johns, and B. Kovatchev, "Reduced daily risk of glycemic variability: comparison of exenatide with

insulin glargine," *Diabetes Technol Ther,* vol. 11, no. 6, pp. 339-44, Jun, 2009.

[26] A. M. Albisser, B. S. Leibel, T. G. Ewart, Z. Davidovac, C. K. Botz, W. Zingg, H. Schipper, and R. Gander, "Clinical control of diabetes by the artificial pancreas," *Diabetes,* vol. 23, no. 5, pp. 397-404, May, 1974.

[27] J. Mirouze, J. L. Selam, T. C. Pham, and D. Cavadore, "Evaluation of exogenous insulin homoeostasis by the artificial pancreas in insulin-dependent diabetes," *Diabetologia,* vol. 13, no. 3, pp. 273-8, May, 1977.

[28] P. G. Jacobs, N. Resalat, J. El Youssef, R. Reddy, D. Branigan, N. Preiser, J. Condon, and J. Castle, "Incorporating an Exercise Detection, Grading, and Hormone Dosing Algorithm Into the Artificial Pancreas Using Accelerometry and Heart Rate," *J Diabetes Sci Technol,* vol. 9, no. 6, pp. 1175-84, Oct 5, 2015.

[29] S. J. Russell, "Progress of artificial pancreas devices toward clinical use: the first outpatient studies," *Current opinion in endocrinology, diabetes, and obesity,* vol. 22, no. 2, pp. 106-111, 2015.

[30] A. Facchinetti, S. Del Favero, G. Sparacino, and C. Cobelli, "Model of glucose sensor error components: identification and assessment for new Dexcom G4 generation devices," *Medical & Biological Engineering & Computing,* vol. 53, no. 12, pp. 1259-1269, 2015/12/01, 2015.

[31] C. D. Man, F. Micheletto, D. Lv, M. Breton, B. Kovatchev, and C. Cobelli, "The UVA/PADOVA Type 1 Diabetes Simulator: New Features," *J Diabetes Sci Technol,* vol. 8, no. 1, pp. 26-34, Jan, 2014.

[32] C. Cobelli, C. D. Man, M. G. Pedersen, A. Bertoldo, and G. Toffolo, "Advancing our understanding of the glucose system via modeling: a perspective," *IEEE Trans Biomed Eng,* vol. 61, no. 5, pp. 1577-92, May, 2014.

[33] V. N. Shah, A. Shoskes, B. Tawfik, and S. K. Garg, "Closed-loop system in the management of diabetes: past, present, and future," *Diabetes Technol Ther,* vol. 16, no. 8, pp. 477-90, Aug, 2014.

[34] R. S. Parker, F. J. Doyle, 3rd, and N. A. Peppas, "A model-based algorithm for blood glucose control in type I diabetic patients," *IEEE Trans Biomed Eng,* vol. 46, no. 2, pp. 148-57, Feb, 1999.

[35] S. Kan, H. Onodera, E. Furutani, T. Aung, M. Araki, H. Nishimura, S. Maetani, and M. Imamura, "Novel control system for blood glucose using a model predictive method," *Asaio j,* vol. 46, no. 6, pp. 657-62, Nov-Dec, 2000.

[36] R. Hovorka, V. Canonico, L. J. Chassin, U. Haueter, M. Massi-Benedetti, M. O. Federici, T. R. Pieber, H. C. Schaller, L. Schaupp, T. Vering, and M. E. Wilinska, "Nonlinear model predictive control of glucose concentration in subjects with type 1 diabetes," *Physiological Measurement,* vol. 25, no. 4, pp. 905-920, 2004.

[37] R. Hovorka, J. M. Allen, D. Elleri, L. J. Chassin, J. Harris, D. Xing, C. Kollman, T. Hovorka, A. M. Larsen, M. Nodale, A. De Palma, M. E. Wilinska, C. L. Acerini, and D. B. Dunger, "Manual closed-loop insulin delivery in children and adolescents with type 1 diabetes: a phase 2 randomised crossover trial," *Lancet,* vol. 375, no. 9716, pp. 743-51, Feb 27, 2010.

[38] D. Elleri, J. M. Allen, M. Nodale, M. E. Wilinska, C. L. Acerini, D. B. Dunger, and R. Hovorka, "Suspended insulin infusion during overnight closed-loop glucose control in children and adolescents with Type 1 diabetes," *Diabet Med,* vol. 27, no. 4, pp. 480-4, Apr, 2010.

[39] K. Kumareswaran, D. Elleri, J. M. Allen, J. Harris, D. Xing, C. Kollman, M. Nodale, H. R. Murphy, S. A. Amiel, S. R. Heller, M. E. Wilinska, C. L. Acerini, M. L. Evans, D. B. Dunger, and R. Hovorka, "Meta-Analysis of Overnight Closed-Loop Randomized Studies in Children and Adults with Type 1 Diabetes: The Cambridge Cohort," *Journal of Diabetes Science and Technology,* vol. 5, no. 6, pp. 1352-1362, 11/01, 2011.

[40] D. Elleri, J. M. Allen, M. Nodale, M. E. Wilinska, J. S. Mangat, A. M. Larsen, C. L. Acerini, D. B. Dunger, and R. Hovorka, "Automated overnight closed-loop glucose control in young children with type 1 diabetes," *Diabetes Technol Ther,* vol. 13, no. 4, pp. 419-24, Apr, 2011.

[41] R. Hovorka, D. Elleri, H. Thabit, J. M. Allen, L. Leelarathna, R. El-Khairi, K. Kumareswaran, K. Caldwell, P. Calhoun, C. Kollman, H. R. Murphy, C. L. Acerini, M. E. Wilinska, M. Nodale, and D. B. Dunger, "Overnight closed-loop insulin delivery in young people with type 1 diabetes: a free-living, randomized clinical trial," *Diabetes Care,* vol. 37, no. 5, pp. 1204-11, 2014.

[42] L. Magni, D. M. Raimondo, L. Bossi, C. D. Man, G. De Nicolao, B. Kovatchev, and C. Cobelli, "Model predictive control of type 1 diabetes: an in silico trial," *J Diabetes Sci Technol,* vol. 1, no. 6, pp. 804-12, Nov, 2007.

[43] L. Magni, M. Forgione, C. Toffanin, C. Dalla Man, B. Kovatchev, G. De Nicolao, and C. Cobelli, "Run-to-run tuning of model predictive control for type 1 diabetes subjects: in silico trial," *J Diabetes Sci Technol,* vol. 3, no. 5, pp. 1091-8, Sep 1, 2009.

[44] L. Magni, D. M. Raimondo, C. Dalla Man, G. De Nicolao, B. Kovatchev, and C. Cobelli, "Model predictive control of glucose concentration in type I diabetic patients: An in silico trial," *Biomedical Signal Processing and Control,* vol. 4, no. 4, pp. 338-346, 2009/10/01/, 2009.

[45] S. Del Favero, D. Bruttomesso, F. Di Palma, G. Lanzola, R. Visentin, A. Filippi, R. Scotton, C. Toffanin, M. Messori, S. Scarpellini, P. Keith-Hynes, B. P. Kovatchev, J. H. Devries, E. Renard, L. Magni, A. Avogaro, and C. Cobelli, "First use of model predictive control in outpatient wearable artificial pancreas," *Diabetes Care,* vol. 37, no. 5, pp. 1212-5, 2014.

[46] B. Grosman, E. Dassau, H. C. Zisser, L. Jovanovic, and F. J. Doyle, 3rd, "Zone model predictive control: a strategy to minimize hyper- and hypoglycemic events," *J Diabetes Sci Technol,* vol. 4, no. 4, pp. 961-75, Jul 1, 2010.

[47] G. P. Forlenza, S. Deshpande, T. T. Ly, D. P. Howsmon, F. Cameron, N. Baysal, E. Mauritzen, T. Marcal, L. Towers, B. W. Bequette, L. M. Huyett, J. E. Pinsker, R. Gondhalekar, F. J. Doyle, 3rd, D. M. Maahs, B. A. Buckingham, and E. Dassau, "Application of Zone Model Predictive Control Artificial Pancreas During Extended Use of Infusion Set and Sensor: A Randomized Crossover-Controlled Home-Use Trial," *Diabetes Care,* vol. 40, no. 8, pp. 1096-1102, Aug, 2017.

[48] E. Dassau, H. Zisser, R. A. Harvey, M. W. Percival, B. Grosman, W. Bevier, E. Atlas, S. Miller, R. Nimri, L. Jovanovic, and F. J. Doyle, 3rd, "Clinical evaluation of a personalized artificial pancreas," *Diabetes Care,* vol. 36, no. 4, pp. 801-9, Apr, 2013.

[49] N. Resalat, J. E. Youssef, R. Reddy, and P. G. Jacobs, "Evaluation of model complexity in model predictive control within an exercise-enabled artificial pancreas," *IFAC-PapersOnLine,* vol. 50, no. 1, pp. 7756-7761, 2017/07/01/, 2017.

[50] V. Bátora, M. Tárnik, J. Murgaš, S. Schmidt, K. Nørgaard, N. K. Poulsen, H. Madsen, and J. B. Jørgensen, "Bihormonal model predictive control of blood glucose in people with type 1 diabetes." pp. 1693-1698.

[51] P. Herrero, P. Georgiou, N. Oliver, M. Reddy, D. Johnston, and C. Toumazou, "A composite model of glucagon-glucose dynamics for in silico testing of bihormonal glucose controllers," *J Diabetes Sci Technol,* vol. 7, no. 4, pp. 941-51, Jul 1, 2013.

[52] N. Resalat, J. E. Youssef, R. Reddy, and P. G. Jacobs, "Design of a dual-hormone model predictive control for artificial pancreas with exercise model." pp. 2270-2273.

[53] B. W. Bequette, "A critical assessment of algorithms and challenges in the development of a closed-loop artificial pancreas," *Diabetes Technol Ther,* vol. 7, no. 1, pp. 28-47, Feb, 2005.

[54] S. Shimoda, K. Nishida, M. Sakakida, Y. Konno, K. Ichinose, M. Uehara, T. Nowak, and M. Shichiri, "Closed-loop subcutaneous insulin infusion algorithm with a short-acting insulin analog for long-term clinical application of a wearable artificial endocrine pancreas," *Front Med Biol Eng,* vol. 8, no. 3, pp. 197-211, 1997.

[55] Y. Matsuo, S. Shimoda, M. Sakakida, K. Nishida, T. Sekigami, S. Ichimori, K. Ichinose, M. Shichiri, and E. Araki, "Strict glycemic control in diabetic dogs with closed-loop intraperitoneal insulin infusion algorithm designed for an artificial endocrine pancreas," *J Artif Organs,* vol. 6, no. 1, pp. 55-63, 2003.

[56] M. J. O'Grady, A. J. Retterath, D. B. Keenan, N. Kurtz, M. Cantwell, G. Spital, M. N. Kremliovsky, A. Roy, E. A. Davis, T. W. Jones, and T. T. Ly, "The use of an automated, portable glucose control system for overnight glucose control in adolescents and young adults with type 1 diabetes," *Diabetes Care,* vol. 35, no. 11, pp. 2182-7, Nov, 2012.

[57] G. M. Steil, K. Rebrin, C. Darwin, F. Hariri, and M. F. Saad, "Feasibility of automating insulin delivery for the treatment of type 1 diabetes," *Diabetes,* vol. 55, no. 12, pp. 3344-50, Dec, 2006.

[58] S. A. Weinzimer, G. M. Steil, K. L. Swan, J. Dziura, N. Kurtz, and W. V. Tamborlane, "Fully automated closed-loop insulin delivery versus semiautomated hybrid control in pediatric patients with type 1 diabetes using an artificial pancreas," *Diabetes Care,* vol. 31, no. 5, pp. 934-9, May, 2008.

[59] A. C. van Bon, Y. M. Luijf, R. Koebrugge, R. Koops, J. B. Hoekstra, and J. H. DeVries, "Feasibility of a portable bihormonal closed-loop system to control glucose excursions at home under free-living conditions for 48 hours," *Diabetes Technol Ther,* vol. 16, no. 3, pp. 131-6, Mar, 2014.

[60] J. R. Castle, J. M. Engle, J. El Youssef, R. G. Massoud, K. C. Yuen, R. Kagan, and W. K. Ward, "Novel use of glucagon in a closed-loop system for prevention of hypoglycemia in type 1 diabetes," *Diabetes Care,* vol. 33, no. 6, pp. 1282-7, Jun, 2010.

[61] B. Gopakumaran, H. M. Duman, D. P. Overholser, I. F. Federiuk, M. J. Quinn, M. D. Wood, and W. K. Ward, "A Novel Insulin Delivery Algorithm in Rats With Type 1 Diabetes: The Fading Memory Proportional-Derivative Method," *Artificial Organs,* vol. 29, no. 8, pp. 599-607, 2005.

[62] F. H. El-Khatib, J. Jiang, and E. R. Damiano, "Adaptive closed-loop control provides blood-glucose regulation using dual subcutaneous insulin and glucagon infusion in diabetic Swine," *J Diabetes Sci Technol,* vol. 1, no. 2, pp. 181-92, Mar, 2007.

[63] A. Haidar, L. Legault, M. Dallaire, A. Alkhateeb, A. Coriati, V. Messier, P. Cheng, M. Millette, B. Boulet, and R. Rabasa-Lhoret, "Glucose-responsive insulin and glucagon delivery (dual-hormone artificial pancreas) in adults with type 1 diabetes: a randomized crossover controlled trial," *Cmaj,* vol. 185, no. 4, pp. 297-305, Mar 5, 2013.

[64] J. R. Castle, J. El Youssef, L. M. Wilson, R. Reddy, N. Resalat, D. Branigan, K. Ramsey, J. Leitschuh, U. Rajhbeharrysingh, B. Senf, S. M. Sugerman, V. Gabo, and P. G. Jacobs, "Randomized Outpatient Trial of Single- and Dual-Hormone Closed-Loop Systems That Adapt to Exercise Using Wearable Sensors," *Diabetes Care,* vol. 41, no. 7, pp. 1471-1477, Jul, 2018.

[65] R. Reddy, J. El Youssef, K. Winters-Stone, D. Branigan, J. Leitschuh, J. Castle, and P. G. Jacobs, "The effect of exercise on sleep in adults with type 1 diabetes," *Diabetes Obes Metab,* vol. 20, no. 2, pp. 443-447, Feb, 2018.

[66] J. L. Ruiz, J. L. Sherr, E. Cengiz, L. Carria, A. Roy, G. Voskanyan, W. V. Tamborlane, and S. A. Weinzimer, "Effect of insulin feedback on closed-loop glucose control: a crossover study," *J Diabetes Sci Technol,* vol. 6, no. 5, pp. 1123-30, Sep 1, 2012.

[67] R. Mauseth, Y. Wang, E. Dassau, R. Kircher, D. Matheson, H. Zisser, L. Jovanovič, and F. J. Doyle, "Proposed Clinical Application for Tuning Fuzzy

Logic Controller of Artificial Pancreas Utilizing a Personalization Factor," *Journal of Diabetes Science and Technology,* vol. 4, no. 4, pp. 913-922, 07/01, 2010.

[68] N. Boumella, J. C. Figueroa, and S. Iqbal, "Enhancing Fuzzy Controllers Using Generalized Orthogonality Principle, Fuzzy Controllers - Recent Advances in Theory and Applications," InTech, 2012.

[69] R. Mauseth, I. B. Hirsch, J. Bollyky, R. Kircher, D. Matheson, S. Sanda, and C. Greenbaum, "Use of a "fuzzy logic" controller in a closed-loop artificial pancreas," *Diabetes Technol Ther,* vol. 15, no. 8, pp. 628-33, Aug, 2013.

[70] Y. C. Kudva, R. E. Carter, C. Cobelli, R. Basu, and A. Basu, "Closed-Loop Artificial Pancreas Systems: Physiological Input to Enhance Next-Generation Devices," *Diabetes Care,* vol. 37, no. 5, pp. 1184-1190, 2014.

[71] K. Turksoy, E. S. Bayrak, L. Quinn, E. Littlejohn, and A. Cinar, "Multivariable adaptive closed-loop control of an artificial pancreas without meal and activity announcement," *Diabetes Technol Ther,* vol. 15, no. 5, pp. 386-400, May, 2013.

[72] P. J. Lenart, and R. S. Parker, "MODELING EXERCISE EFFECTS IN TYPE I DIABETIC PATIENTS," *IFAC Proceedings Volumes,* vol. 35, no. 1, pp. 247-252, 2002/01/01/, 2002.

[73] M. Hernandez-Ordonez, and D. U. Campos-Delgado, "An extension to the compartmental model of type 1 diabetic patients to reproduce exercise periods with glycogen depletion and replenishment," *J Biomech,* vol. 41, no. 4, pp. 744-52, 2008.

[74] J. S. Sibold, and K. M. Berg, "Mood enhancement persists for up to 12 hours following aerobic exercise: a pilot study," *Percept Mot Skills,* vol. 111, no. 2, pp. 333-42, Oct, 2010.

[75] D. Elleri, J. M. Allen, J. Harris, K. Kumareswaran, M. Nodale, L. Leelarathna, C. L. Acerini, A. Haidar, M. E. Wilinska, N. Jackson, A. M. Umpleby, M. L. Evans, D. B. Dunger, and R. Hovorka, "Absorption patterns of meals containing complex carbohydrates in type 1 diabetes," *Diabetologia,* vol. 56, no. 5, pp. 1108-17, May, 2013.

[76] R. Hovorka, K. Kumareswaran, J. Harris, J. M. Allen, D. Elleri, D. Xing, C. Kollman, M. Nodale, H. R. Murphy, D. B. Dunger, S. A. Amiel, S. R. Heller, M. E. Wilinska, and M. L. Evans, "Overnight closed loop insulin delivery

(artificial pancreas) in adults with type 1 diabetes: crossover randomised controlled studies," *Bmj,* vol. 342, pp. d1855, Apr 13, 2011.

[77] H. J. Woerle, M. Albrecht, R. Linke, S. Zschau, C. Neumann, M. Nicolaus, J. Gerich, B. Goke, and J. Schirra, "Importance of changes in gastric emptying for postprandial plasma glucose fluxes in healthy humans," *Am J Physiol Endocrinol Metab,* vol. 294, no. 1, pp. E103-9, Jan, 2008.

[78] S. A. Weinzimer, J. L. Sherr, E. Cengiz, G. Kim, J. L. Ruiz, L. Carria, G. Voskanyan, A. Roy, and W. V. Tamborlane, "Effect of pramlintide on prandial glycemic excursions during closed-loop control in adolescents and young adults with type 1 diabetes," *Diabetes Care,* vol. 35, no. 10, pp. 1994-9, Oct, 2012.

[79] A. American Diabetes, "Standards of Medical Care in Diabetes—2013," *Diabetes Care,* vol. 36, no. Suppl 1, pp. S11-S66, 12/10, 2013.

[80] A. Bertachi, A. Beneyto, C. M. Ramkissoon, and J. Vehi, "Assessment of Mitigation Methods to Reduce the Risk of Hypoglycemia for Announced Exercise in a Uni-hormonal Artificial Pancreas," *Diabetes Technol Ther,* vol. 20, no. 4, pp. 285-295, Apr, 2018.

[81] C. Manohar, J. A. Levine, D. K. Nandy, A. Saad, C. Dalla Man, S. K. McCrady-Spitzer, R. Basu, C. Cobelli, R. E. Carter, A. Basu, and Y. C. Kudva, "The Effect of Walking on Postprandial Glycemic Excursion in Patients With Type 1 Diabetes and Healthy People," *Diabetes Care,* vol. 35, no. 12, pp. 2493-2499, 2012.

[82] A. Maran, P. Pavan, B. Bonsembiante, E. Brugin, A. Ermolao, A. Avogaro, and M. Zaccaria, "Continuous glucose monitoring reveals delayed nocturnal hypoglycemia after intermittent high-intensity exercise in nontrained patients with type 1 diabetes," *Diabetes Technol Ther,* vol. 12, no. 10, pp. 763-8, Oct, 2010.

[83] K. E. Iscoe, and M. C. Riddell, "Continuous moderate-intensity exercise with or without intermittent high-intensity work: effects on acute and late glycaemia in athletes with Type 1 diabetes mellitus," *Diabet Med,* vol. 28, no. 7, pp. 824-32, Jul, 2011.

[84] J. E. Yardley, G. P. Kenny, B. A. Perkins, M. C. Riddell, N. Balaa, J. Malcolm, P. Boulay, F. Khandwala, and R. J. Sigal, "Resistance Versus Aerobic Exercise: Acute effects on glycemia in type 1 diabetes," *Diabetes Care,* vol. 36, no. 3, pp. 537-542, 2013.

[85] J. E. Yardley, G. P. Kenny, B. A. Perkins, M. C. Riddell, J. Malcolm, P. Boulay, F. Khandwala, and R. J. Sigal, "Effects of performing resistance exercise before versus after aerobic exercise on glycemia in type 1 diabetes," *Diabetes Care,* vol. 35, no. 4, pp. 669-75, Apr, 2012.

[86] C. Tonoli, E. Heyman, B. Roelands, L. Buyse, S. S. Cheung, S. Berthoin, and R. Meeusen, "Effects of different types of acute and chronic (training) exercise on glycaemic control in type 1 diabetes mellitus: a meta-analysis," *Sports Med,* vol. 42, no. 12, pp. 1059-80, Dec 1, 2012.

[87] J. E. Yardley, K. E. Iscoe, R. J. Sigal, G. P. Kenny, B. A. Perkins, and M. C. Riddell, "Insulin pump therapy is associated with less post-exercise hyperglycemia than multiple daily injections: an observational study of physically active type 1 diabetes patients," *Diabetes Technol Ther,* vol. 15, no. 1, pp. 84-8, Jan, 2013.

[88] D. Elleri, J. M. Allen, K. Kumareswaran, L. Leelarathna, M. Nodale, K. Caldwell, P. Cheng, C. Kollman, A. Haidar, H. R. Murphy, M. E. Wilinska, C. L. Acerini, D. B. Dunger, and R. Hovorka, "Closed-loop basal insulin delivery over 36 hours in adolescents with type 1 diabetes: randomized clinical trial," *Diabetes Care,* vol. 36, no. 4, pp. 838-44, Apr, 2013.

[89] M. Breton, A. Farret, D. Bruttomesso, S. Anderson, L. Magni, S. Patek, C. Dalla Man, J. Place, S. Demartini, S. Del Favero, C. Toffanin, C. Hughes-Karvetski, E. Dassau, H. Zisser, F. J. Doyle, 3rd, G. De Nicolao, A. Avogaro, C. Cobelli, E. Renard, and B. Kovatchev, "Fully integrated artificial pancreas in type 1 diabetes: modular closed-loop glucose control maintains near normoglycemia," *Diabetes,* vol. 61, no. 9, pp. 2230-7, Sep, 2012.

[90] S. J. Russell, F. H. El-Khatib, D. M. Nathan, K. L. Magyar, J. Jiang, and E. R. Damiano, "Blood glucose control in type 1 diabetes with a bihormonal bionic endocrine pancreas," *Diabetes Care,* vol. 35, no. 11, pp. 2148-55, Nov, 2012.

[91] S. J. Russell, F. H. El-Khatib, M. Sinha, K. L. Magyar, K. McKeon, L. G. Goergen, C. Balliro, M. A. Hillard, D. M. Nathan, and E. R. Damiano, "Outpatient Glycemic Control with a Bionic Pancreas in Type 1 Diabetes," *The New England journal of medicine,* vol. 371, no. 4, pp. 313-325, 06/15, 2014.

[92] A. Roy, and R. S. Parker, "Dynamic modeling of exercise effects on plasma glucose and insulin levels," *J Diabetes Sci Technol,* vol. 1, no. 3, pp. 338-47, May, 2007.

[93] R. N. Bergman, L. S. Phillips, and C. Cobelli, "Physiologic evaluation of factors controlling glucose tolerance in man: measurement of insulin sensitivity and beta-cell glucose sensitivity from the response to intravenous glucose," *Journal of Clinical Investigation,* vol. 68, no. 6, pp. 1456-1467, 1981.

[94] N. P. Balakrishnan, L. Samavedham, and G. P. Rangaiah, "Personalized mechanistic models for exercise, meal and insulin interventions in children and adolescents with type 1 diabetes," *J Theor Biol,* vol. 357, pp. 62-73, Sep 21, 2014.

[95] G. A. Borg, "Psychophysical bases of perceived exertion," *Med Sci Sports Exerc,* vol. 14, no. 5, pp. 377-81, 1982.

[96] N. Resalat, J. El Youssef, N. Tyler, J. Castle, and P. G. Jacobs, "A statistical virtual patient population for the glucoregulatory system in type 1 diabetes with integrated exercise model," *PLOS ONE,* vol. 14, no. 7, pp. e0217301, 2019.

[97] A. Facchinetti, S. Del Favero, G. Sparacino, and C. Cobelli, "An online failure detection method of the glucose sensor-insulin pump system: improved overnight safety of type-1 diabetic subjects," *IEEE Trans Biomed Eng,* vol. 60, no. 2, pp. 406-16, Feb, 2013.

[98] B. P. Kovatchev, M. Breton, C. D. Man, and C. Cobelli, "In silico preclinical trials: a proof of concept in closed-loop control of type 1 diabetes," *J Diabetes Sci Technol,* vol. 3, no. 1, pp. 44-55, Jan, 2009.

[99] Y. Wang, M. W. Percival, E. Dassau, H. C. Zisser, L. Jovanovic, and F. J. Doyle, 3rd, "A novel adaptive basal therapy based on the value and rate of change of blood glucose," *J Diabetes Sci Technol,* vol. 3, no. 5, pp. 1099-108, Sep 1, 2009.

[100] M. W. Percival, Y. Wang, B. Grosman, E. Dassau, H. Zisser, L. Jovanovic, and F. J. Doyle, 3rd, "Development of a multi-parametric model predictive control algorithm for insulin delivery in type 1 diabetes mellitus using clinical parameters," *J Process Control,* vol. 21, no. 3, pp. 391-404, Mar 1, 2011.

[101] K. Zarkogianni, A. Vazeou, S. G. Mougiakakou, A. Prountzou, and K. S. Nikita, "An insulin infusion advisory system based on autotuning nonlinear model-predictive control," *IEEE Trans Biomed Eng,* vol. 58, no. 9, pp. 2467-77, Sep, 2011.

[102] R. Visentin, C. Dalla Man, B. Kovatchev, and C. Cobelli, "The university of Virginia/Padova type 1 diabetes simulator matches the glucose traces of a clinical trial," *Diabetes Technol Ther,* vol. 16, no. 7, pp. 428-34, Jul, 2014.

[103] R. Visentin, C. D. Man, and C. Cobelli, "One-Day Bayesian Cloning of Type 1 Diabetes Subjects: Toward a Single-Day UVA/Padova Type 1 Diabetes Simulator," *IEEE Trans Biomed Eng,* vol. 63, no. 11, pp. 2416-2424, Nov, 2016.

[104] M. E. Wilinska, L. J. Chassin, C. L. Acerini, J. M. Allen, D. B. Dunger, and R. Hovorka, "Simulation environment to evaluate closed-loop insulin delivery systems in type 1 diabetes," *J Diabetes Sci Technol,* vol. 4, no. 1, pp. 132-44, Jan 1, 2010.

[105] A. Haidar, M. E. Wilinska, J. A. Graveston, and R. Hovorka, "Stochastic Virtual Population of Subjects With Type 1 Diabetes for the Assessment of Closed-Loop Glucose Controllers," *IEEE Trans Biomed Eng,* vol. 60, no. 12, pp. 3524-33, Dec, 2013.

[106] M. C. Riddell, I. W. Gallen, C. E. Smart, C. E. Taplin, P. Adolfsson, A. N. Lumb, A. Kowalski, R. Rabasa-Lhoret, R. J. McCrimmon, C. Hume, F. Annan, P. A. Fournier, C. Graham, B. Bode, P. Galassetti, T. W. Jones, I. S. Millan, T. Heise, A. L. Peters, A. Petz, and L. M. Laffel, "Exercise management in type 1 diabetes: a consensus statement," *Lancet Diabetes Endocrinol,* vol. 5, no. 5, pp. 377-390, May, 2017.

[107] J. R. Castle, J. El Youssef, L. M. Wilson, R. Reddy, N. Resalat, D. Branigan, K. Ramsey, J. Leitschuh, U. Rajhbeharrysingh, B. Senf, S. M. Sugerman, V. Gabo, and P. G. Jacobs, "Randomized Outpatient Trial of Single- and Dual-Hormone Closed-Loop Systems That Adapt to Exercise Using Wearable Sensors," *Diabetes Care*, May 11, 2018.

[108] R. Hovorka, V. Canonico, L. J. Chassin, U. Haueter, M. Massi-Benedetti, M. Orsini Federici, T. R. Pieber, H. C. Schaller, L. Schaupp, T. Vering, and M. E. Wilinska, "Nonlinear model predictive control of glucose concentration in subjects with type 1 diabetes," *Physiol Meas,* vol. 25, no. 4, pp. 905-20, Aug, 2004.

[109] D. Lv, M. D. Breton, and L. S. Farhy, "Pharmacokinetics modeling of exogenous glucagon in type 1 diabetes mellitus patients," *Diabetes Technol Ther,* vol. 15, no. 11, pp. 935-41, Nov, 2013.

[110] I. Zakeri, A. L. Adolph, M. R. Puyau, F. A. Vohra, and N. F. Butte, "Application of cross-sectional time series modeling for the prediction of energy expenditure from heart rate and accelerometry," *J Appl Physiol (1985),* vol. 104, no. 6, pp. 1665-73, Jun, 2008.

[111] J. Walsh, R. Roberts, and T. Bailey, "Guidelines for insulin dosing in continuous subcutaneous insulin infusion using new formulas from a retrospective study of individuals with optimal glucose levels," *J Diabetes Sci Technol,* vol. 4, no. 5, pp. 1174-81, Sep 1, 2010.

[112] M. R. Rickels, S. M. Kong, C. Fuller, C. Dalton-Bakes, J. F. Ferguson, M. P. Reilly, K. L. Teff, and A. Naji, "Insulin sensitivity index in type 1 diabetes and following human islet transplantation: comparison of the minimal model to euglycemic clamp measures," *Am J Physiol Endocrinol Metab,* vol. 306, no. 10, pp. E1217-24, May 15, 2014.

[113] P. Herrero, J. Bondia, O. Adewuyi, P. Pesl, M. El-Sharkawy, M. Reddy, C. Toumazou, N. Oliver, and P. Georgiou, "Enhancing automatic closed-loop glucose control in type 1 diabetes with an adaptive meal bolus calculator - in silico evaluation under intra-day variability," *Comput Methods Programs Biomed,* vol. 146, pp. 125-131, Jul, 2017.

[114] A. Facchinetti, S. Del Favero, G. Sparacino, J. R. Castle, W. K. Ward, and C. Cobelli, "Modeling the glucose sensor error," *IEEE Trans Biomed Eng,* vol. 61, no. 3, pp. 620-9, Mar, 2014.

[115] M. C. Palumbo, M. Morettini, P. Tieri, F. Diele, M. Sacchetti, and F. Castiglione, "Personalizing physical exercise in a computational model of fuel homeostasis," *PLOS Computational Biology,* vol. 14, no. 4, pp. e1006073, 2018.

[116] N. Resalat, J. El Youssef, R. Reddy, J. Castle, and P. G. Jacobs, "Adaptive tuning of basal and bolus insulin to reduce postprandial hypoglycemia in a hybrid artificial pancreas," *Journal of Process Control,* vol. 80, pp. 247-254, 2019/08/01/, 2019.

[117] C. C. Palerm, H. Zisser, W. C. Bevier, L. Jovanovič, and F. J. Doyle, "Prandial Insulin Dosing Using Run-to-Run Control," *Application of clinical data and medical expertise to define a suitable performance metric,* vol. 30, no. 5, pp. 1131-1136, 2007.

[118] C. C. Palerm, H. Zisser, L. Jovanovič, and F. J. Doyle, "A run-to-run framework for prandial insulin dosing: handling real-life uncertainty,"

International Journal of Robust and Nonlinear Control, vol. 17, no. 13, pp. 1194-1213, 2007.

[119] E. Dassau, and J. E. Pinsker, "Twelve-Week 24/7 Ambulatory Artificial Pancreas With Weekly Adaptation of Insulin Delivery Settings: Effect on Hemoglobin A1c and Hypoglycemia," vol. 40, no. 12, pp. 1719-1726, Dec, 2017.

[120] E. Dassau, S. A. Brown, A. Basu, J. E. Pinsker, Y. C. Kudva, R. Gondhalekar, S. Patek, D. Lv, M. Schiavon, J. B. Lee, C. Dalla Man, L. Hinshaw, K. Castorino, A. Mallad, V. Dadlani, S. K. McCrady-Spitzer, M. McElwee-Malloy, C. A. Wakeman, W. C. Bevier, P. K. Bradley, B. Kovatchev, C. Cobelli, H. C. Zisser, and F. J. Doyle, 3rd, "Adjustment of Open-Loop Settings to Improve Closed-Loop Results in Type 1 Diabetes: A Multicenter Randomized Trial," *J Clin Endocrinol Metab,* vol. 100, no. 10, pp. 3878-86, Oct, 2015.

[121] C. Toffanin, A. Sandri, M. Messori, C. Cobelli, and L. Magni, "Automatic adaptation of basal therapy for Type 1 diabetic patients: a Run-to-Run approach," *IFAC Proceedings Volumes,* vol. 47, no. 3, pp. 2070-2075, 2014/01/01/, 2014.

[122] C. Toffanin, R. Visentin, M. Messori, F. D. Palma, L. Magni, and C. Cobelli, "Towards a Run-to-Run Adaptive Artificial Pancreas: In Silico Results," *IEEE Transactions on Biomedical Engineering,* vol. PP, no. 99, pp. 1-1, 2017.

[123] K. Turksoy, L. T. Quinn, E. Littlejohn, and A. Cinar, "An integrated multivariable artificial pancreas control system," *J Diabetes Sci Technol,* vol. 8, no. 3, pp. 498-507, May, 2014.

[124] S. J. Galati, and E. J. Rayfield, "Approach to the patient with postprandial hypoglycemia," *Endocr Pract,* vol. 20, no. 4, pp. 331-40, Apr, 2014.

[125] N. Resalat, J. El Youssef, R. Reddy, and P. G. Jacobs, "Design of a dual-hormone model predictive control for artificial pancreas with exercise model," *Conf Proc IEEE Eng Med Biol Soc,* vol. 2016, pp. 2270-2273, Aug, 2016.

[126] R. Hovorka, F. Shojaee-Moradie, P. V. Carroll, L. J. Chassin, I. J. Gowrie, N. C. Jackson, R. S. Tudor, A. M. Umpleby, and R. H. Jones, "Partitioning glucose distribution/transport, disposal, and endogenous production during

IVGTT," *Am J Physiol Endocrinol Metab,* vol. 282, no. 5, pp. E992-1007, May, 2002.

[127] "Defining and reporting hypoglycemia in diabetes: a report from the American Diabetes Association Workgroup on Hypoglycemia," *Diabetes Care,* vol. 28, no. 5, pp. 1245-9, May, 2005.

[128] L. M. Huyett, E. Dassau, H. C. Zisser, and F. J. Doyle, "Design and Evaluation of a Robust PID Controller for a Fully Implantable Artificial Pancreas," *Industrial & Engineering Chemistry Research,* vol. 54, no. 42, pp. 10311-10321, 2015.

[129] Y. Ramprasad, G. P. Rangaiah, and S. Lakshminarayanan, "Robust PID Controller for Blood Glucose Regulation in Type I Diabetics," *Industrial & Engineering Chemistry Research,* vol. 43, no. 26, pp. 8257-8268, 2004/12/01, 2004.

[130] D. Boiroux, V. Bátora, M. Hagdrup, M. Tárnik, J. Murgaš, S. Schmidt, K. Nørgaard, N. K. Poulsen, H. Madsen, and J. B. Jørgensen, "Comparison of Prediction Models for a Dual-Hormone Artificial Pancreas∗∗Funded by the Danish Diabetes Academy supported by the Novo Nordisk Foundation. Contact information: John Bagterp J_rgensen(jbjo@dtu.dk)," *IFAC-PapersOnLine,* vol. 48, no. 20, pp. 7-12, 2015/01/01/, 2015.

[131] M. E. Wilinska, L. J. Chassin, H. C. Schaller, L. Schaupp, T. R. Pieber, and R. Hovorka, "Insulin kinetics in type-I diabetes: continuous and bolus delivery of rapid acting insulin," *IEEE Trans Biomed Eng,* vol. 52, no. 1, pp. 3-12, Jan, 2005.

[132] L. Wang, "Model Predictive Control System Design and Implementation Using MATLAB®," *Advances in Industrial Control,*, pp. 1-39, 2009.

[133] B. W. Bequette, "Algorithms for a closed-loop artificial pancreas: the case for model predictive control," *J Diabetes Sci Technol,* vol. 7, no. 6, pp. 1632-43, Nov 01, 2013.

[134] G. M. Steil, "Algorithms for a closed-loop artificial pancreas: the case for proportional-integral-derivative control," *J Diabetes Sci Technol,* vol. 7, no. 6, pp. 1621-31, Nov 01, 2013.

[135] H. Thabit, M. Tauschmann, J. M. Allen, L. Leelarathna, S. Hartnell, M. E. Wilinska, C. L. Acerini, S. Dellweg, C. Benesch, L. Heinemann, J. K. Mader, M. Holzer, H. Kojzar, J. Exall, J. Yong, J. Pichierri, K. D. Barnard, C. Kollman, P. Cheng, P. C. Hindmarsh, F. M. Campbell, S. Arnolds, T. R.

Pieber, M. L. Evans, D. B. Dunger, and R. Hovorka, "Home Use of an Artificial Beta Cell in Type 1 Diabetes," *N Engl J Med*, Sep 17, 2015.

[136] B. Kovatchev, C. Cobelli, E. Renard, S. Anderson, M. Breton, S. Patek, W. Clarke, D. Bruttomesso, A. Maran, S. Costa, A. Avogaro, C. Dalla Man, A. Facchinetti, L. Magni, G. De Nicolao, J. Place, and A. Farret, "Multinational study of subcutaneous model-predictive closed-loop control in type 1 diabetes mellitus: summary of the results," *J Diabetes Sci Technol,* vol. 4, no. 6, pp. 1374-81, Nov 01, 2010.

[137] N. Resalat, R. Reddy, J. El Youssef, and P. G. Jacobs, "Design of a Dual-Hormone Model Predictive Control for Artificial Pancreas with Exercise Model," in 38th Annual International Conference of the IEEE Engineering in Medicine and Biology Society, Orlando, FL, 2016, pp. 2270-2273.

[138] R. N. Bergman, Y. Z. Ider, C. R. Bowden, and C. Cobelli, "Quantitative estimation of insulin sensitivity," *Am J Physiol,* vol. 236, no. 6, pp. E667-77, Jun, 1979.

[139] C. Cobelli, A. Caumo, and M. Omenetto, "Minimal model SG overestimation and SI underestimation: improved accuracy by a Bayesian two-compartment model," *Am J Physiol,* vol. 277, no. 3 Pt 1, pp. E481-8, Sep, 1999.

[140] T. Kobayashi, S. Sawano, T. Itoh, K. Kosaka, H. Hirayama, and Y. Kasuya, "The pharmacokinetics of insulin after continuous subcutaneous infusion or bolus subcutaneous injection in diabetic patients," *Diabetes,* vol. 32, no. 4, pp. 331-6, Apr, 1983.

[141] G. M. Ward, K. M. Weber, I. M. Walters, P. M. Aitken, B. Lee, J. D. Best, R. C. Boston, and F. P. Alford, "A modified minimal model analysis of insulin sensitivity and glucose-mediated glucose disposal in insulin-dependent diabetes," *Metabolism,* vol. 40, no. 1, pp. 4-9, Jan, 1991.

[142] B. W. Bequette, "Glucose Clamp Algorithms and Insulin Time-Action Profiles," *J Diabetes Sci Technol,* vol. 3, no. 5, pp. 1005-13, Sep, 2009.

[143] K. Osei, D. A. Cottrell, M. L. Henry, R. J. Tesi, R. M. Ferguson, and T. M. O'Dorisio, "Minimal model analysis of insulin sensitivity and glucose-mediated glucose disposal in type 1 (insulin-dependent) diabetic pancreas allograft recipients," *Diabetologia,* vol. 35, no. 7, pp. 676-80, Jul, 1992.

[144] W. L. Clarke, S. Anderson, M. Breton, S. Patek, L. Kashmer, and B. Kovatchev, "Closed-loop artificial pancreas using subcutaneous glucose sensing and insulin delivery and a model predictive control algorithm: the

Virginia experience," *J Diabetes Sci Technol,* vol. 3, no. 5, pp. 1031-8, Sep 1, 2009.

[145] D. Boiroux, A. K. Duun-Henriksen, S. Schmidt, K. Nørgaard, S. Madsbad, N. K. Poulsen, H. Madsen, and J. B. Jørgensen, "Overnight glucose control in people with type 1 diabetes," *Biomedical Signal Processing and Control,* vol. 39, no. Supplement C, pp. 503-512, 2018/01/01/, 2018.

[146] A. J. Laguna Sanz, F. J. Doyle, 3rd, and E. Dassau, "An Enhanced Model Predictive Control for the Artificial Pancreas Using a Confidence Index Based on Residual Analysis of Past Predictions," *J Diabetes Sci Technol,* vol. 11, no. 3, pp. 537-544, May, 2017.

[147] C. Toffanin, R. Visentin, M. Messori, F. D. Palma, L. Magni, and C. Cobelli, "Toward a Run-to-Run Adaptive Artificial Pancreas: In Silico Results," *IEEE Trans Biomed Eng,* vol. 65, no. 3, pp. 479-488, Mar, 2018.

[148] K. Turksoy, C. Monforti, M. Park, G. Griffith, L. Quinn, and A. Cinar, "Use of Wearable Sensors and Biometric Variables in an Artificial Pancreas System," *Sensors (Basel),* vol. 17, no. 3, Mar 7, 2017.

[149] M. D. Breton, S. A. Brown, C. H. Karvetski, L. Kollar, K. A. Topchyan, S. M. Anderson, and B. P. Kovatchev, "Adding heart rate signal to a control-to-range artificial pancreas system improves the protection against hypoglycemia during exercise in type 1 diabetes," *Diabetes Technol Ther,* vol. 16, no. 8, pp. 506-11, Aug, 2014.